

**ANKARA YILDIRIM BEYAZIT UNIVERSITY**  
**GRADUATE SCHOOL OF NATURAL AND APPLIED**  
**SCIENCES**



**A NOVEL AND EFFICIENT METHOD FOR FACE**  
**RECOGNITION USING ORIGINAL AND**  
**SYMMETRICAL SAMPLES**

**Ph.D. Thesis by**

**Saad Omran Elhashmi ALLAGWAIL**

**Department of Electrical and Computer Engineering**

**August, 2019**

**ANKARA**

**A NOVEL AND EFFICIENT METHOD FOR FACE  
RECOGNITION USING ORIGINAL AND  
SYMMETRICAL SAMPLES**

**A Thesis Submitted to the  
Graduate School of Natural and Applied Sciences of  
Ankara Yıldırım Beyazıt University  
In Partial Fulfillment of the Requirements for the Ph.D.  
in Electrical and Computer Engineering, Department of Electrical and  
Computer Engineering**

**by**

**Saad Omran Elhashmi ALLAGWAIL**

**August, 2019**

**ANKARA**

## Ph.D. THESIS EXAMINATION RESULT FORM

We have read the thesis entitled “**A NOVEL AND EFFICIENT METHOD FOR FACE RECOGNITION USING ORIGINAL AND SYMMETRICAL SAMPLES**” completed by **SAAD OMRAN ELHASHMI ALLAGWAIL** under the supervision of **ASSIST. PROF. DR. OSMAN SERDAR GEDİK** and we certify that in our opinion it is fully adequate, in scope and in quality, as a thesis for the degree of Ph.D.

Assist. Prof. Dr. Osman Serdar GEDİK

---

Supervisor

Assist. Prof. Dr. Özkan KILIÇ

---

Jury Member

Assis. Prof. Dr. Javad RAHEBI

---

Jury Member

Assist. Prof. Dr. Muhammed BÜLBÜL

---

Jury Member

Assis. Prof. Dr. Elif VURAL

---

Jury Member

Prof. Dr. Ergün ERASLAN

---

Director

Graduate School of Natural and Applied Sciences

I hereby declare that, in this thesis which has been prepared in accordance with the Thesis Writing Manual of Graduate School of Natural and Applied Sciences,

- All data, information and documents are obtained in the framework of academic and ethical rules,
- All information, documents and assessments are presented in accordance with scientific ethics and morals,
- All the materials that have been utilized are fully cited and referenced,
- No change has been made on the utilized materials,
- All the works presented are original,

and in any contrary case of above statements, I accept to renounce all my legal rights.

**Date:** August, 2019    **Signature** :.....

**Name & Surname:** Saad Omran Elhashmi ALLAGWAIL

## **ACKNOWLEDGMENT**

It is a pleasure for me to express my sincere gratitude to my thesis supervisor Assist. Prof. Dr. Osman Serdar GEDİK for his continuous supervision, sharing his experience, encouragement and guidance throughout my study.

Also, I would like to thank the members of my thesis committee, for their support and valuable suggestions that made great contributions to this work.

Finally, the greatest thanks go to my family members for their infinite support. This thesis is dedicated to them.

**2019, August**

**Saad Omran Elhashmi ALLAGWAIL**

# **A NOVEL AND EFFICIENT METHOD FOR FACE RECOGNITION USING ORIGINAL AND SYMMETRICAL SAMPLES**

## **ABSTRACT**

In the practical case of face recognition applications, the human face can have only a limited number of training images. However, it is known that, in general, increasing the number of training images also increases the performance of face recognition systems. In this case, a new set of training samples can be generated from the original samples, using the symmetry property of the face. Although many face recognition methods have been proposed in the literature, a robust face recognition system is still a challenging task. In this thesis, recognition performance is improved by using the property of face symmetry. Moreover, by this way we observe that the effects of illumination and pose variations are reduced. The proposed method has three main stages: preprocessing, feature extraction and classification. A Two-Dimensional Discrete Wavelet Transform with Single-Level, Gaussian Low-Pass Filter and Difference of Gaussian are used, separately, for preprocessing. The Local Binary Pattern, Gray Level Co-Occurrence Matrix, Gabor Filter and Histogram of Oriented Gradients are used for feature extraction, and finally, the Euclidean distance and cosine similarity are used for classification. The proposed method is tested and evaluated using the Olivetti Research Laboratory (ORL), Yale and AR datasets. The proposed method is a new approach for face recognition using symmetry. Also, a new algorithm for feature extraction is proposed and the experimental results show that it is faster than state of the art methods in the literature. The new proposed algorithm can use the benefit of symmetry property either in the image space or in the feature space. This thesis also examines the importance of the preprocessing stage in a face recognition system. The experimental results show that the proposed method has a recognition accuracy rates higher than the state-of-the art methods in the literature.

**Keywords:** face recognition; symmetry; wavelet transform; local binary pattern; gray-level co-occurrence matrix; Gabor; histogram of oriented gradients.

# ORİJİNAL VE SİMETRİK ÖRNEKLERİ KULLANARAK YÜZ TANIMI İÇİN YENİ VE ETKİLİ BİR YÖNTEM

## ÖZ

Pratik yüz tanıma uygulamalarında, insan yüzü yalnızca sınırlı sayıda eğitim görüntüsüne sahip olabilir. Bununla birlikte, genel olarak, eğitim görüntülerinin sayısının artırılmasının, yüz tanıma sistemlerinin performansını da arttırdığı bilinmektedir. Bu durumda, yüzün simetri özelliğini kullanarak orijinal örneklerden yeni bir dizi eğitim örneği üretilebilir. Literatürde birçok yüz tanıma yöntemi önerilmiş olmasına rağmen, gürbüz yüz tanıma hala zor bir problem olarak karşımıza çıkmaktadır. Bu tezde, yüz simetrisi özelliği kullanılarak tanıma performansı artırılmıştır. Ayrıca, bu şekilde aydınlatma ve poz değişikliklerinin etkilerinin azaldığı gözlemlenmiştir. Önerilen yöntemin üç ana aşaması vardır: ön işleme, öznitelik çıkarma ve sınıflandırma. Tek Seviyeli iki-boyutlu ayrık parçacık dönüşümü, alçak geçiren Gauss filtresi ve Gaussların farkı yöntemleri ayrı ayrı ön işleme için kullanılmıştır. Öznitelik çıkarımı için ise yerel ikili örüntü, gri seviye eşzamanlılık matrisi, Gabor filtresi ve yönlendirilmiş gradyanların histogramı kullanılmış ve son olarak Öklid mesafesi ve kosinüs benzerliği sınıflandırma için kullanılmıştır. Önerilen yöntem Olivetti Araştırma Laboratuvarı (ORL), Yale ve AR veri setleri kullanılarak test edilmiş ve değerlendirilmiştir. Önerilen yöntem, simetri kullanarak yüz tanıma için yeni bir yaklaşımdır. Ayrıca, öznitelik çıkarımı için yeni bir algoritma önerilmiş olup deneysel sonuçlar, yöntemin tekniğin bilinen durumundan daha hızlı olduğunu göstermektedir. Önerilen yeni yöntem, simetri özelliğinin avantajını görüntü uzayında veya öznitelik uzayında kullanabilir. Bu tez aynı zamanda ön işleme aşamasının bir yüz tanıma sisteminde önemini incelemektedir. Deneysel sonuçlar, önerilen yöntemin tekniğin bilinen durumuna göre daha yüksek bir tanıma doğruluğu oranına sahip olduğunu göstermektedir.

**Anahtar Kelimeler:** yüz tanıma, simetri, parçacık dönüşümü, yerel ikili örüntü, gri seviye eşzamanlılık matrisi, Gabor, yönlendirilmiş gradyanların histogramı

## CONTENTS

Ph.D. THESIS EXAMINATION RESULT FORM .....	ii
ETHICAL DECLARATION .....	iii
ACKNOWLEDGMENT .....	iv
ABSTRACT .....	v
ÖZ .....	vi
NOMENCLATURE .....	x
LIST OF TABLES .....	xi
LIST OF FIGURES .....	xii

## CHAPTER 1- INTRODUCTION..... 1

1.1 Background .....	1
1.2 Methods Used for Face Recognition .....	4
1.2.1 Holistic Methods .....	4
1.2.2 Local Methods .....	5
1.2.3 Hybrid Methods .....	6
1.3 Proposal Work .....	6
1.4 Contributions .....	8
1.5 Outline .....	9

## CHAPTER 2 - LITERATURE REVIEW..... 10

2.1 Background .....	10
2.2 Face Recognition by PCA .....	15
2.3 The Traditional FR System .....	17
2.3.1 Preprocessing .....	18
2.3.2 Feature Extraction .....	19
2.3.3 Classification (Feature Matching) .....	20
2.4 The Symmetry Property in Nature .....	20
2.5 Face Recognition and Symmetry .....	22
2.6 The Symmetry and the Problem of Small Size Training Samples .....	22
2.7 The Symmetry and the Problem of Illumination Variations .....	23
2.8 The Proposed FR System .....	24

<b>CHAPTER 3 - METHODS AND MATERIALS .....</b>	<b>25</b>
3.1    Preprocessing.....	25
3.1.1    Wavelet Transforms .....	25
3.1.2    Gaussian Low-Pass Filter (GLPF) .....	26
3.1.3    Difference of Gaussians (DoG).....	27
3.2    Feature Extraction Methods .....	27
3.2.1    Feature Extraction Using GLCM .....	27
3.2.2    Feature Extraction Using LBP .....	29
3.2.3    Feature Extraction Using the Gabor Filter .....	31
3.2.4    Feature Extraction Using Histograms of Oriented Gradients (HOG)..	34
3.3    Classification .....	39
3.3.1    Euclidean Distance .....	40
3.3.2    Cosine Similarity.....	40
3.4    Datasets .....	41
3.4.1    The ORL Dataset.....	41
3.4.2    The Yale Dataset .....	42
3.4.3    AR Face Database .....	43
 <b>CHAPTER 4 - EXPERIMENTS AND RESULTS.....</b>	 <b>44</b>
4.1    Generating New Images .....	44
4.2    Experiments on the Original ORL Dataset.....	45
4.3    Experimental Result on the Symmetrical ORL Dataset .....	46
4.4    Using a Preprocessing Stage .....	47
4.5    The GLCM Method .....	48
4.6    Combining Feature Extraction Methods .....	48
4.7    The Gabor Filter Method.....	49
4.8    Other Experiments .....	50
4.9    Experiments on the Yale Dataset .....	51
4.10    Symmetrical and Low-Quality Face Images .....	54
4.11    Experiments on the AR Dataset .....	55
4.11.1    Experimental Results Using All Images in AR Dataset.....	55
4.11.2    Experimental Results: Illumination and Occlusion.....	63
 <b>CHAPTER 5 - SYMMETRY IN FEATURE DOMAIN .....</b>	 <b>68</b>

5.1	Feature Extraction Using Image Stripes (FEIS).....	68
5.1.1	The FEIS Method and Symmetry .....	72
5.1.2	The Symmetry Procedure in the Features Space.....	73
5.1.3	The FEIS Method for Face Recognition .....	75
5.1.4	The Effect of $\lambda$ on Recognition Rates.....	75
5.1.5	Comparing the FR Performance Using the Original Features and the FR Performance Using the Original with Symmetrical Features .....	79
5.1.6	The Speed of the Proposed Method Compared with Other Methods ..	80
5.1.7	The Performance of the FR System Using the Proposed Method Compared with the Other Methods.....	81
<b>CHAPTER 6 - CONCLUSION AND FUTURE WORK .....</b>		<b>84</b>
6.1	Future Directions .....	85
<b>REFERENCES.....</b>		<b>87</b>
<b>CURRICULUM VITAE.....</b>		<b>98</b>

## **NOMENCLATURE**

### **Acronyms**

PCA	Principle Component Analysis
LDA	Linear discriminant analysis
SVD	Singular Value Decomposition
DTCWT	Dual Tree Complex Wavelet Transform
LBP	Local Binary Pattern
DCT	Discrete Cosine Transformation
GLCM	Gray Level Co-Occurrence matrix
WT	Wavelets Transform
DWT	Discrete Wavelet Transformation
GLPF	Gaussian Low Pass Filter
DoG	Difference of Gaussians
SVM	Support Vector Machine
JPEG	Joint Photographic Experts Group
LPP	Locality Preserving Projections
SIC	Symmetrical image correction
BPFF	Bit-plane feature fusion
2DPCA	Two-dimensional PCA
WLDs	Weber Local Descriptors
LRC	Linear regression-based classification
DCT	Discrete Cosine Transformation
ORL	Olivetti Research Laboratory
HOG	Histograms of Oriented Gradients
FEIS	Feature Extraction using Image Stripes

## LIST OF TABLES

<b>Table 4.1</b> The recognition rates of the different methods on the ORL dataset, using the OTS compared with the OSTs.....	51
<b>Table 4.2</b> The recognition rates of the different methods on the Yale dataset, using the OTS and the OSTs.....	52
<b>Table 4.3</b> The recognition rates of the different methods on the AR dataset, using the OTS and the OSTs.....	63
<b>Table 5.1</b> The results using original features with different values of $\lambda$ and different training sample sizes .....	78
<b>Table 5.2</b> The results using original with symmetrical features with different values of $\lambda$ and different training sample sizes .....	79
<b>Table 5.3</b> The speed of the proposed method compared with other methods .....	80
<b>Table 5.4</b> The performance of the proposed method compared with other methods .....	81
<b>Table 5.5</b> The recognition rates of the FEIS method on the ORL dataset compared with the other methods.....	82
<b>Table 5.6</b> The recognition rates of the FEIS method on the Yale dataset compared with the other methods. ....	82
<b>Table 5.7</b> The recognition rates of the FEIS method on the AR dataset compared with the other methods. ....	83

## LIST OF FIGURES

<b>Figure 1.1</b> Enrollment to a biometric system [2].	2
<b>Figure 1.2</b> Authentication with a biometric system [2].	2
<b>Figure 1.3</b> A general framework of face recognition	3
<b>Figure 1.4</b> (a) Holistic face representation, (b) local face representation with salient regions and (c) with partitioning (example face images are from the ORL Dataset) [26].	6
<b>Figure 1.5</b> Face recognition system (example face images are from the Yale Dataset).	7
<b>Figure 2.1</b> The traditional system for face recognition (FR)	18
<b>Figure 2.2</b> The symmetry property in nature	21
<b>Figure 2.3</b> The Symmetry in the human face (example face image is from the Yale Dataset)	22
<b>Figure 2.4</b> Genrating two extra face images form one face image; (a) original face image; (b) first new face image generated from the left side of the face; (c) second new face image generated from the right side of the face (example face images are from the Yale Dataset)	23
<b>Figure 2.5</b> (a) original face image with different distribution of light between the left and right sides of the face; (b) & (c) new generated images with a uniform distribution of light in both sides of the face (example face images are from the Yale Dataset)..	23
<b>Figure 2.6</b> The proposed system for face recognition (FR)	24
<b>Figure 3.1</b> Two-dimensional Discrete Wavelet Transform (DWT) [110].	25
<b>Figure 3.2</b> Gaussian Low-Pass Filter for ( $\sigma = 2$ )	26
<b>Figure 3.3</b> The representation of Gray Level Co-Occurrence Matrix (GLCM) with different angles ( $\theta$ ) and different distances (D) from the pixel of interest [115].	27
<b>Figure 3.4</b> The Local Binary Pattern (LBP) architecture.	30
<b>Figure 3.5</b> Circular (8, 2) neighborhood [117].	30
<b>Figure 3.6</b> Example of a preprocessed face image partitioned into thirty-six windows and its feature histogram using the Local Binary Pattern (LBP).	31
<b>Figure 3.7</b> Different wavelength values: (a) 25; (b) 50 [121].	32
<b>Figure 3.8</b> Different orientation: (a) 0; (b) 45 [121]	32
<b>Figure 3.9</b> Changing the phase shift values: (a) 180; (b) 90 [121]	33
<b>Figure 3.10</b> Aspect ratio: (a) Very large; (b) Very small [121].	33
<b>Figure 3.11</b> Different bandwidth values: (a) Large; (b) Small [121].	34
<b>Figure 3.12</b> The blocks and the cells	36
<b>Figure 3.13</b> The histogram quantization to 9 bins	36

<b>Figure 3.14</b> The HOG interpolation .....	38
<b>Figure 3.15</b> Concatenating the histograms .....	38
<b>Figure 3.16</b> The HOG visualization .....	39
<b>Figure 3.17</b> Sample images from the Olivetti Research Laboratory (ORL) dataset .	42
<b>Figure 3.18</b> Sample images from the Yale face dataset. ....	42
<b>Figure 3.19</b> AR face database .....	43
<b>Figure 4.1</b> (a) Original image; (b) left side; (c) right side; (d) mirror of left side; (e) mirror of right side; (f) integrating left side with mirror; (g) integrating right side with mirror; and (h) Discrete Wavelet Transform (DWT) of the original image in the first level. ....	44
<b>Figure 4.2</b> Recognition rates using LBP with original training sample (LBP-OTS) compared with LBP with original and symmetrical training samples (LBP-OSTS).	46
<b>Figure 4.3</b> Recognition rates using LBP, LBP with Discrete Wavelet Transform (DWT-LBP), LBP with Gaussian Low-Pass filter (GLPF-LBP), and LBP with Difference of Gaussian (DoG-LBP) methods, versus size of the training set of the ORL dataset (OSTS). ....	47
<b>Figure 4.4</b> Recognition rates using the LBP, the Gray Level Co-Occurrence Matrix (GLCM), and the combination of the LBP with the GLCM (LBP-GLCM) methods versus the size of the training set of the ORL dataset (OSTS).....	48
<b>Figure 4.5</b> Recognition rates using different methods: Principal Component Analysis (PCA), Local Binary Pattern (LBP), LBP with Discrete Wavelet Transform (DWT LBP), LBP with Gaussian Low-Pass filter (GLPF-LBP) Gray Level Co-Occurrence Matrix (GLCM), combination of LBP with GLCM (LBP-GLCM), and the Gabor versus size of the training set of the ORL dataset (OSTS). ....	49
<b>Figure 4.6</b> Rates of recognition using different methods: Principal Component Analysis (PCA), Collaborative Representation-Based Classification (CRC), Sparse Representation-Based Classification (SRC), Collaborative Representation-Based Classification Using Symmetry (SCRC), and the Gabor Method Using Original and Symmetrical Training Samples (Gabor-OSTS), versus the size of the training set on the Yale dataset. ....	53
<b>Figure 4.7</b> The accuracy versus compression level on YALE database .....	54
<b>Figure 4.8</b> The recognition rate using LBP with different cell size .....	57
<b>Figure 4.9</b> The recognition rate using LBP with cell size of 8x8.....	58
<b>Figure 4.10</b> The recognition rate using HOG for OTS and OSTs .....	59
<b>Figure 4.11</b> The recognition rate using Gabor Filter.....	60
<b>Figure 4.12</b> The recognition rate using LBP with cell size of 8x8, HOG, and Gabor with OSTs .....	61
<b>Figure 4.13</b> Illumination difference. (a) normal illumination. (b) high illumination. (c) and (d) variations in illumination. (Example images from AR dataset) .....	64

<b>Figure 4.14</b> The recognition rate using LBP 8x8, Gabor and HOG using images of illumination form AR dataset.....	64
<b>Figure 4.15</b> The recognition rate using LBP 8x8, Gabor and HOG using images of occlusion (sunglasses) form AR dataset .....	65
<b>Figure 4.16</b> The recognition rate using LBP 8x8, Gabor and HOG using images of occlusion (scarf) form AR dataset.....	66
<b>Figure 5.1</b> An example of an image .....	69
<b>Figure 5.2</b> An example of extracted features for different values of $\lambda$ .....	70
<b>Figure 5.3</b> The original image (a), and its stripes (b), (Example image from ORL dataset) .....	71
<b>Figure 5.4</b> Features example for an image from ORL dataset .....	71
<b>Figure 5.5</b> Different sets of features using different values of $\lambda$ .....	72
<b>Figure 5.6</b> Original image, b) left side, c) right side, d) mirror of left side, e) mirror of right side, f) integrating left side with mirror, g) integrating right side with mirror..	72
<b>Figure 5.7</b> The symmetry procedure in the image space.....	73
<b>Figure 5.8</b> The symmetry procedure in the features space.....	74
<b>Figure 5.9</b> The features of the original image (parent) .....	74
<b>Figure 5.10</b> Generating the symmetrical features (children) from the original features (parent) .....	75
<b>Figure 5.11</b> Recognition rates vs size of training set for different values of $\lambda$ using original features.....	76
<b>Figure 5.12</b> Recognition rates vs size of training set for different values of $\lambda$ using original with symmetrical features .....	76
<b>Figure 5.13</b> Recognition rates vs $\lambda$ for different sizes of training set using original features .....	77
<b>Figure 5.14</b> Recognition rates vs $\lambda$ for different sizes of training set using original with symmetrical features .....	78
<b>Figure 5.15</b> The FR performance using the original features and the FR performance using the original with symmetrical features for different values of $\lambda$ .....	79
<b>Figure 5.16</b> A 112x92 image from ORL dataset used for speed test .....	80
<b>Figure 5.17</b> The speed of the proposed method compared with other methods.....	80

# CHAPTER 1

## INTRODUCTION

### 1.1 Background

With the development of the computers and computer-based systems, their application areas for computer vision-based systems have been increased based on demand for the daily life, and hence computers ease our daily life and change it day by day. One of the important demands for the computer-based systems is face detection and recognition for security systems.

Humans are identified by their physiological, behavioral and biological properties by biometrics. Biometrics are divided into two categories: physiological biometrics, which include the identification of individuals by physiological and biological characteristics such as face, fingerprint, iris, eye, etc. The second category is the behavioral biometrics, which include the identification of individuals through human situations such as handwriting, signature, walking, etc. [1].

The enrollment to a biometric system is achieved by capturing the biometric data using a biometric device, then storing the extracted information in an enrollment templates and finally, the template is stored in the database as shown in **Figure 1.1**.

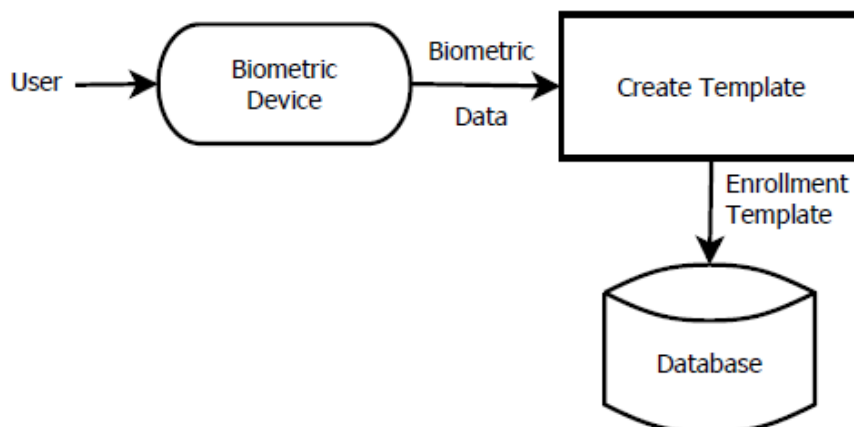


**Figure 1.1** Enrollment to a biometric system [2].

On the other hand, the Authentication with a biometric system is achieved by capturing the biometric data by a biometric device, then storing the extracted information in an enrollment templates and finally the templated is compared to the one in the database [2], as shown in **Figure 1.2**.

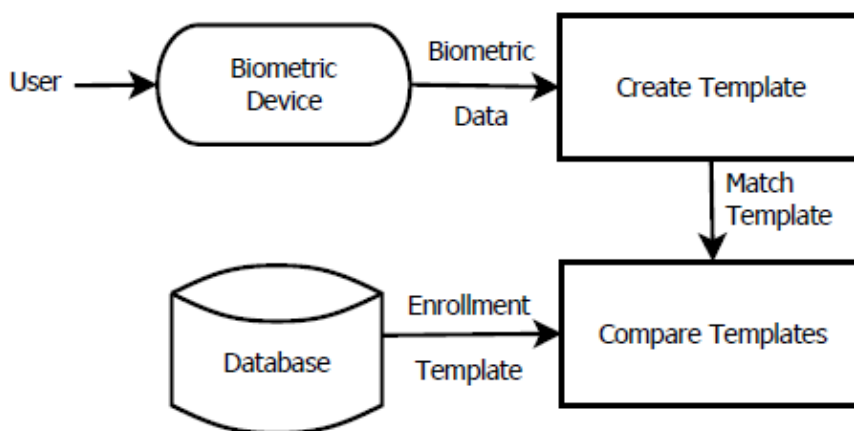


**Figure 1.2** Authentication with a biometric system [2]

A general framework of face recognition is shown in **Figure 1.3**.

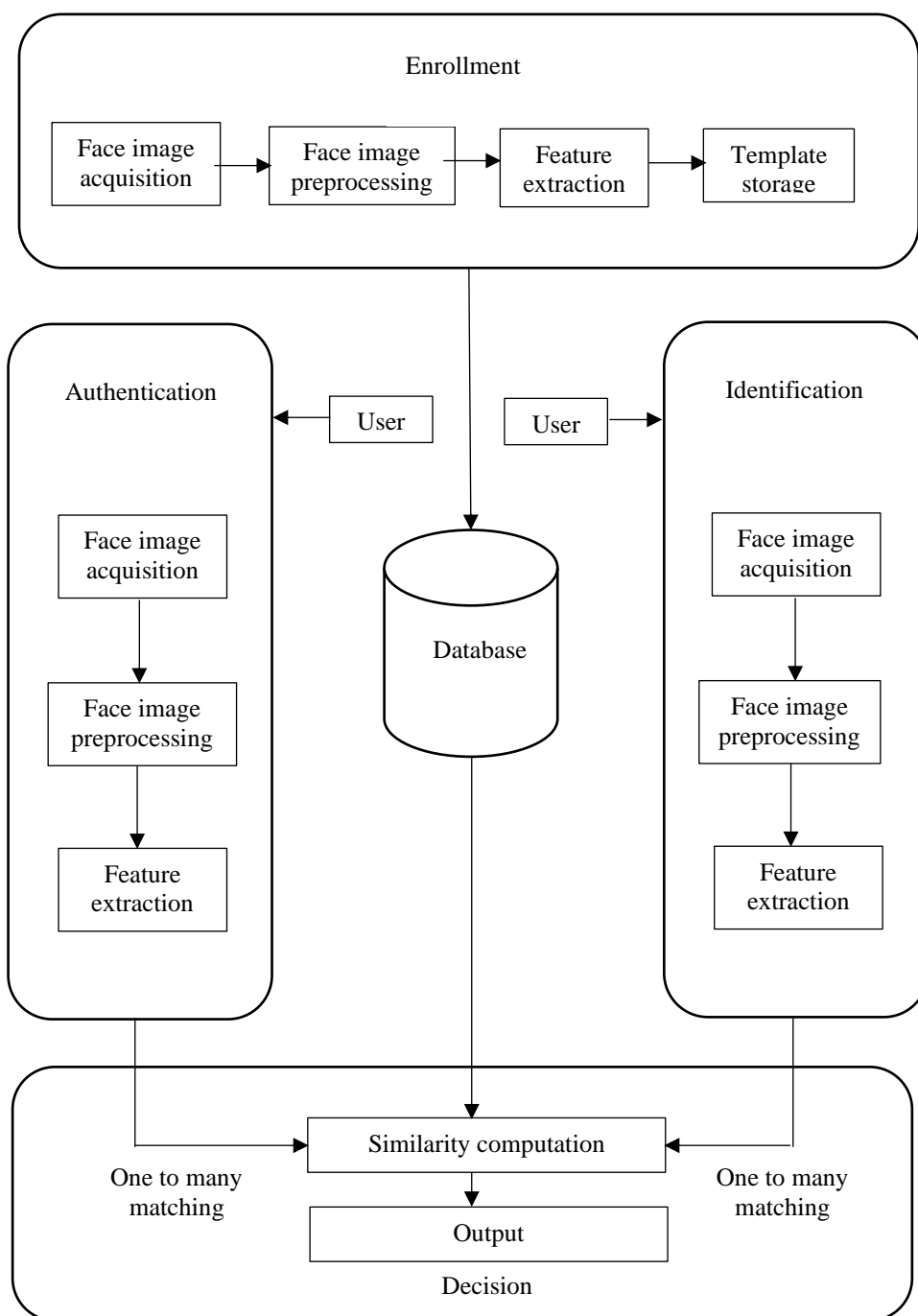


**Figure 1.3** A general framework of face recognition

Robust and accurate face recognition (FR) is one of the most important problems in computer vision applications. In literature, there are several methods used for FR, including holistic, local, and hybrid methods [3, 4]. However, recent research has revealed that a symmetry-based approach for FR is a useful method to increase the

performance of the FR system; thus, it is possible to realize FR using the property of face symmetry [5, 6].

There are many methods can be used to extract the features from the face images such as: the Local Binary Pattern (LBP) [7-9], the Gray Level Co-Occurrence Matrix (GLCM) [10], and the Gabor Filter [11], since these methods performed well for a texture feature extraction that could be used for the FR [12-14].

Moreover, any two methods from the list could be combined [11, 15], such as for instance LBP with GLCM, in order to make the feature extraction operation more robust.

Also, the images of the face can be enhanced, before extracting their features. This enhancement operation is accomplished by a preprocessing step using well-known techniques, namely the Gaussian low-pass filter (GLPF) [16], Difference of Gaussian (DoG) [17], and the Discrete Wavelet Transform (DWT) [18].

There are some benchmark facial datasets that are widely used to test the performance of the FR methods [5, 19, 20] such as: Olivetti Research Laboratory (ORL) [21], Yale [22] and AR datasets [6, 23, 24].

## **1.2 Methods Used for Face Recognition**

Although there are many image processing methods, only some of them are able to solve face recognition problem [25]. These methods are classified, for face representation, to three main types: the global-based face representation approaches that use holistic characteristics of the face (Holistic Methods), the local-based face representation methods (Local Methods) and finally, the hybrid approaches that use and combine holistic and local methods (Hybrid Methods).[26]

### **1.2.1 Holistic methods**

Holistic (or global) face recognition is based on using the entire region of the face for recognition [27]. There are many methods proposed, for instance, Principle Component Analysis (PCA) [28], which is also called as Eigen faces [29], Linear

Discriminant Analysis (LDA) [30]. The two most popular methods are eigenfaces [31], and Fisherfaces [32].

#### ***1.2.1.1 Eigenfaces***

The eigenfaces approach is the most well-known face recognition algorithm [31], it is based on principal components analysis (PCA) [27]. Eigenfaces is a subspace projection face recognition method, which is based on reduction from high-dimensional data in the original image to a low-dimensional face space. This technique returns a set of orthogonal basis vectors. Each training image and testing image is then projected into the ‘face space’ and the vectors of the test image is classified as the most likely to the vectors of the training images [27].

#### ***1.2.1.2 Fisherfaces***

Fisherfaces is another well-known face recognition approach, it is the use of linear discriminant analysis (LDA) to face recognition [32]. In eigenfaces, the variance between vectors is used to find a linear subspace for projection, without taking into consideration the class associations of each training vector [27].

### **1.2.2 Local methods**

Face recognition based on local facial regions has attracted a significant amount of interest because local features are believed to be more robust to the variations of facial expression, illumination and occlusions [26]. Local methods provide additional flexibility to recognize a face based on its parts, thus the common and class-specific features can be easily identified [4]. The local methods use various descriptions of the face for recognition, for example, purely geometric approaches that uses the distances and ratios of distances between landmarks on the face (such as corners of the eyes and mouth) [27]. There are many method use local facial regions, for instance, Elastic Bunch Graph Matching (EBGM) [33], Local Binary Patterns [11, 34] and Gray Level Co-occurrence Matrix [10].

Approaches that utilize local regions either use salient regions or they just partition the face image into rectangular blocks.

**Figure 1.4** shows an example for holistic and local face representations.

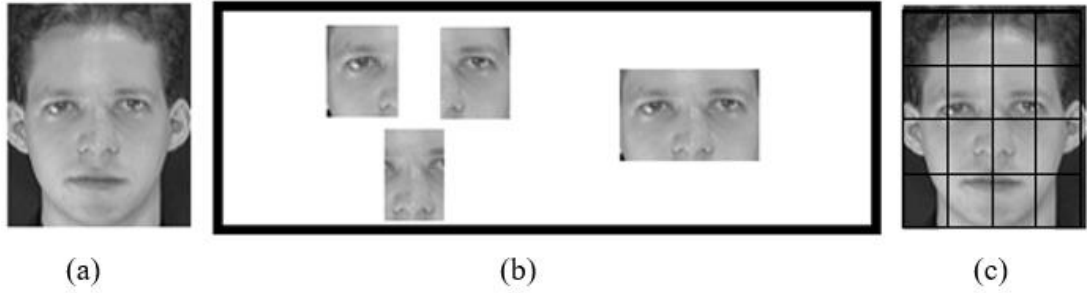


**Figure 1.4** (a) Holistic face representation, (b) local face representation with salient regions and (c) with partitioning (example face images are from the ORL Dataset) [26].

### 1.2.3 Hybrid methods

Since singular approaches cannot give a sufficient solution to the face recognition problem, researchers have had a tendency to combine both holistic and local techniques to improve the recognition performance. These approaches are called hybrid approaches. There are many approaches that use both holistic and local features, for instance, Gabor filters, that are used for extraction of the global and local facial features. When the global features represented are not clear, the local features are combined and fused to form a feature vector to be used as a face descriptor for recognition [35]. The modular eigenface approach is another approach that uses both global eigenfaces and local eigenfeatures [36] [37].

## 1.3 Proposal work

The property of face symmetry is useful for solving two main problems in FR that are still prevalent—the limited number of face training samples and the variations in poses and facial expressions, in addition to the lighting conditions. The proposed method uses the property of face symmetry to reduce the effect of these two problems.

In this thesis, we have implemented a face recognition system based on the original and symmetrical samples of the face images, however, our study is concerned with the case of aligned faces. We use DWT based on LBP (which is a new approach for symmetrical face databases), where we use DWT for compression of symmetrical face

training data, and we extract the features from the face images using LBP. The proposed face recognition system is developed and used for different aims. Furthermore, we try to improve the accuracy of the results. The proposed FR system has three main stages: Preprocessing, Feature Extraction, and Classification, as shown in **Figure 1.5**.

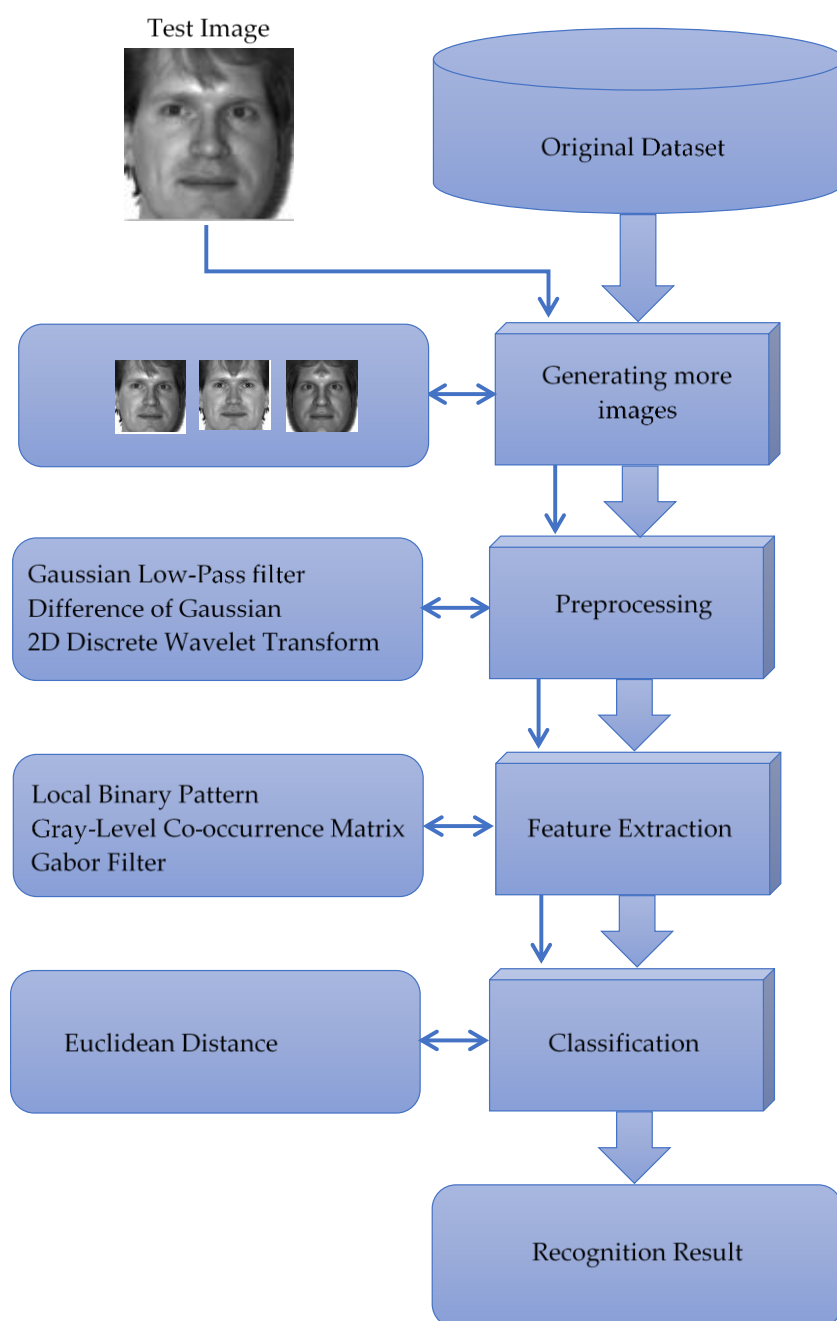


**Figure 1.5** Face recognition system (example face images are from the Yale Dataset).

The preprocessing stage is used to enhance the face images before extracting their features. Accordingly, the GLPF, DoG and the Two-Dimensional Discrete Wavelet Transform (2-D DWT), are used, separately, in this stage.

Also, the LBP, GLCM, Gabor Filter and Histogram of oriented gradients (HOG) are used in the second stage, feature extraction stage, to extract the feature of the face images.

And finally, we use the Euclidean Distance and the Cosine similarity classifiers in the final stage, the classification stage.

The proposed method is analyzed and examined using three benchmark facial datasets, namely the ORL, Yale and AR datasets.

## **1.4 Contributions**

Although there exist many methods using the symmetry property of the face for face detection, the use of this property for face recognition is limited to one algorithm. In this thesis, we propose a method to use the benefit of this property for face recognition. In addition, the idea is generalized using many algorithms, moreover it is examined using a number of benchmark facial datasets.

This thesis confirms that the use of the symmetry property of the face is very useful in the case of low-quality face images.

After proving that the use of symmetry property of the face boosts the performance of the existing feature extraction methods, a new feature extraction algorithm, based on the symmetry property, is proposed. This algorithm is the first algorithm that can benefit from the symmetry property of the face in the feature space. As the existing algorithms can use the symmetry property of the face only in the image space, and this is the main contribution of this thesis.

The mechanism of the newly proposed algorithm makes it faster than the existing feature extraction algorithms.

## 1.5 Outline

In this thesis, we present an overview of the face recognition issue, the associated problems and the proposed solutions. The methodology can be utilized for recognition under a limited number of training samples, in addition, the illumination and pose variations. The organization of this thesis is explained as follows:

Chapter 1 is devoted to explaining a general background and the methods that are used for face recognition, in addition of proposal work, the contributions and the outline of this thesis.

Chapter 2 presents the literature review, the difference between the traditional and the proposed face recognition system and the stages of the face recognition procedure, also, we address the symmetry property in nature including human faces and the idea of summery property to overcome the limited training samples and the illumination and pose variation problems.

Chapter 3 explains a variety of methods and materials that are used for the different stages of the face recognition system, in addition to a number of datasets that are used for measuring the performance of the face recognition system.

Chapter 4 includes the carried-out experiments and the obtained results using different scenarios.

In Chapter 5, we propose a new algorithm for feature extraction for face recognition, and its advantages over the existing algorithms for symmetry purposes.

Finally, in Chapter 6, we present the conclusions and future work of this thesis.

# CHAPTER 2

## LITERATURE REVIEW

### 2.1 Background

Face recognition (FR) is a biometric technique that belongs to biometrics, which uses physiological characteristics such as (the face, fingerprint, eye, etc.), and anatomy characteristics such as (signature, walking, etc.). These characteristics are special for each person to identify the identity of individuals and available to all people, unique to each person, and are permanent and difficult to emulate or falsify, unlike other traditional techniques such as passwords and identity cards that can be stolen or used fraudulently by others [38].

For the human brain, face recognition is considered as a high-level visual work where a person can detect and identify faces in a scene in an easy way, on another hand, developing a computer system that performs these tasks is a major challenge that hides many complex processes. This challenge becomes even greater because of some factors that may hinder facial recognition, especially when the conditions for getting a facial image are inappropriate and uncontrollable. There are two types of facial differences: one resulting from the physical similarity between individuals and this type is generally limited. By contrast, the changes in the person itself are much greater and can be attributed to several factors: facial expressions, lighting conditions, etc., which may cause the face recognition system to fail. In general, several scientific researchers have tried to solve these problems, but they are not perfect yet [39].

The face, certainly, is a biological characteristic used by humans to identify and know each other. The purpose of designing a face recognition system is to simulate the human recognition system and has been extensively studied [40, 41]. However, these studies are not effective in the case of a problem of small sample size, and thus the results are still modest, this study presents a solution to this problem.

Some studies have shown that the human visual system is more sensitive to changes in the low-frequency band. Some research has suggested that the techniques implemented in the low-frequency have improved the efficiency of facial recognition [42] which led this study to use some techniques related to low-frequency.

Researchers are also focusing on developing techniques to improve the efficiency of facial recognition systems or in developing techniques to reduce processing time and calculations. Thus, the balance between system efficiency and the processing time is important in this area, this study takes care of this issue.

Robust and accurate FR is among the most important and well-studied problems in computer vision [43]. However, illumination and pose variations are still some open problems that need to be solved. Facial images are taken in environments that are usually not under control, which contain variations in viewpoint and illumination; therefore, these two factors play a vital role in the efficiency of recognition. Developing an algorithm that can handle variations in illumination, pose, facial expression, and occlusion, etc., altogether, still seems to be a very challenging task.

There are many studies related to FR, such as the authors of [44], who have presented a robust method for FR, using a sparse representation-based classification (SRC). Although the results are good, the method had a high computational cost. Zhang et al. in [45] proposed an SRC-based classification algorithm, based on the Gabor feature, by combining the features from SRC and Gabor. Furthermore, they succeeded in reducing the complexity of computation and improving the FR rate. Mairal et al. [46] added a new step to SRC for signals, by successfully using their method to recognize a handwritten digit and to classify the textures. In [47], the authors mapped the facial images to the so-called face subspace. Here, Locality Preserving Projections (LPP) are used to calculate a basis set, called Laplacian Faces. Linear Discriminant Analysis (LDA) has been used in [32] to construct a subspace on which the inter-person variance is optimally large, while the intra-person variance is efficiently small. The main disadvantage of this technique, the same as that of Principal Component Analysis (PCA) [48], is the data-space Euclidean consideration, since the method fails when data points lie in a nonlinear subspace, which is usually true with multimodally distributed facial images.

Although there exists many studies [17, 49, 50] on invariant representations for handling certain variations, apparently, a generic approach to model different variations at once, has not yet come to light. It has been known for a long time that feature-based methods, such as elastic bunch graph matching, are promisingly successful against many factors, including variations of illumination and viewpoint [51]. Nevertheless, their extreme sensitivity to feature extraction and the measurement of extracted features makes them unreliable [52]. Many authors have studied the effect of variations in illumination conditions on FR [17, 50, 52-55]. As a result, appearance-based methods have dominated the literature.

FR with LBP has been proposed by Ahonen et al. [9], in which the algorithm is not sensitive to light, and accordingly, this point is considered to be the robustness of their study. The authors of [56] used discriminative dictionary learning and SRC, along with the Gabor filter bank and the LBP, for feature extraction, and reduced the influences of illumination changes. One of the milestones for FR under variations, could be stated as the Fisherfaces and Eigenfaces [32] technique, which is insensitive to illumination variations. A good improvement has been recommended in [57], in which local linear transformations are used instead of one global transformation. Although the technique suggests different mapping functions for different pose classes, it could not treat the case of critical variations. Facial images with different poses, facial expressions, and illumination conditions are studied and the performances of the recognition are shown to be higher, compared to the Fisherfaces or Eigenfaces [58].

Pose variation has also been studied in [59], by using view-based Eigenfaces. For each view, Eigenfaces are calculated and applied as separate transformations into a standard lower-dimensional subspace. The authors in [60] introduced Eigen features, in which a feature-based scheme is incorporated. In fact, their performance highly depended on discretization, where the Eigen light-field technique is used to define the subspace of poses. Moreover, uncommon poses could be treated by this technique.

The authors of [61] combined the generalized photometric stereo and Eigen light field concept to generate a generic method which is also insensitive to illumination changes. The authors of [62] presented a method to arrange the variation of poses and illumination, including shadows and reflections; however, the computational cost in

their method decreased the efficiency of the recognition system, since they generated 3D models from 2D images.

Shashua et al. proposed a method in [53], based on the illumination invariant signature image, since they showed that it is possible, even in bad conditions, to use a small dataset to generate more images with varying illumination. However, their method is not appropriate when the images included some shadows. Then, Zhou et al. in [54] reduced the effect of the shadow issued, by utilizing extra limitations on the albedo.

Georghiades et al. showed that in [52], when the pose is fixed, all possibilities of illumination in the image space had a convex cone. In addition, they used their method to reconstruct the shape and albedo of the face by training the system using only a few images, with different directions of light. The authors proved in [63] that all possible illumination variations are accomplished using only a nine-dimensional linear subspace, by using spherical harmonics. The authors of [64] examined different illumination conditions and also hypothetically analyzed the subspace for images of a convex Lambertian object.

The authors of [65] proposed a nonlinear subspace approach using the tensor representation of faces in different cases, including facial expressions, illuminations, and poses, since they used the  $n$  mode tensor Singular Value Decomposition (SVD), to generate an image base. Even though this technique gave good results, it still requires several images under different variations, for each training identity.

Another nonlinear subspace analysis has been proposed in [66], using the manifold assumption in which a gallery manifold for each identity is stored in the database. To define a test identity with several new poses, first its probe manifold is constructed, by its identity being defined using a manifold-to-manifold distance. The method is fairly good, but the necessity for various images of the test person, could be considered a disadvantage.

In [67], the illumination invariance is analyzed, using a ridge regression technique to overcome the matrix inversion that is required in the symmetric bilinear model. The authors of [68] introduced a modified asymmetric model to overcome pose variations.

However, the performance of their method is affected by the discretization resolution of the pose space.

Kusuma and Chua proposed an investigation about the use of image recombination for face recognition. They combined 2D and 3D face recognition methods by using the maximum amount of variance in images and finding the axis transformation of data of distinctive facial expressions of 2D and 3D images. The results of using image pixel recombination or other face recognition systems based on score level fusion showed good performance [69]. Also, they proposed image at the level of dependency between modalities in image recombination for face recognition. They again combined 2D and 3D face recognition methods, and results are useful as in their research a year before [69].

Abeer et al examined multi-linear neighborhood preserving projection for face recognition. They proposed a novel method of supervised and unsupervised multi-linear neighborhood preserving projection for face recognition. They determined the number of subspaces derived by the method using the order of the tensor space. The performance of the supposed method in the research is analyzed using ORL, AR and FERET face datasets. The results of the study showed that the MNPP outperforms the standard approaches in terms of the error rate [70].

Banerjee et al proposed a frequency domain nonlinear correlation technique for face recognition under varying lighting conditions. Their technique is based on phase correlation between an optimum projecting image correlation filter and an optimum reconstructed image correlation filter. The improvement in performance is achieved by exploiting point wise nonlinearities of image pixels. They also suggested that, by minimizing the energy at the correlation plane while maximizing the correlation peak would lead to more optimization. The proposed scheme is analyzed using standard face data bases, it shows that the performance is improved compared with other standard unconstrained correlation filters [71].

Givens et al examined biometric performance evaluation for the face recognition using statistical methods. Statistical reasoning has been applied predominantly in the design of recognition algorithms. One of the approaches seeks to identity, compares and

interprets how characteristics of subjects. Another approach is illustrated with generalized linear mixed model analysis of some challenging face datasets. Although some of face recognition algorithms suffering from familiar statistical ideas in multivariate statistics, dimension reduction, classification, etc. the field presents some unique features and challenges [72].

Li et al developed a method for face recognition using multi-scale Weber Local Descriptors (WLDs) and multi-level information fusion. In their research, they introduce a method including four steps as follows [73]:

1. Image partition
2. Feature extraction
3. Features measurement
4. Voting

Their suggested model and its results showed effectiveness upon three popular data sets.

Luan et al examined face recognition with contiguous occlusion using linear regression and level set methods. They proposed a novel method for face recognition against contiguous occlusion without using partition scheme. The idea behind this is to eliminate the impact of occlusions on the linear regression-based classification (LRC) method. In their approach, they analyzed that error image derived from the LRC is a better choice than original image for identifying occluded regions. they presented how to effectively use the spatial continuity of corrupted pixels to determine the occluded regions. Their results show the efficacy of the proposed approach against different types of occlusion [74].

## **2.2 Face recognition by PCA**

Although there are many researches on face recognition and PCA method, there have been restricted researches on face recognition using PCA method. In this part of the

study, some of important researches focusing on face recognition using PCA have been mentioned.

Zhou et al examined the use of PCA and Linear Discriminant Analysis (LDA) for face recognition. They suggested to use the inner-classes covariance matrix for feature extraction as generating matrix, and eigenvectors from each person obtained. Afterwards, they obtained reconstructed images. The suggested method is effective on ORL face database [75].

Wang et al proposed novel generalized PCA based face recognition algorithm. They improved symmetrical image correction (SIC) and bit-plane feature fusion (BPFF) in order to improve the illumination robustness of the algorithm. Afterwards, they applied Generalized PCA to the virtual faces to achieve face recognition. Results of the illustration showed that, combined approach to face recognition algorithm is effective to reduce the differences in sensitivity [76].

Hsieh and Tung developed a new hybrid approach depending on sub-pattern technique and whitened PCA for face recognition. In their research, they combined sub-pattern technique with PCA I and PCA II respectively for the face recognition. The study showed that sub-pattern technique is useful for PCA I, but not useful for PCA II and PCA. Afterwards, they combined PCA II and Sp-PCA I for face recognition. The results of the experiments showed that the proposed approach gives more sophisticated recognition performance than that obtained using other traditional methods [77].

Luh and Lin proposed a face recognition method with help of artificial immune networks based on PCA. They optimized antibodies of the immune networks using genetic algorithms. The results of their study showed that proposed method have better recognition rate in contrast with most of the developed methods [78].

Oh et al proposed one of the functional components of general face recognition system based polynomial radial basis function neural networks. Their system consisted of preprocessing and recognition module. They presented efficiency of PCA-LDA combined algorithm compared with other algorithms such as PCA, LPP, 2D-PCA and 2D-LPP [79].

Zhang and Zhou proposed an alternative two-dimensional PCA (2DPCA) for efficient face representation and recognition which is working in the column direction of images. They developed the two-directional 2DPCA. Experimental results on ORL and subset of FERET face datasets showed that their method achieves the same or even higher recognition accuracy than 2DPCA [80].

Tan and Chen examined adaptively weighted sub-pattern PCA for face recognition. Their method operated directly on sub-pattern of the image that partitioned from the original whole pattern of the image. Also, their method can adaptively compute the contributions of each part and then endows them to a classification task in order to improve the robustness of the system for both expression and illumination variations. Experiments on three standard face databases show that their method is competitive [81].

Authors of recent researches use deep learning methods to solve the problem of face recognition as stated in [82-87], although these methods give good results, they require a lot of computation and consuming a lot of time, in addition, they need to use a large amount of data [88], which make them unsuitable for the FR systems that require to give fast results.

Authors in [89] present a deep learning framework and evaluate residual nets on the ImageNet dataset, they show that the results won the 1<sup>st</sup> place on the ILSVRC 2015 classification task.

### **2.3 The traditional FR system**

The traditional FR system is normally consisting of three main stages, these stages are: The preprocessing stage, the feature extraction stage and the classification stage, as shown in **Figure 2.1**. However, the first stage, the preprocessing stage, in some system is not used.

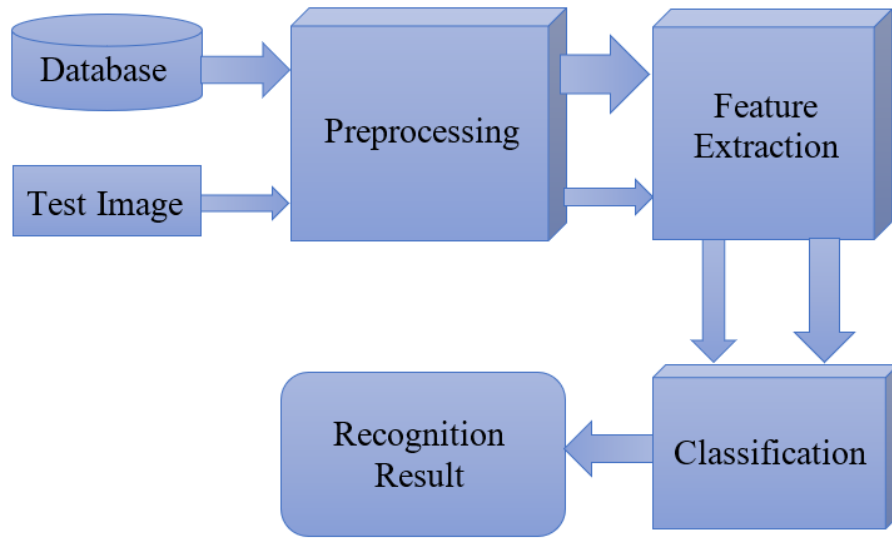


**Figure 2.1** The traditional system for face recognition (FR)

### 2.3.1 Preprocessing

The preprocessing step stabilizes and prepares the input for feature extraction step so that good features can be extracted from the image [90].

Face image preprocessing includes different processes depending on the application, like alignment (translation, rotation, scaling), illumination normalization, and illumination correlation. And accordingly, an ideal preprocessing is supposed to eliminate the irrelevant information (e.g., illumination, background) [11].

The preprocessing step is used by many authors in their studies [7, 11, 17, 91], since they use many different techniques such as the authors in [92] present a wavelet-based illumination invariant algorithm as a preprocessing technique for face recognition. In their study, they show that wavelet multiresolution analysis is promising for illumination normalization because the illumination component resides in the wavelet approximation coefficient; this can be removed easily by setting the approximation sub band to zero values. Wavelet transform is also presented in [18], where the authors suggest a new pattern recognition framework for face recognition based on the combination of Radon and wavelet transforms (WT). They also show that it is invariant to variations in facial expressions and illumination. More details are in section 3.1.1.

Also, the Gaussian low-pass filter is used as in [93], where the authors suggest blurring the face image and the reference face image by a Gaussian filter improves the recognition rates, as in section 3.1.2. In addition, the authors in [17] use the Difference of Gaussian (DOG) to enhance the image and to eliminate the shadowing effects hence reducing the light variations effect. Moreover, the authors also in [17], state that using gamma correction enhance the local dynamic range of the image in dark or shadowed regions while compressing it in bright regions and this solve the problem of lighting variations of real capture system. The preprocessing methods are explained in section 3.1.

### **2.3.2 Feature Extraction**

The feature extraction's goal is to extract relevant features from a face image. However, extracting information from the image is easy for a human but it is a very challenging task for computer vision [94].

There exist many algorithms that are used for feature extraction including Local Binary Pattern (LBP) as in [7] where the authors stated that the LBP have emerged as one of the most prominent local texture descriptors. Moreover, the LBP is most widely used in face recognition because of its unique feature and less computation time [94].

In addition, the authors of [10] propose a use of Gray Level Co-occurrence Matrix (GLCM) to achieve a high texture classification accuracy. In their method, they calculate the GLCM of each sub-image and they use the statistical values to construct the final feature vector.

Moreover, the Gabor filter is used for feature extraction as in [14] where the authors state that the Gabor filtering, in recent years, has emerged as one of the most popular among various approaches to texture feature extraction. In their paper, they use the Gabor filter to improve the performance of texture classification.

The feature extraction methods are explained in more details in section 3.2.

### 2.3.3 Classification (Feature Matching)

The classification step is the last and actual recognition process. It is used to match the feature vector of the test image that is obtained from the feature extraction step with the feature vectors of the train images which are already stored in a database.

There are many techniques that are used for classification [95] and they vary from the Euclidean Distance [20], K-Nearest Neighbor [94], Support Vector Machine (SVM) [30] to advanced algorithms like Neural Networks [96, 97]. More details are in section 3.3.

## 2.4 The symmetry property in nature

Symmetry is a natural characteristic that can exist in by many objects, including natural objects such as human, tree leaves insects and crystals, etc., and non-natural objects such as geometric shapes and mathematical equations, etc., as shown in **Figure 2.2**. This has made many authors notice its important role [98, 99].

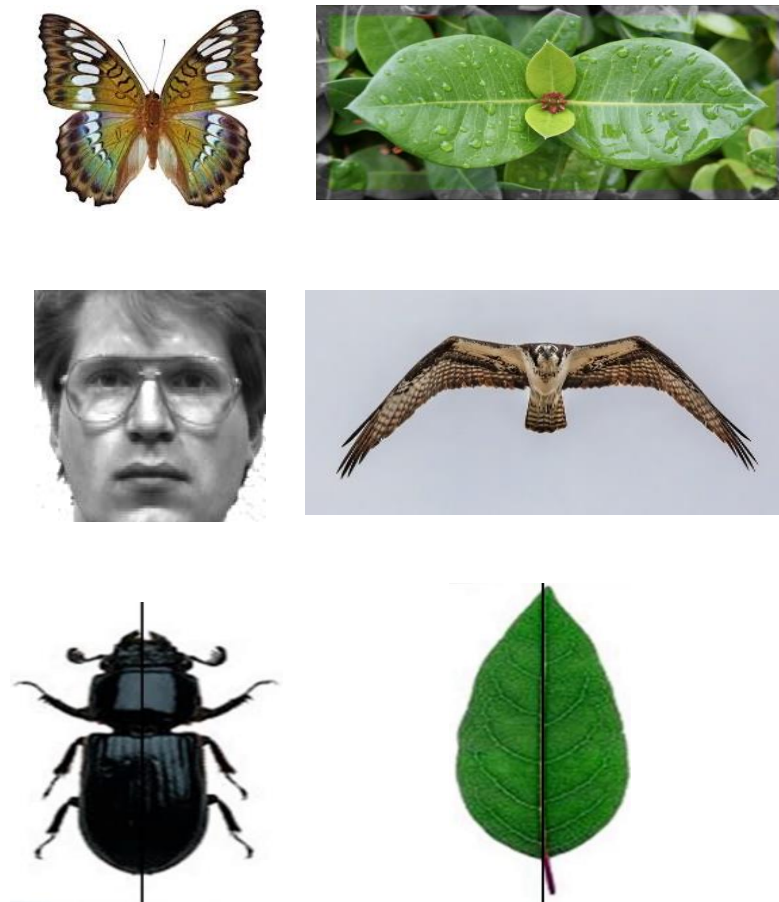


**Figure 2.2** The symmetry property in nature

In general, the object is considered to be a symmetrical to some operation if this operation does not have any effect of a change on that object. The operation could be a rotation, or a reflection or some type of a transformation. So, the symmetry is defined scientifically as "a transformation that leaves an object unchanged" [100, 101].

Some types of symmetry are so familiar, that sometimes cannot be noticed. The mirror is a famous example of one of the symmetry-creating tools, which turns the sides of the objects so that the right side is left, and the left side is right.

The process of discrimination becomes easier when the left and right sides of the object are radically different. But symmetry in biology and especially in humans is so sophisticated that it is difficult to see such differences, thus this encourages the authors to study and use it to improve the face recognition techniques.

## 2.5 Face Recognition and Symmetry

One of the most important properties in nature, and particularly in human faces, is that of symmetry. It has been observed that the human face is almost symmetrical, as shown in **Figure 2.3**, so the use of this property for face detection (FD) has been previously studied [102], where the authors have developed a technique to automatically compute bilateral symmetry axis and use it in their research.



**Figure 2.3** The Symmetry in the human face (example face image is from the Yale Dataset)

Zhao and Chellappa in [103] used the symmetry of the face to reduce the effects of illumination in FD. It has been shown that symmetry is also useful for extracting the facial profile in facial recognition techniques [104, 105]. The authors of [106] successfully applied the symmetry property to FD, and they concluded that the expressions of the face are also symmetrical.

## 2.6 The symmetry and the problem of small size training samples

The main idea behind using the symmetry property of the face is to increase the limited size of the training samples by generating more images from the original images as shown in **Figure 2.4**. These generated images are used along with the original images to train the FR system.

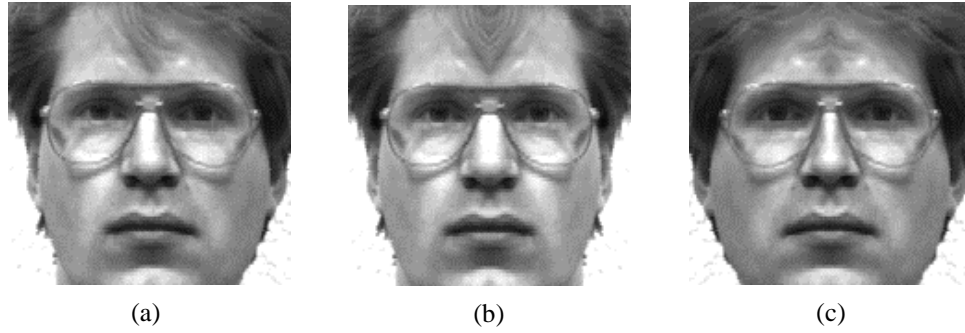


**Figure 2.4** Generating two extra face images from one face image; (a) original face image; (b) first new face image generated from the left side of the face; (c) second new face image generated from the right side of the face (example face images are from the Yale Dataset)

## 2.7 The Symmetry and the problem of illumination variations

The new generated images have a very interesting characteristic property which is a uniform distribution in lighting in both sides of the face, as shown in **Figure 2.5**. This property makes the system work better than if there is a difference in lighting between the two sides of the face.

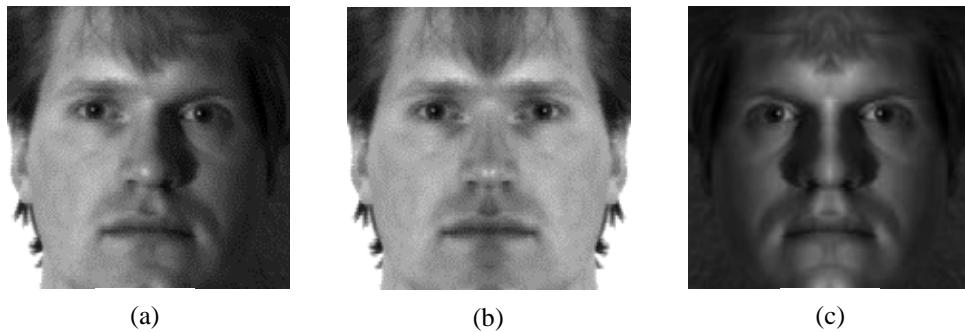


**Figure 2.5** (a) original face image with different distribution of light between the left and right sides of the face; (b) & (c) new generated images with a uniform distribution of light in both sides of the face (example face images are from the Yale Dataset)

The face recognition algorithms suffer from these two problems, the limited number of training samples and the variations in poses and expressions as well as illumination conditions. Although there are several proposed methods trying to overcome these problems, these problems are still considered as open problems yet. One of the recent methods has been proposed by Yong et al [107]; in their paper, they used dictionary

learning algorithms for face recognition, and because the conventional dictionary learning algorithms suffer from the mentioned problems, they proposed a novel dictionary learning framework to obtain a robust dictionary for face recognition. In their algorithm, they first produce virtual face images and then designs an elaborate objective function. Based on this objective function, they obtained a mathematically tractable and computationally efficient algorithm to generate a robust dictionary. Also, a recent method has been proposed by the authors of [5, 6], wherein, they improve the rate of FR recognition accuracy by using the symmetry property of the face, to using Symmetry for Collaborative Representation-Based Classification (SCRC). This thesis presents a solution for these problems by proposing a FR system based on using the benefits of facial symmetry.

## 2.8 The proposed FR system

The proposed FR system contains an additional stage compared to the traditional FR system as shown in **Figure 2.6**. This stage generates a new set of images, for training, from the original images, using the face symmetry property, which increases the limited size of the training samples, also, the new generated images have a very useful advantage over the original images in case of illumination and pose variations as explained in the last section. These benefits increase the ability of the FR system to improve the accuracy of facial recognition.

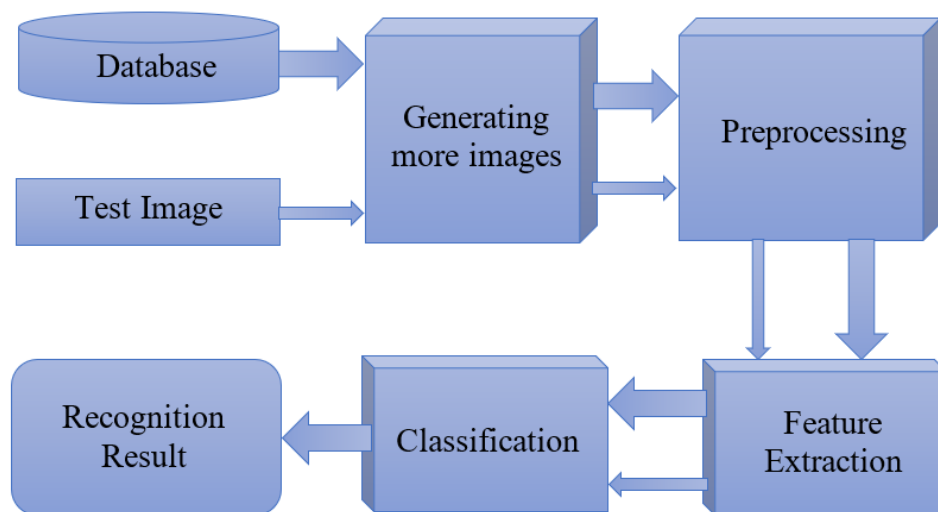


**Figure 2.6** The proposed system for face recognition (FR)

# CHAPTER 3

## METHODS AND MATERIALS

In this thesis, many methods are implemented, these methods including the preprocessing methods such as GLPF, DoG and DWT. Also, the Feature extraction methods such as GLCM, LBP, Gabor Filter and HOG and finally, the classification methods such as euclidean distance and cosine similarity.

### 3.1 Preprocessing

#### 3.1.1 Wavelet Transforms

Wavelet transforms are selected for preprocessing, since they examine images in a time–frequency localization, which helps to implement many methods, based on the wavelet for image processing [108]. The wavelet transform is invariant to variations in illumination and facial expressions as stated in [18]. The image is dismantled into two parts, using an LP filter and an HP filter, and each of these parts is down-sampled by two [109], as illustrated in Figure 3.1.

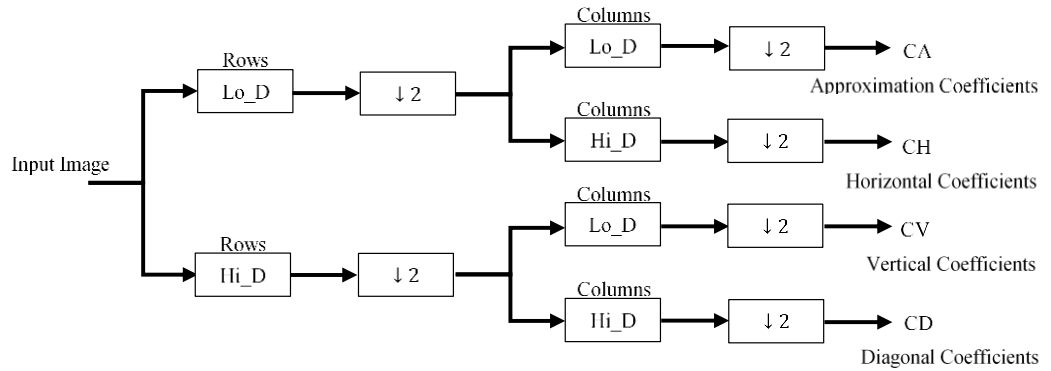


**Figure 3.1** Two-dimensional Discrete Wavelet Transform (DWT) [110].

where Lo\_D is a low-pass filter, Hi\_D is a high-pass filter, ↓ 2 denotes a down-sampling with a factor of two (keeping the even indexed rows or columns).

### 3.1.2 Gaussian Low-Pass Filter (GLPF)

The Gaussian Low-Pass filter or Gaussian smoothing is a filter that results in the smoothing of an image, by using a Gaussian function. It is used to filter images and reduce image noise [111].

The GLPF is used in many image processing systems that require a pre-preparing for their inputs, since it reduces the image noise [93] and allows only the lower-frequency components of the image to pass [16]. Moreover, some research has suggested that the techniques implemented in the low-frequency have improved the efficiency of facial recognition [42]. The equation of a Gaussian function in two dimensions is given by the following formula:

$$G(x, y) = \frac{1}{2\pi\sigma^2} e^{-\frac{x^2+y^2}{2\sigma^2}} \quad (3.1)$$

where,  $x$  and  $y$  are, respectively, the distance from the origin, in the horizontal and vertical axes,  $\sigma$  represents the standard deviation of the Gaussian distribution. **Figure 3.2** shows the Gaussian Low-Pass Filter for ( $\sigma = 2$ ).

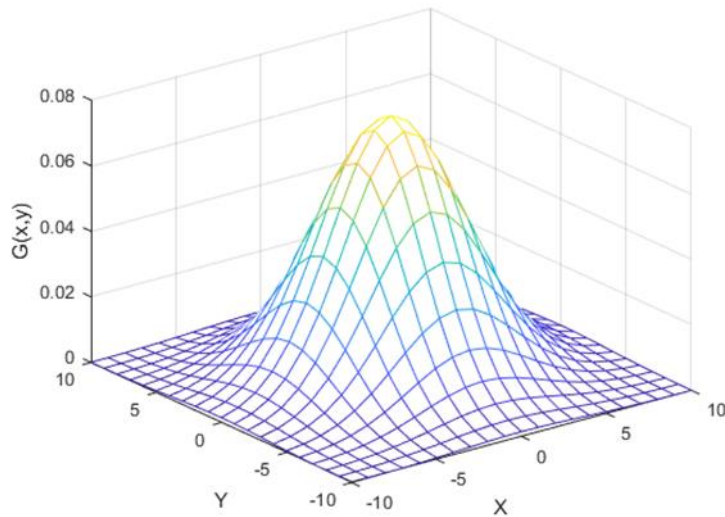


**Figure 3.2** Gaussian Low-Pass Filter for ( $\sigma = 2$ )

### 3.1.3 Difference of Gaussians (DoG)

If there are two copies of the same image and these two copies are being filtered using two Gaussian filters with different variances  $\sigma_1^2$  and  $\sigma_2^2$  (where  $\sigma_2 > \sigma_1$ ), to produce two new images, the result of subtracting these two new images is the DoG [112]. It is used to reduce the effect of light variations as in [17]. The filtering process is the convolution of the image with the filter kernel. Filtering the image keeps only the low-frequency spatial information. Therefore, subtracting one result from the other becomes a bandpass operation [113]. If  $\sigma_1 = \sigma$  and  $\sigma_2 = K\sigma$ , then the DoG of image  $I$ , for the two-dimensional case, is the function:

$$F_{\sigma, K\sigma}(x, y) = I * \frac{1}{2\pi\sigma^2} e^{-\frac{(x^2+y^2)}{2\sigma^2}} - I * \frac{1}{2\pi K^2\sigma^2} e^{-\frac{(x^2+y^2)}{2K^2\sigma^2}} \quad (3.2)$$

where  $F$  is the DoG function,  $I$  is the original image.

## 3.2 Feature Extraction Methods

### 3.2.1 Feature Extraction Using GLCM

The GLCM is one of the methods used for feature extraction. Its concept is introduced by Harlick et al. [114]. It perform a high texture classification [10]. In GLCM, the extracted features depend on the direction (angle  $\theta$ ) and the distance ( $D$ ) from the pixel of interest [10], as illustrated in **Figure 3.3**.

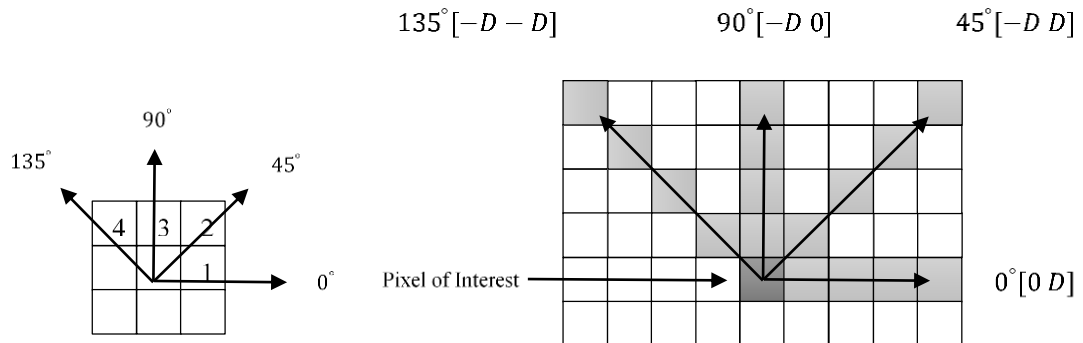


**Figure 3.3** The representation of Gray Level Co-Occurrence Matrix (GLCM) with different angles ( $\theta$ ) and different distances ( $D$ ) from the pixel of interest [115].

In this study, a number of values ( $D = 1, 2$ , and  $3$  and  $\theta = 0^\circ, 45^\circ, 90^\circ$ , and  $135^\circ$ ) are examined to calculate the best scenario. The used features are the correlations, contrast, maximum probability, angular second moment, mean, homogeneity, entropy, and dissimilarity [114]. These features are calculated using the following formula:

1. Correlation:

$$f_1 = \sum_i \sum_j \frac{(i - \mu_x)(j - \mu_y)p(x, y)}{\sigma_x \sigma_y} \quad (3.3)$$

2. Contrast:

$$f_2 = \sum_i \sum_j (i - j)^2 p(x, y) \quad (3.4)$$

3. Maximum probability:

$$f_3 = \max \left( \frac{p(x, y)}{|i \times j|} \right) \quad (3.5)$$

4. Angular Second Moment:

$$f_4 = \sum_i \sum_j p(x, y)^2 \quad (3.6)$$

5. Mean:

$$f_5 = \frac{\sum p(x, y)}{i \times j} \quad (3.7)$$

6. Homogeneity:

$$f_6 = \sum_i \sum_j \left( \frac{p(x, y)}{1 + |i - j|} \right) \quad (3.8)$$

7. Entropy:

$$f_7 = \sum_i \sum_j \left( \frac{p(x,y)}{\log p(x,y)} \right) \quad (3.9)$$

8. Dissimilarity:

$$f_8 = \sum_i \sum_j |i - j| p(x,y) \quad (3.10)$$

where  $\mu_x$  is the mean of the column values in the image,  $\mu_y$  is the mean of the row values in the image,  $p(x,y)$  denotes the elements of the Gray Level Co-Occurrence Matrix,  $i$  and  $j$  are, respectively, the lengths of the row and column of the image [116].

### 3.2.2 Feature Extraction Using LBP

One of the most widely used methods to analyze and model texture is the LBP method [12]. It could be basically described as a  $3 \times 3$  square operator. In each square, the eight-neighborhood pixels are compared with the one in the center. If the pixel values of the neighbors are greater than or equal to the pixel value at the center, they are replaced by 1. If not, then their values are replaced by 0. Then, the new binary values of the neighbors are concatenated to produce one decimal value that is considered to be a new value for the pixel in the center. The window is passed to the next pixel and the same operation is repeated. These new decimal values represented the histogram of the input texture. Equation 11 described the algorithm of the LBP operation:

$$LBP_{N_p, R(x,y)} = \sum_{N_p=0}^{N_p-1} s(g_p - g_c) 2^{N_p} \quad (3.11)$$

where  $s$  is the sign function,  $N_p$  is the number of neighborhood pixels,  $g_p$  represents the gray level value of the neighboring pixels, and  $g_c$  represents the gray level value of the central pixels.  $2^P$  is required to produce decimal values.

The traditional LBP [9] analyzes the texture of the image and thresholds a  $3 \times 3$  square neighborhood as the center pixel value. It only uses the sign information to produce the LBP, as illustrated in **Figure 3.4** [7].

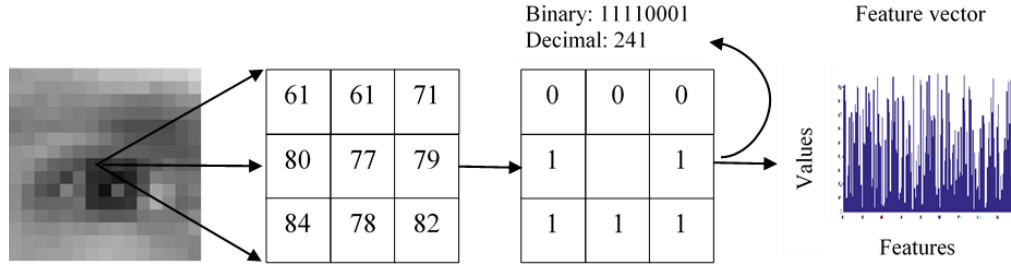


**Figure 3.4** The Local Binary Pattern (LBP) architecture.

In a newer implementation, the LBP operation has been upgraded to deal with any neighborhood size, by replacing the square with a circle [12]. This can be described by  $(N_p, R)$ , where  $R$  is the radius of the circle used. **Figure 3.5** illustrates an  $(8, 2)$  neighborhood. Additionally, there are a number of other modifications to the LBP [7].

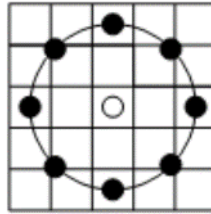


**Figure 3.5** Circular  $(8, 2)$  neighborhood [117]

The term  $LBP_{P,R}^{u^2}$  is used to describe the LBP operation, where  $u^2$  denotes the use of a uniform pattern. The resulting histogram results in the necessary information distributed in the image, such as edges, corners, uniform areas, etc. The effective operation must take care of the spatial information in the image, during the representation. One strategy to accomplish this is to partition the image into a number of small areas  $R_0, R_1, \dots, R_{m-1}$  [9], where  $m$  is the number of areas. If the size of the histogram is  $B$ , then the length of the feature vector is  $mB$ . It is obvious from this relation that the number of areas  $m$  determines the length of the feature vector, which means selecting small areas results in long feature vectors, leading to extreme use of

memory and a slow classification processing. Selecting large areas causes a loss of spatial information. An example of a preprocessed face image partitioned into thirty-six windows and the resulting face feature histogram are illustrated in **Figure 3.6** [96].

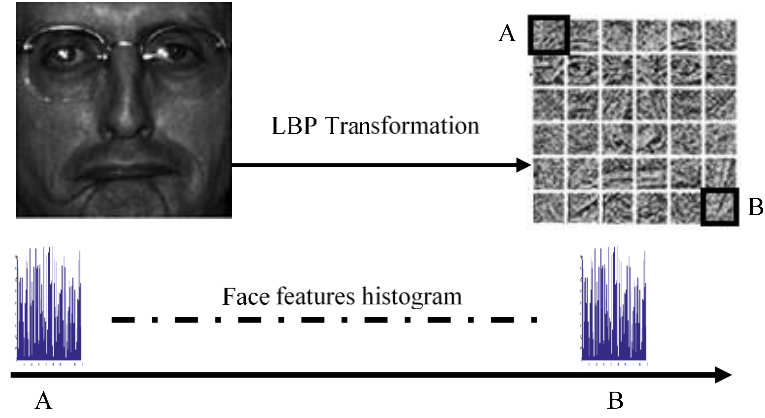


**Figure 3.6** Example of a preprocessed face image partitioned into thirty-six windows and its feature histogram using the Local Binary Pattern (LBP).

### 3.2.3 Feature Extraction Using the Gabor Filter

The Gabor filter is a very helpful tool in image processing, especially in FR [118]. In the spatial domain, the Gabor filter with two dimensions is the modulation of a Gaussian kernel function, by a complex sinusoidal plane wave with a center frequency  $f$  and orientation  $\theta$  [119], and is defined as:

$$G(x, y) = \frac{f^2}{\pi\gamma\eta} e^{\left(-\frac{x'^2 + \gamma^2 y'^2}{2\sigma^2}\right)} e^{(j2\pi f x' + \phi)}$$

$$x' = x \cos \theta + y \sin \theta \quad (3.12)$$

$$y' = -x \sin \theta + y \cos \theta$$

where  $\gamma$  and  $\eta$  denote the ratio between the envelope of the Gaussian function with standard deviation  $\sigma$  and the center frequency, and  $\phi$  defines the phase offset.

The frequency (or wavelength) governs the width of the stripes in the function, and by increasing the frequency, the stripes become thinner. The orientation governs the rotation of the Gabor envelope and the aspect ratio controls the height of the function. For a very large aspect ratio, the envelope approaches a height of one pixel, and for a very small aspect ratio, the height stretches across the image. The bandwidth controls the overall size of the Gabor envelope, such that for a large bandwidth, the envelope increases, allowing more stripes [120]. **Figure 3.7** up to **Figure 3.11** show the effect of changing some parameters for the function of a Gabor.



**Figure 3.7** Different wavelength values: (a) 25; (b) 50 [121]

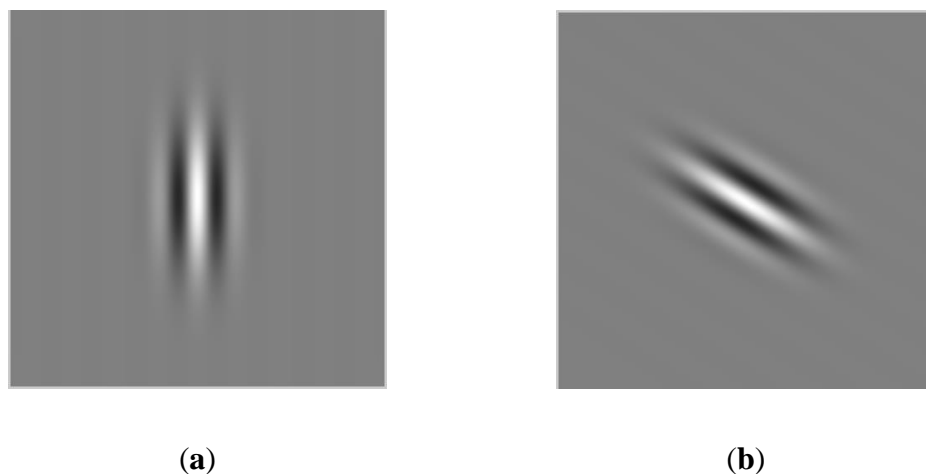


**Figure 3.8** Different orientation: (a) 0; (b) 45 [121]

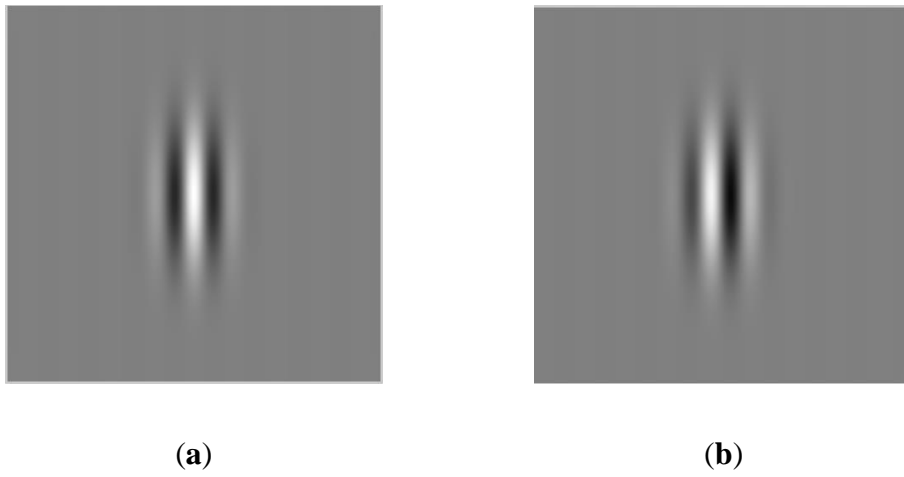


**Figure 3.9** Changing the phase shift values: (a) 180; (b) 90 [121]



**Figure 3.10** Aspect ratio: (a) Very large; (b) Very small [121]

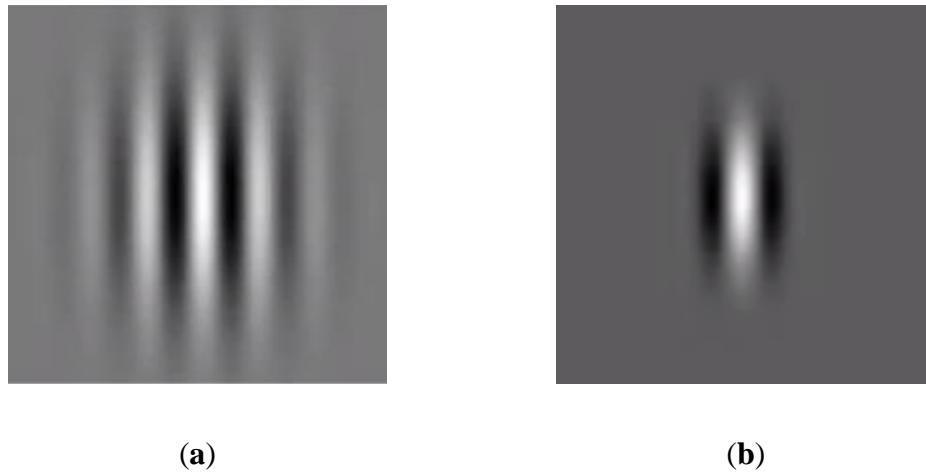


**Figure 3.11** Different bandwidth values: (a) Large; (b) Small [121]

Gabor filters have many advantages, such as invariance to rotation, scale, and translation. Moreover, they are robust against disturbances in images, such as change in illumination [122],[30], and they have been found to be particularly appropriate to extract many features from an image, using different frequencies and orientation for Gabor filters [120].

They are useful, especially in feature extraction for texture analysis and segmentation. The varying orientation observes the texture that is oriented in a particular direction, while the varying Gaussian envelope standard deviation controls the region size of the image that is being analyzed [123].

### **3.2.4 Feature extraction using Histograms of Oriented Gradients (HOG)**

Another very popular method for feature extrication is the Histograms of Oriented Gradients (HOG). It is one type of descriptors that is used a lot in the human detection [124]. The HOG concept is to compute the gradient orientation and the gradient direct magnitude. To obtain the HOG of an image, first, the changes in X and Y are computed, then the magnitude and direction are obtained.

### 3.2.4.1 Computing Gradients

The main operation of HOG is the derivative, or the center difference, since, there are two derivatives, the x derivative and the y derivative, once these derivatives are obtained, the gradient magnitude and the gradient orientation can be computed.

$$f'(x) = \lim_{h \rightarrow 0} \frac{f(x+h) - f(x-h)}{2h} \quad (3.13)$$

The magnitude is given by:

$$s = \sqrt{s_x^2 + s_y^2} \quad (3.14)$$

And the orientation is given by:

$$\theta = \arctan\left(\frac{s_y}{s_x}\right) \quad (3.15)$$

### 3.2.4.2 Blocks and Cells

**Figure 3.12** shows a face image, it is assumed that this image is a 64x128 image, if this image is divided to 128 cells, then some blocks are taken, for example the first block is block 1 with 2x2 cells, then the second block is 50 % overlapped, which block 2, so, each block is consist of 2x2 cells with size 8x8 which means 16x16, with 7x15 = 105 blocks in total.

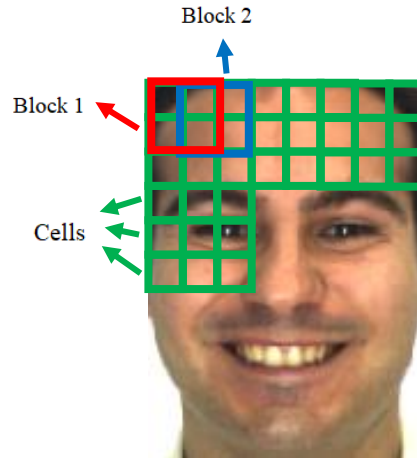


**Figure 3.12** The blocks and the cells

### 3.2.4.3 HOG Feature Extraction Steps

To calculate the HOG for an image with  $64 \times 128$ , for example, the image is divided onto  $16 \times 16$  blocks with 50% overlap, so therefore there are  $7 \times 15$  with total of 105 of blocks, and each block consists of  $2 \times 2$  cells, and the size is  $8 \times 8$ , then the HOG is quantized with 9 directions or bins, if the direction is not one of the bins then some kind of interpolation can be done, also, the Gaussian can be applied to smooth the histogram, then all the descriptors can be concatenated since there are 105 of these block and each one is 9 dimensional, this gives a very large described, about 3780 dimension descriptor and this for the whole image of the block in the image, as shown in **Figure 3.13**.

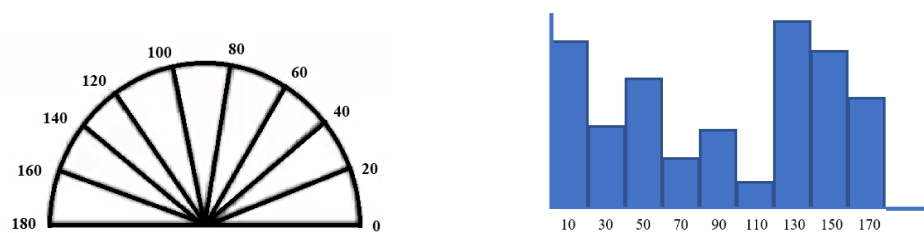


**Figure 3.13** The histogram quantization to 9 bins

The procedure of HOG for feature extraction can be summarized in the following steps:

1. Compute the centered horizontal and vertical gradients with no smoothing.
2. Compute gradient orientation and magnitudes.
  - For color image, pick the color channel with the highest gradient magnitude for each pixel.
3. For 64x128 image,
4. Divide the image into 16x16 of 50% overlap.
  - $7 \times 15 = 105$  blocks in total
5. Each block should consist of 2x2 size 8x8.
6. Quantize the gradient orientation into 9 bins.
  - The vote is the gradient magnitude.
  - Interpolate votes bi-linearly between neighboring bin center.
  - The vote can also be weighted with Gaussian to down-weight the pixel near the edges of the block.
7. Concatenate histograms (Feature dimension:  $105 \times 4 \times 9 = 3780$ )

#### 3.2.4.4 *The Linear Interpolation*

The better histograms can be found by doing the interpolation. If there are 9 bins, and the range of the gradient orientation is between  $[0^\circ \ 180^\circ]$ , this range is quantized into these 9 bins as shown in figure 5.3, if the orientation has  $85^\circ$ , and since, there is no bin with  $85^\circ$ , in this case, this is split into couple of bins which are closest to that, these bins are  $70^\circ$  and  $90^\circ$ , since the difference between  $70^\circ$  and  $85^\circ$  is  $15^\circ$ , and the difference between  $90^\circ$  and  $85^\circ$  is  $5^\circ$ , the values is divided proportionally according to this ratio, that means  $(5/20 = 1/4)$  and  $(15/20 = 3/4)$ , and the histogram is distributed according to this concept, as shown in **Figure 3.14**.

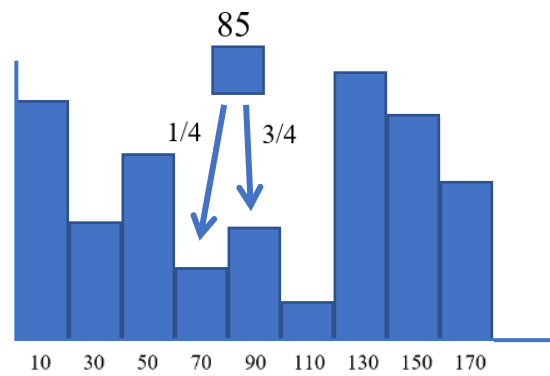


**Figure 3.14** The HOG interpolation

#### 3.2.4.5 Feature Vector

Each block has its histogram, all the histograms are concatenated to produce the final feature vector of the all image as shown in **Figure 3.15**.

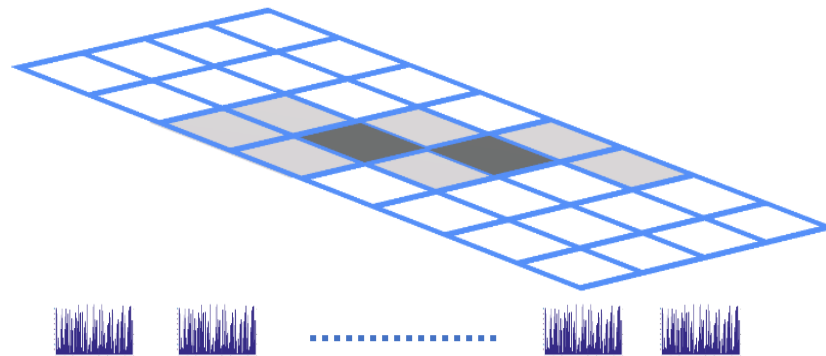


**Figure 3.15** Concatenating the histograms

#### 3.2.4.6 Visualization

The visualization of the HOG, as in **Figure 3.16**, with some blocks and each block has its histogram which corresponds to the face regions, and some blocks give the dominating direction for some certain region, which give the visualization of the representation that represents the face and calculates how much the distance from these different parts of the face.

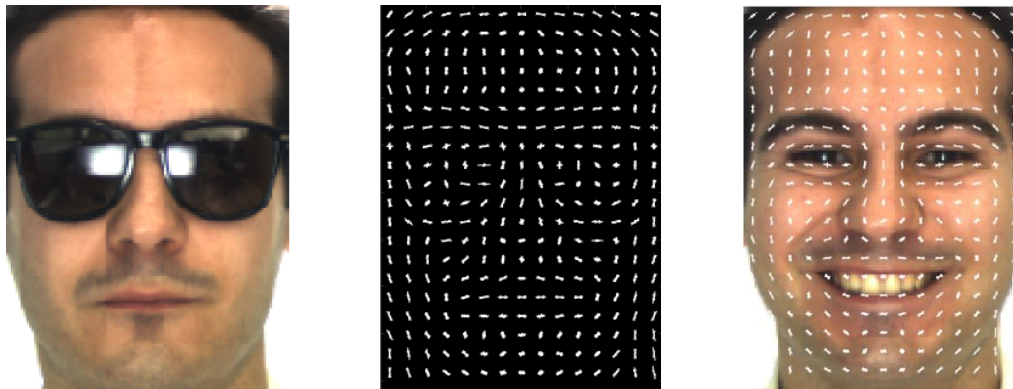


**Figure 3.16** The HOG visualization

By looking to the presentation (middle figure), it is clear it is representing a face, and this is used to recognize the face. Once the descriptor exists, for lots of training examples (faces), then any train techniques such of machine learning can be used for face recognition by classifying the face according to their features.

The HOG is a very strong and popular descriptor, and it is a kind of global descriptor which looks at the whole image. Authors of [124] propose this descriptor and they use it for human detection.

### 3.3 Classification

Although there are many classifiers used for the classification, such as the Euclidean Distance, the Cosine Distance, Linear Discriminant Analysis, Quadratic Discriminant Analysis, Learning Vector Quantization, and Support Vector Machines [95]. The Minimum Euclidean Distance classifier is considered to be one of the most popular classifiers that could be easily designed [125] and widely used [97, 126]. In general, it is used to examine the similarities between objects. For this reason, we use this classifier in this study.

### 3.3.1 Euclidean Distance

The Euclidean distance  $d$  between two points  $i$  and  $j$ , where  $I = (i_1, i_2, \dots, i_n)$  and  $j = (j_1, j_2, \dots, j_n)$ , in Cartesian coordinates, is the length of the straightest line between them. This distance is given by the formula:

$$d(i, j) = \sqrt{(i_1 - j_1)^2 + (i_2 - j_2)^2 + \dots + (i_n - j_n)^2} = \sqrt{\sum_{k=1}^n (i_k - j_k)^2} \quad (3.16)$$

Therefore, if the two points are close to each other, then the value of  $d$  is small; otherwise, it is large. The Euclidean vector is the location of a point in a Euclidean  $n$ -space, where the length of this vector is measured by the formula of the Euclidean norm, given by:

$$\|I\| = \sqrt{i_1^2 + i_2^2 + \dots + i_n^2} \quad (3.17)$$

This tool is used to test how similar one object (face) is to another, by testing the similarities between their respective feature vectors.

The Euclidean distance is used to check how similar vectors are, if the distance between two instances is low enough they are probably describing the same thing we take two instances from the data set and we calculated the difference between the corresponding properties, we can use threshold to decide if they are similar enough.

### 3.3.2 Cosine Similarity

The Cosine Distance is a way to measure the similarity between two vectors by measuring the angle between them. So, it considers the orientation not the magnitude. The angle between two vectors with the same orientation is  $0^\circ$ , and for those vectors diametrically opposed is  $90^\circ$ , independent of their magnitude. Cosine distance is particularly used in positive space. Cosine distance is applicable for any number of dimensions and is most commonly used in high-dimensional positive spaces.

The cosine of the angle between two non-zero vectors can be obtained from the Euclidean dot product formula

$$\mathbf{a} \cdot \mathbf{b} = \|\mathbf{a}\|_2 \|\mathbf{b}\|_2 \cos \theta \quad (3.18)$$

Given two vectors of  $A$  and  $B$ , the cosine of the angle between them  $\cos(\theta)$ , can be represented using a dot product and as

$$\cos(\theta) = \frac{\mathbf{A} \cdot \mathbf{B}}{\|\mathbf{A}\|_2 \|\mathbf{B}\|_2} \quad (3.19)$$

$$\cos(\theta) = \frac{\sum_{i=1}^n A_i B_i}{\sqrt{\sum_{i=1}^n A_i^2} \sqrt{\sum_{i=1}^n B_i^2}} \quad (3.20)$$

where  $A_i$  and  $B_i$  are components of vector  $A$  and  $B$  respectively.

### 3.4 Datasets

The datasets in this thesis is taken from the ORL, Yale and AR datasets.

#### 3.4.1 The ORL Dataset

The ORL is a well-known face dataset that is used to test FR algorithms. It has 400 images of 40 distinct persons, 10 images for each person. The dataset is varied in many aspects. First, the images are taken at different times during the lives of the people. Second, the images include different variations and different facial expressions, such as closed or open eyes. Some of the people are smiling, others are not. In addition, there are a number of people wearing spectacles while others are not wearing spectacles. Furthermore, a number of the images include up to twenty degrees of tilting and rotation of the face [5].

A number of face images from the ORL dataset are illustrated in **Figure 3.17**.

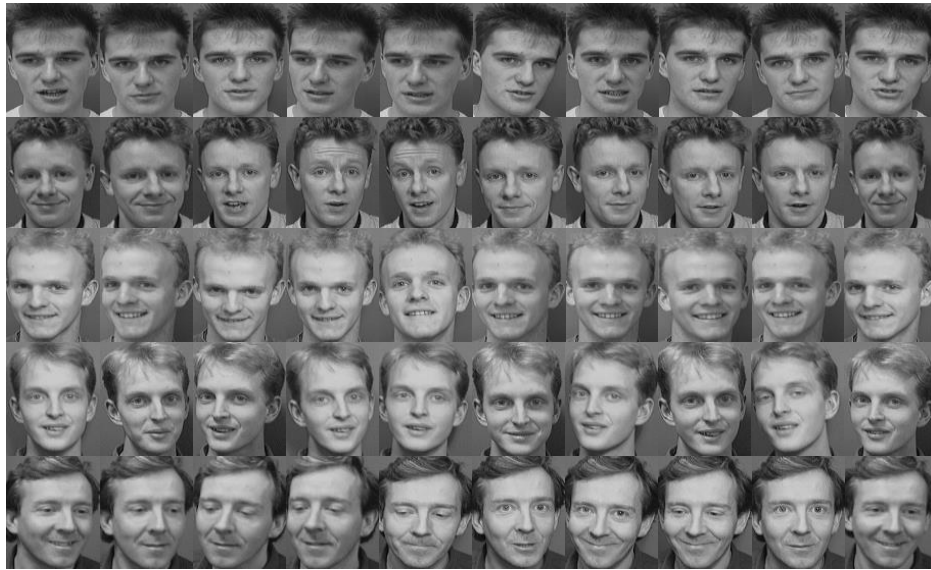


**Figure 3.17** Sample images from the Olivetti Research Laboratory (ORL) dataset

### 3.4.2 The Yale Dataset

In this dataset, there exists 165 images for 15 unique people, 11 images for each person with different cases, such as normal, sad, sleepy, etc. The dataset includes many variations of pose, illumination, and expression [5]. A number of images from the Yale dataset are illustrated in **Figure 3.18**.



**Figure 3.18** Sample images from the Yale face dataset.

### 3.4.3 AR Face Database

The AR dataset is used in many face recognition papers, it contains over 4000 color face images of 126 people, including 26 frontal views of faces with different facial expressions, illumination conditions and occlusions, like (smile, anger, scream, left light on, right light on, all side lights on, wearing sun glasses, wearing sun glasses and left light on, wearing sun glasses and right light on, wearing scarf, wearing scarf and left light on, wearing scarf and right light on). The images of 120 individuals are captured in two sessions and each session contains 26 color images [23].

**Figure 3.19** shows some images form AR dataset.



**Figure 3.19** AR face database

# CHAPTER 4

## EXPERIMENTS AND RESULTS

This section shows some results obtained from simulations using MATLAB 2015b. The experiments are implemented on images from the ORL, Yale and AR datasets, using the proposed method. The proposed method is compared with the performance of PCA [48], Collaborative Representation-Based Classification (CRC) [127], SRC [44], and SCRC [5, 6].

The FR system consisted of three stages. The first stage is the preprocessing stage, in which the 2-D DWT, the GLPF, and the DoG are used separately. The second stage is the feature extraction stage, where the LBP, the GLCM, Gabor Filter and the HOG are examined; all these algorithms are first tested separately, then, the two methods from the list are combined in the Feature Extraction Stage. In the final stage (the Classification Stage), the Euclidean distance and Cosine similarity are examined as classifiers. The procedure is carried out and tested using the Original Training Samples (OTS) and the Original with Symmetrical Training Samples (OSTS) from the ORL, Yale and the AR datasets.

### 4.1 Generating New Images

In order to increase the size of the training data, new training images are generated using the property of face symmetry, since those images reflect some part of the face that is not shown by the original images, as illustrated in **Figure 4.1**.

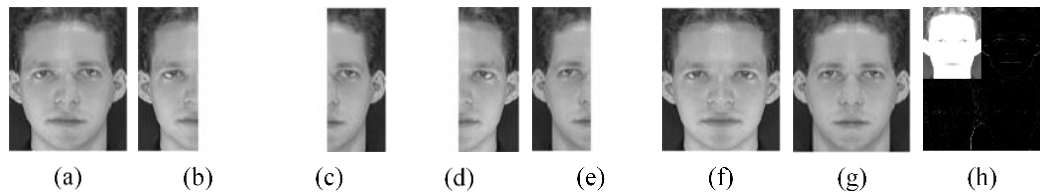


**Figure 4.1** (a) Original image; (b) left side; (c) right side; (d) mirror of left side; (e) mirror of right side; (f) integrating left side with mirror; (g) integrating right side with mirror; and (h) Discrete Wavelet Transform (DWT) of the original image in the first level.

## 4.2 Experiments on the original ORL Dataset

In the experiment, one, two, up to nine face images of each person from the ORL dataset with size 112 x 92 are used, respectively, as the training samples and the rest of images are used as the testing samples. The features of the training and testing images are extracted using the LBP, the GLCM, and the Gabor Filter. Each image had one feature vector,  $f = [f_1, f_2 \cdots f_m]$ , where  $m$  is the number of one-image features.

The similarity between the feature vector of the test image and the feature vectors of the training images is measured using the Euclidean distance classifier. The person who had a training image feature vector with a minimum Euclidean distance is considered to be the result of recognition. The experiments are run ten times, with random image selection in each experiment. The recognition rate is calculated as the average of each set of these experiments.

### 4.3 Experimental result on the symmetrical ORL Dataset

In this experiment, the original and symmetrical images are used for training. The experiment revealed the use of symmetrical images, along with the original images, improved the accuracy of FR, as compared to only using the original images as training samples. **Figure 4.2** shows the results of using the LBP for feature extraction with OTS and OSTs.

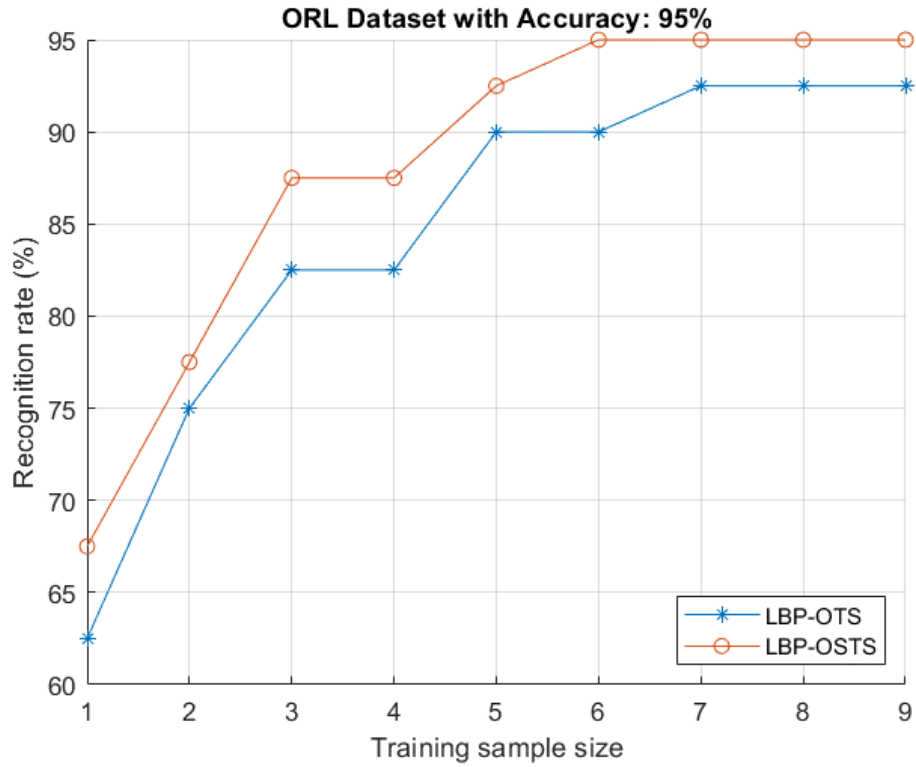


**Figure 4.2** Recognition rates using LBP with original training sample (LBP-OTS) compared with LBP with original and symmetrical training samples (LBP-OSTS).

#### 4.4 Using a Preprocessing Stage

In this experiment, three different methods for preprocessing are separately examined with LBP. First, LBP is used without any preprocessing stage, followed by the GLPF being used for the preprocessing stage, with a standard deviation of  $\sigma = 1$  and a window size of 5 pixels. Then the DoG with  $\sigma_1 = 0.1$ ,  $\sigma_2 = 2.0$ , and a window size of 5 pixels is used for the preprocessing stage. Finally, the 2-D DWT is also used for the preprocessing stage.

The results show that the use of GLPF or 2-D DWT as a preprocessing stage improves the accuracy of FR, as compared to not using any of the preprocessing stages, as in **Figure 4.3**. The experiments are implemented using OSTs.

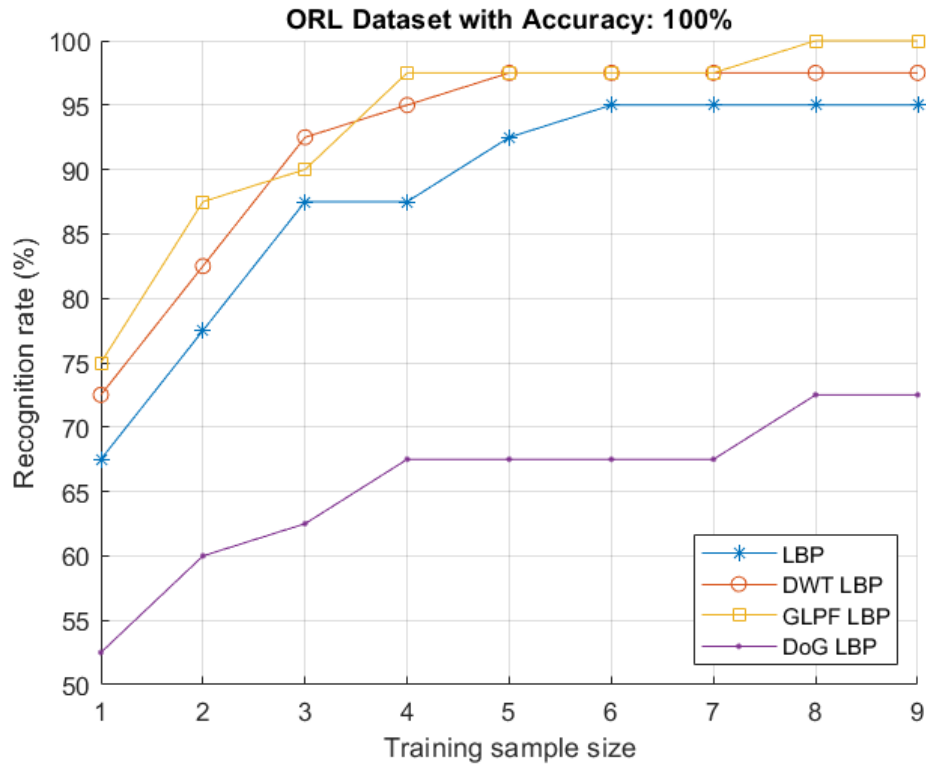


**Figure 4.3** Recognition rates using LBP, LBP with Discrete Wavelet Transform (DWT-LBP), LBP with Gaussian Low-Pass filter (GLPF-LBP), and LBP with Difference of Gaussian (DoG-LBP) methods, versus size of the training set of the ORL dataset (OSTS).

## 4.5 The GLCM Method

In this experiment, the GLCM method is used to extract the features. The parameters of the GLCM method are selected to be  $D = 1$  and  $\theta = 0^\circ$ .

## 4.6 Combining Feature Extraction Methods

In this experiment, two methods are used separately for feature extraction, the LBP and the GLCM. Then, the two feature vectors obtained from these two methods are normalized and concatenated to produce one longer feature vector, which is used for training and testing. The results show that the combination of the two methods could help to improve the accuracy of FR, as compared to using one method for feature extraction, as shown in **Figure 4.4**. The experiments are implemented using OSTs.

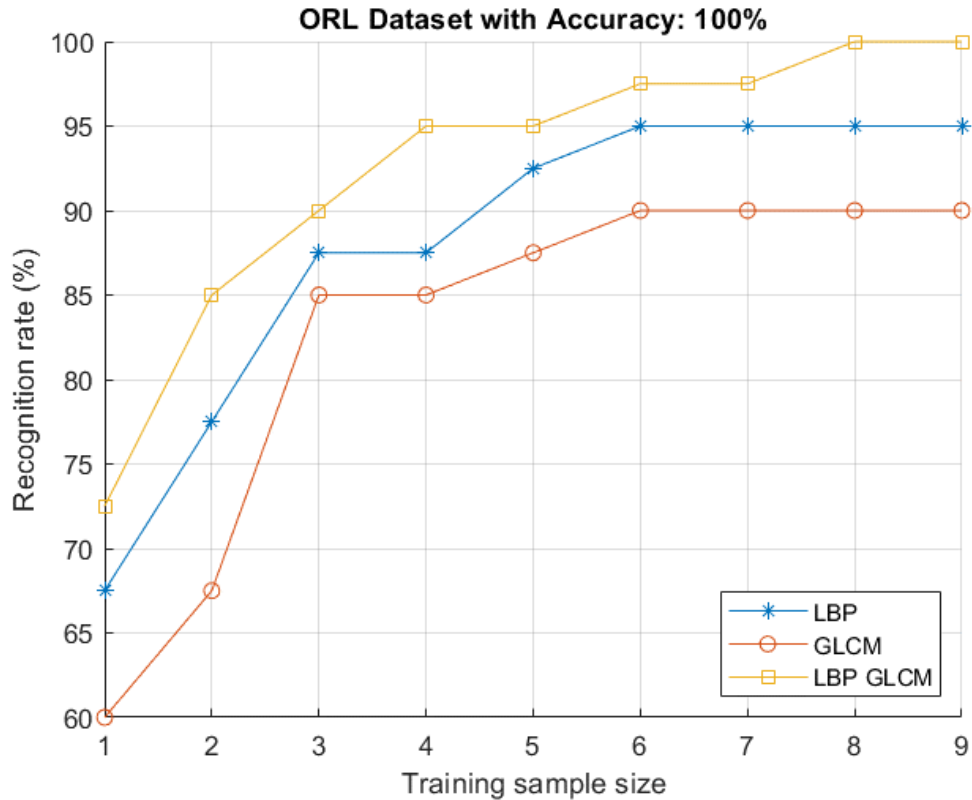


**Figure 4.4** Recognition rates using the LBP, the Gray Level Co-Occurrence Matrix (GLCM), and the combination of the LBP with the GLCM (LBP-GLCM) methods versus the size of the training set of the ORL dataset (OSTS).

## 4.7 The Gabor Filter Method

In this experiment, the Gabor Filter is examined to extract the features. The parameters of the Gabor filter bank are set as following. The number of scales is set to 5, the number of orientations is set to 8, and the number of rows and columns in a 2-D Gabor filter are each set to 39. Additionally, the parameter of the Gabor function is set as following. The factor of down-sampling along the rows is set to 4 and the factor of down-sampling along the columns is set to 4. The experiment revealed that the best results are obtained using the Gabor Filter, as compared to the other methods. **Figure 4.5** shows the results of the recognition rates for different methods on the OSTs–ORL dataset. These methods are: the LBP without any preprocessing stage (LBP), the LBP with DWT as a preprocessing stage (DWT-LBP), the LBP with GLPF as a preprocessing stage (GLPF-LBP), the GLCM, the LBP combined with the GLCM and the Gabor. For the sake of comparison, the performance of the PCA has also been shown in the figure.

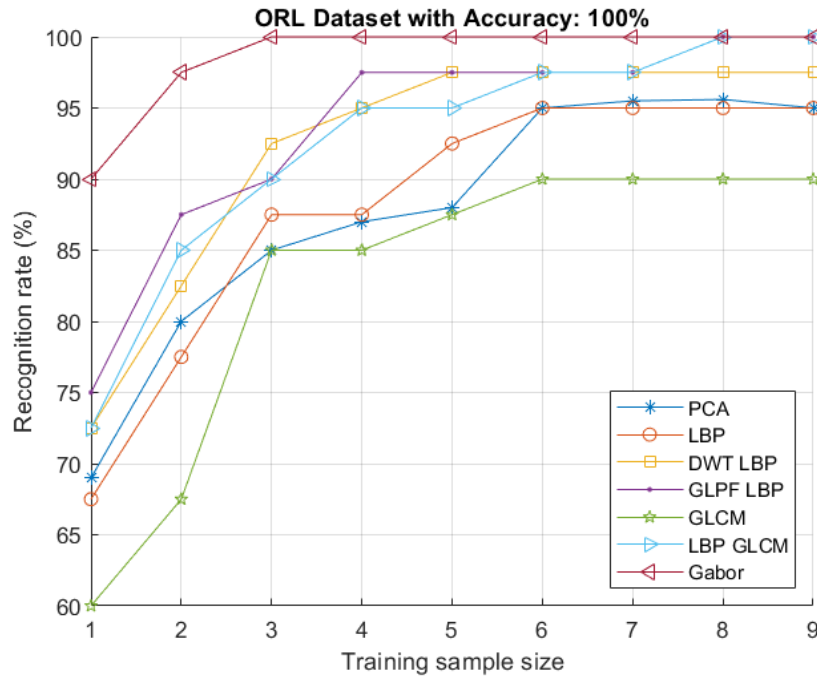


**Figure 4.5** Recognition rates using different methods: Principal Component Analysis (PCA), Local Binary Pattern (LBP), LBP with Discrete Wavelet Transform (DWT LBP), LBP with Gaussian Low-Pass filter (GLPF-LBP) Gray Level Co-Occurrence Matrix (GLCM), combination of LBP with GLCM (LBP-GLCM), and the Gabor versus size of the training set of the ORL dataset (OSTS).

## 4.8 Other Experiments

The proposed method is examined in various cases and situations. For this purpose, different experiments are carried out, using different preprocessing techniques and different feature extraction methods. These experiments are implemented to compare the performance of the FR system when the original training samples (OTS) are used alone and when the original training samples are used, along with the symmetrical training samples (OSTS).

For the sake of completeness, the results are compared with the methods in the literature PCA [48], CRC [127], SRC [44], and SCRC [5, 6]. The obtained results are summarized in **Table 4.1**.

As we can see from the table, as the number of training samples increase, the accuracy increases too. Also, in general, the results using original with symmetrical samples are better than using the original samples alone.

In addition, it is observed that the using of preprocessing stage improves the results of the LBP form (95%) to (100%) using GLPF and to (97.5%) using DWT. On the opposite side, using DoG is not recommended with LBP.

Moreover, using LBP combined with GLCM performs better than using one of them alone, for instance, the best result for LBP is (95%) and the best result for GLCM is (90%), but for the combined LBP-GLCM the accuracy is (100%).

And lastly, the best results are obtained using Gabor, it reaches (100%).

**Table 4.1** The recognition rates of the different methods on the ORL dataset, using the OTS compared with the OSTs.

Preprocessing Method	Feature Extraction Method		No. of Training Images								
			1	2	3	4	5	6	7	8	9
			Recognition Rate %								
No	LBP	OTS	62.5	75	82.5	82.5	90	90	92.5	92.5	92.5
		OSTS	67.5	77.5	87.5	87.5	92.5	95	95	95	95
DWT	LBP	OTS	70	80	90	92.5	95	95	95	97.5	97.5
		OSTS	72.5	82.5	92.5	95	97.5	97.5	97.5	97.5	97.5
GLPF	LBP	OTS	72.5	80	87.5	92.5	95	95	97.5	97.5	97.5
		OSTS	75	87.5	90	97.5	97.5	97.5	97.5	100	100
DoG	LBP	OTS	50	55	62.5	62.5	65	65	65	67.5	70
		OSTS	52.5	60	62.5	67.5	67.5	67.5	67.5	72.5	72.5
No	GLCM	OTS	55	65	77.5	77.5	80	87.5	87.5	87.5	90
		OSTS	60	67.5	85	85	87.5	90	90	90	90
DWT	GLCM	OTS	50	55	60	60	62.5	62.5	62.5	65	62.5
		OSTS	57.5	70	70	80	77.5	75	80	80	82.5
DoG	GLCM	OTS	37.5	40	40	40	42.5	42.5	45	45	45
		OSTS	40	42.5	50	50	50	50	50	52.5	55
GLPF	GLCM	OTS	57.5	67.5	80	80	80	82.5	82.5	82.5	82.5
		OSTS	57.5	75	82.5	82.5	87.5	90	90	90	90
No	LBP–GLCM	OTS	70	82.5	87.5	92.5	92.5	95	95	95	95
		OSTS	72.5	85	90	95	95	97.5	97.5	100	100
No	Gabor	OTS	87.5	95	100	100	100	100	100	100	100
		OSTS	90	97.5	100	100	100	100	100	100	100
No	PCA [48]	OTS	69	79	84	87	89	95	96	96	95
No	CRC [127]	OTS	72	84	86	91	91	94	93	94	93
No	SRC [44]	OTS	76	89	90	94	94	94	95	96	95
No	SCRC [5, 6]	OSTS	76	90	92	94	94	95	96	96	95

## 4.9 Experiments on the Yale Dataset

In this experiment, from the Yale dataset, either one, two, or up to ten facial images of size 154 x 154, are chosen for each person, which are then used as the training samples, and the rest of images are used as the testing samples. These experiments are similar in procedure to those in the ORL dataset, where a variety of methods are tested for preprocessing and feature extraction. These methods are tested and examined using the OTS and the OSTs. Many results are obtained using the different cases, these

results are summarized in **Table 4.2** and **Figure 4.6**, along with the performance of the methods in the literature PCA [48], CRC [127], SRC [44], and SCRC [5, 6].

As we can see from the **Table 4.2**, as the number of training samples increase, the accuracy increases too. Also, in general, the results using original with symmetrical samples are better than using only the original samples. In addition, for Yale dataset, it is easy to reach accuracy of (100%) using only LBP, either using only original samples or using original with symmetrical samples. the difference between using only original samples or using original with symmetrical samples is that, for original with symmetrical samples we need less images for training. Furthermore, GLCM does not perform well with DWT, since the DWT is filtering and compressing the images, which means reducing the quality of the images, we can conclude that the GLCM is sensitive to low-quality images. And finally, the best results are obtained using Gabor where we need only two training samples to reach (100%) using original with symmetrical samples.

**Table 4.2** The recognition rates of the different methods on the Yale dataset, using the OTS and the OSTs.

Preprocessing Method	Feature Extraction Method		No. of Training Images									
			1	2	3	4	5	6	7	8	9	10
			Recognition Rate %									
No	LBP	OTS	90	93	96	98	100	100	100	100	100	100
		OSTS	95	98	100	100	100	100	100	100	100	100
No	GLCM	OTS	70	75	87	87	87	87	87	87	87	87
		OSTS	75	80	93	93	93	93	93	93	93	93
DWT	GLCM	OTS	12	15	18	20	20	20	20	20	20	20
		OSTS	20	23	27	30	33	33	33	33	33	33
DoG	GLCM	OTS	60	60	73	73	73	73	80	80	80	80
		OSTS	65	67	87	87	87	87	87	87	87	87
GLPF	GLCM	OTS	80	85	87	87	87	87	87	87	87	87
		OSTS	80	93	93	93	93	93	93	93	93	93
No	Gabor	OTS	95	97	100	100	100	100	100	100	100	100
		OSTS	97	100	100	100	100	100	100	100	100	100
No	PCA [48]	OTS	69	89	89	93	87	87	98	95	96	100
No	CRC [127]	OTS	87	93	94	99	98	96	98	95	96	100
No	SRC [44]	OTS	87	90	90	98	92	92	98	100	100	100
No	SCRC [5, 6]	OSTS	88	95	97	99	100	100	100	100	100	100

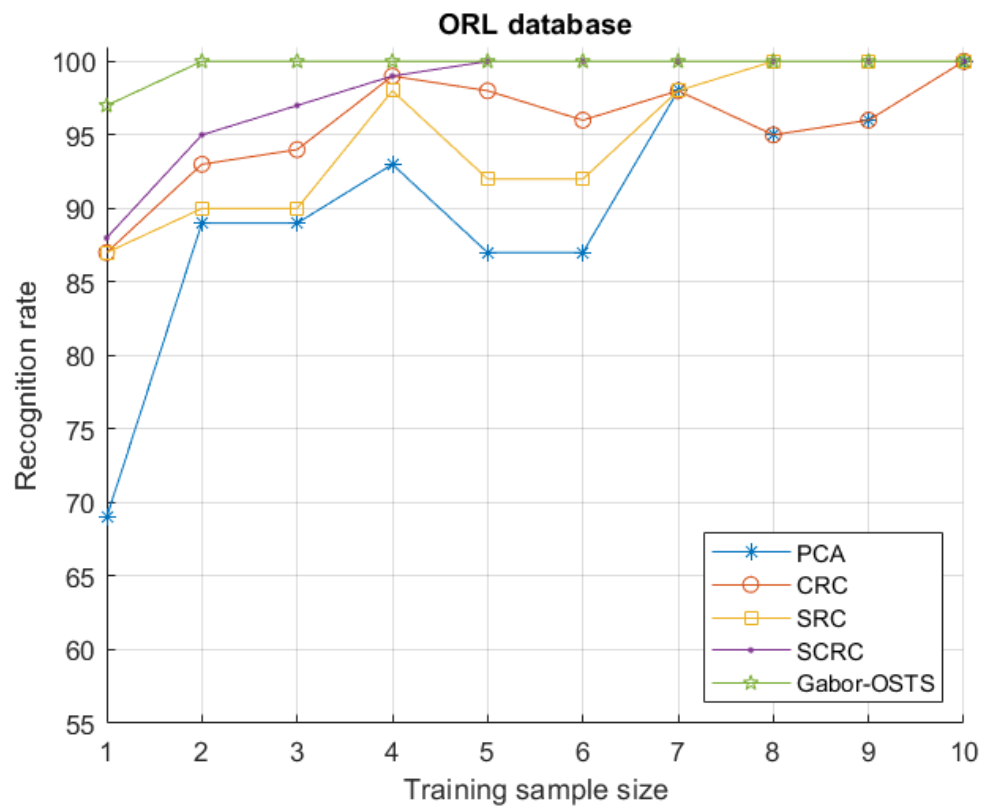


**Figure 4.6** Rates of recognition using different methods: Principal Component Analysis (PCA), Collaborative Representation-Based Classification (CRC), Sparse Representation-Based Classification (SRC), Collaborative Representation-Based Classification Using Symmetry (SCRC), and the Gabor Method Using Original and Symmetrical Training Samples (Gabor-OSTS), versus the size of the training set on the Yale dataset.

### 4.10 Symmetrical and Low-Quality Face Images

The proposed method of symmetry improves the recognition techniques, especially when we process low quality face images. In this experiment, the quality of face images is reduced using different compression levels of Discrete Wavelet Transform (DWT), the recognition rates are tested using 10-training images from YALE database, one time using original training samples only, and second time using original with symmetrical training samples. **Figure 4.7** shows the accuracy versus compressional level on YALE dataset.

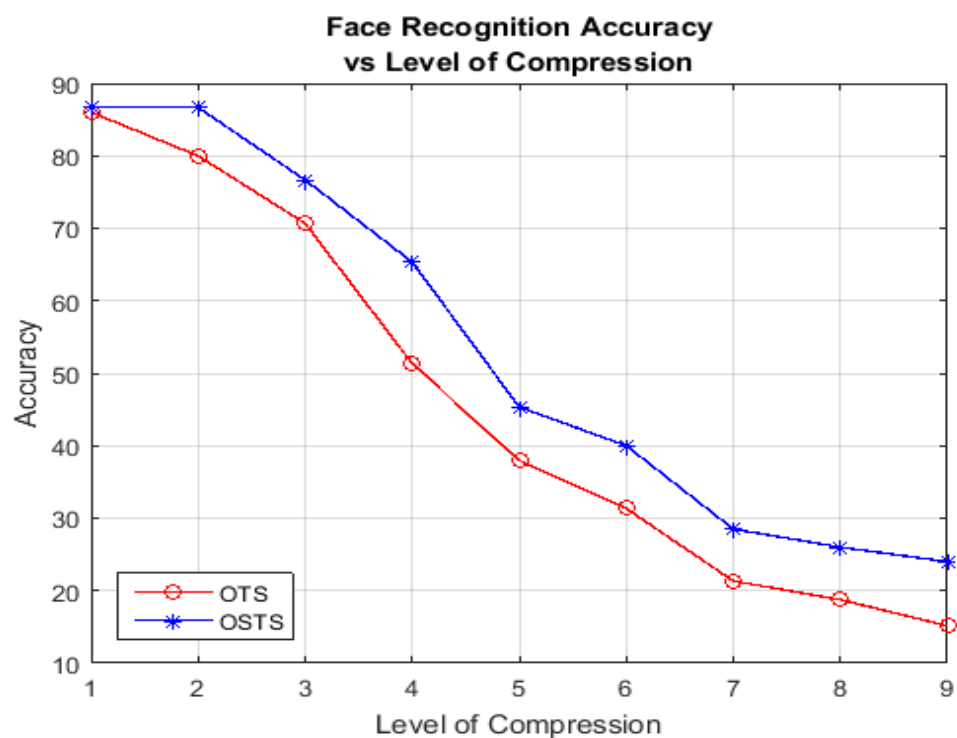


**Figure 4.7** The accuracy versus compression level on YALE database

## 4.11 Experiments on the AR Dataset

These results are carried out using the images from AR dataset, different feature extraction methods are used, LBP, GLCM, Extended GLCM, HOG and Gabor. Also, for each method, different cases have been studied. In additions, the feature fusion is studied too by combining two or more of feature vectors that are obtained from different methods. The recognition system is examined one time using original training samples (OTS) and the second time using original with symmetrical training samples (OSTS). The following figures show the obtained results.

### 4.11.1 Experimental Results using all images in AR dataset

In this part, all AR dataset is used to test the recognition system, the system is trained using 10% of dataset and the rest 90% is used for testing, then 20% for training and 80% for testing, up to 95% for training and 5% for testing.

#### 4.11.1.1 Experiment 1: LBP

In this experiment, the LBP is used for feature extraction without a preprocessing stage, the Euclidean classifier is used for classification.

#### 4.11.1.2 Experiment 2: GLCM

In this experiment, the traditional GLCM method is used for feature extraction, the traditional GLCM calculates four different properties or features for each image, these properties are, the Contrast, the Correlation, the Energy and the Homogeneity, as explained in as in section 3.2.1.

#### 4.11.1.3 Experiment 3: Extended GLCM

In this experiment, some improvements are added to the traditional GLCM where the four features that can be obtained from the traditional GLCM is extended to 23 features for each image, these 23 features such as: Autocorrelation, Contrast, Correlation, Maximum probability, Angular Second Moment, Mean, Energy, Entropy,

Homogeneity, Dissimilarity, Sum of squares, Sum of average, Sum of variance, Sum of entropy as in section 3.2.1.

#### ***4.11.1.4 Experiment 4: Normalized Extended GLCM***

In this experiment, more improvements are added by normalizing the feature vector, the normalization indeed improves the recognition accuracy.

#### ***4.11.1.5 Experiment 5: Features Fusion***

In this experiment, two vectors of features that are obtained using two different methods, are fused, the features that are obtained from the LBP method are fused with the features that are obtained from the Normalized Extended GLCM. This experiment shows that, using the combination of two methods is better than using one method alone.

#### ***4.11.1.6 Experiment 6: LBP with different cell size***

The face recognition system is examined using LBP with different cell size, the choosing of a proper value for cell size for LBP is not an easy task, because the decreasing of the cell size would produce more features thus more computation complexity, but at the same time it does improve the recognition accuracy, as shown in **Figure 4.8**.

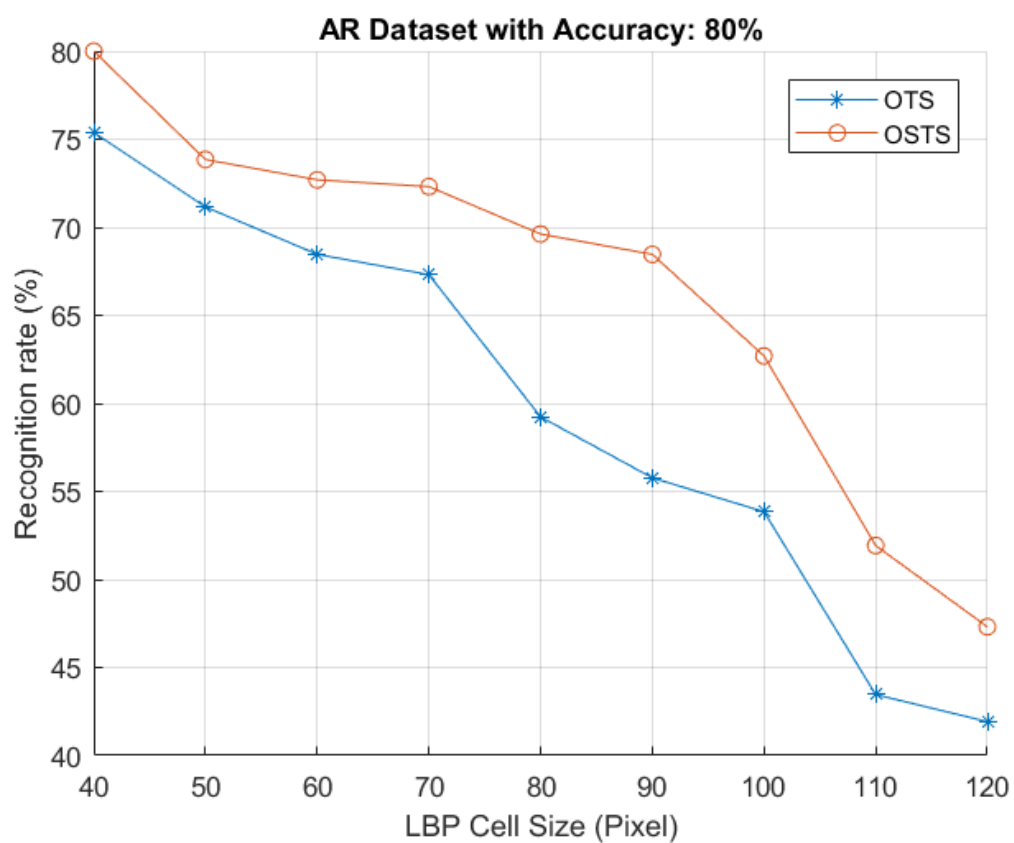


**Figure 4.8** The recognition rate using LBP with different cell size

#### 4.11.1.7 Experiment 7: LBP with a Small Cell Size

A small cell size for LBP which is 8x8 is selected to perform the recognition, although it takes time for training, it gives good results, the experiment is carried out using OSTs, the accuracy reaches 99.23% as shown in **Figure 4.9**.

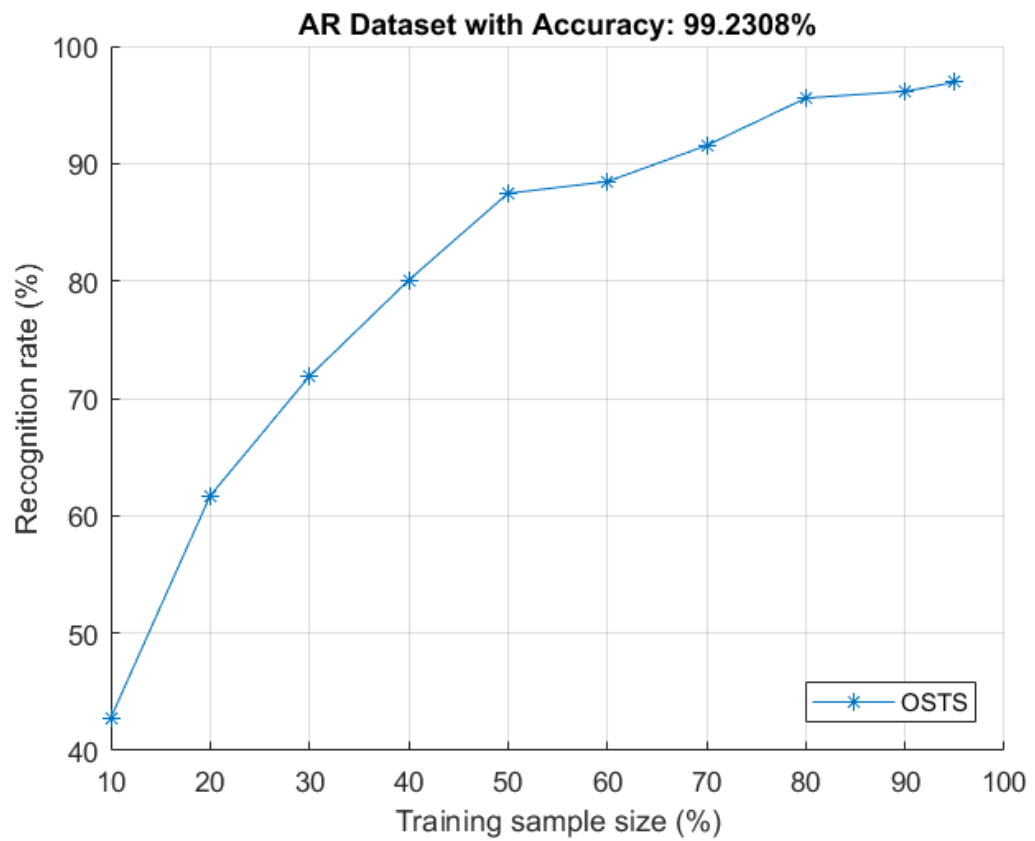


**Figure 4.9** The recognition rate using LBP with cell size of 8x8

#### 4.11.1.8 Experiment 8: HOG

In this experiment, the Histograms of Oriented Gradients HOG is used for feature extraction, this technique extracts a lot of feature from the image and produce a long feature vector that describe the information in the image. The results are shown in **Figure 4.10**.

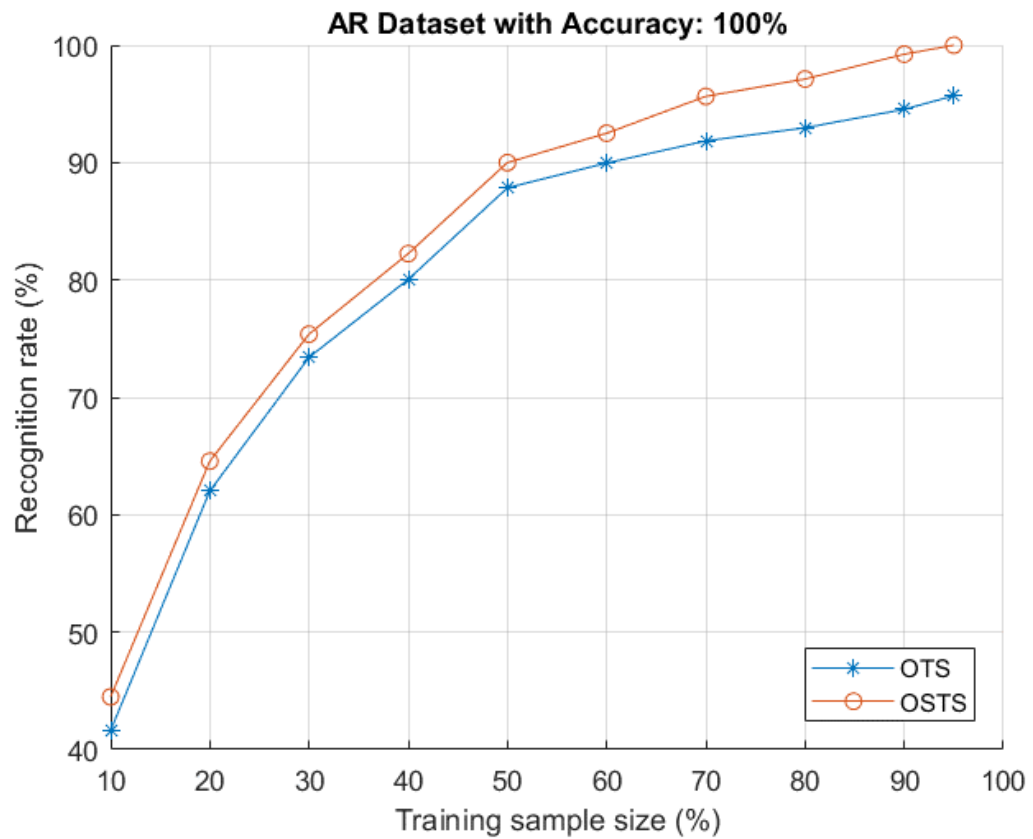


**Figure 4.10** The recognition rate using HOG for OTS and OSTs

#### 4.11.1.9 Experiment 9: Gabor

In this experiment, the Gabor Filter is used for feature extraction, the system is examined using OTS and OSTS, the results are illustrated in **Figure 4.11**.

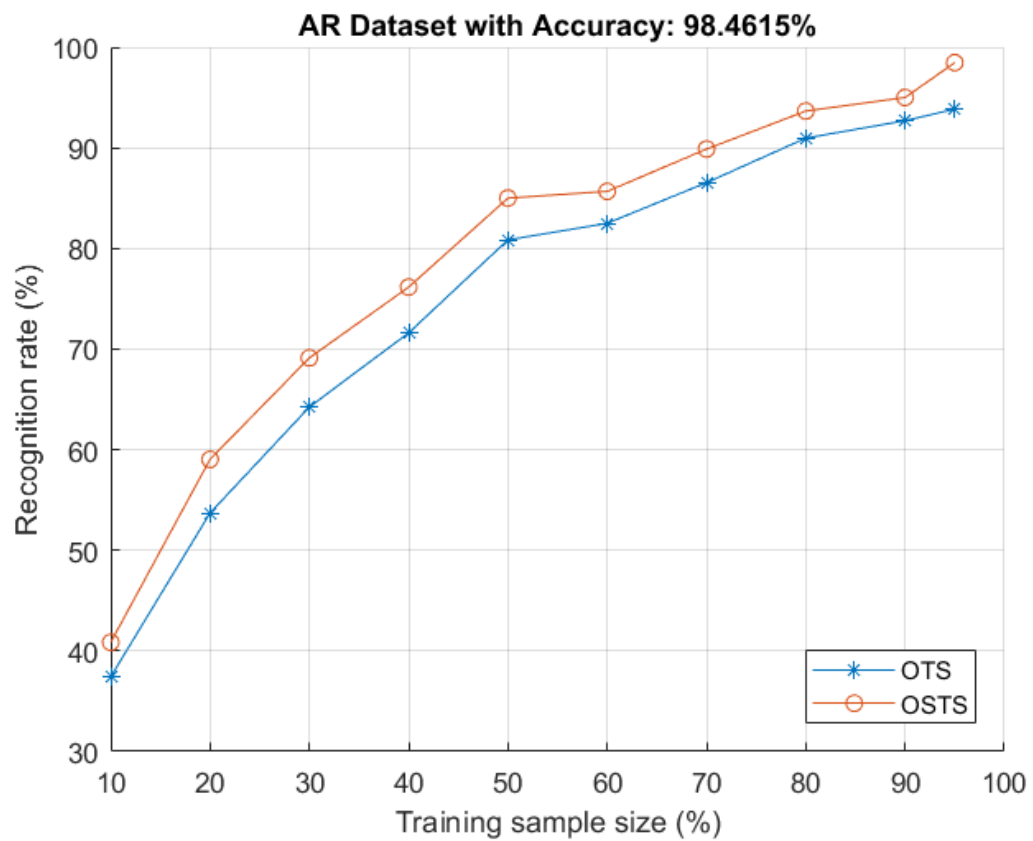


**Figure 4.11** The recognition rate using Gabor Filter

#### 4.11.1.10 Experiment 10: LBP, HOG and Gabor

The results of LBP with cell size of 8x8, HOG and Gabor using OSTs are compared, as shown in **Figure 4.12**.

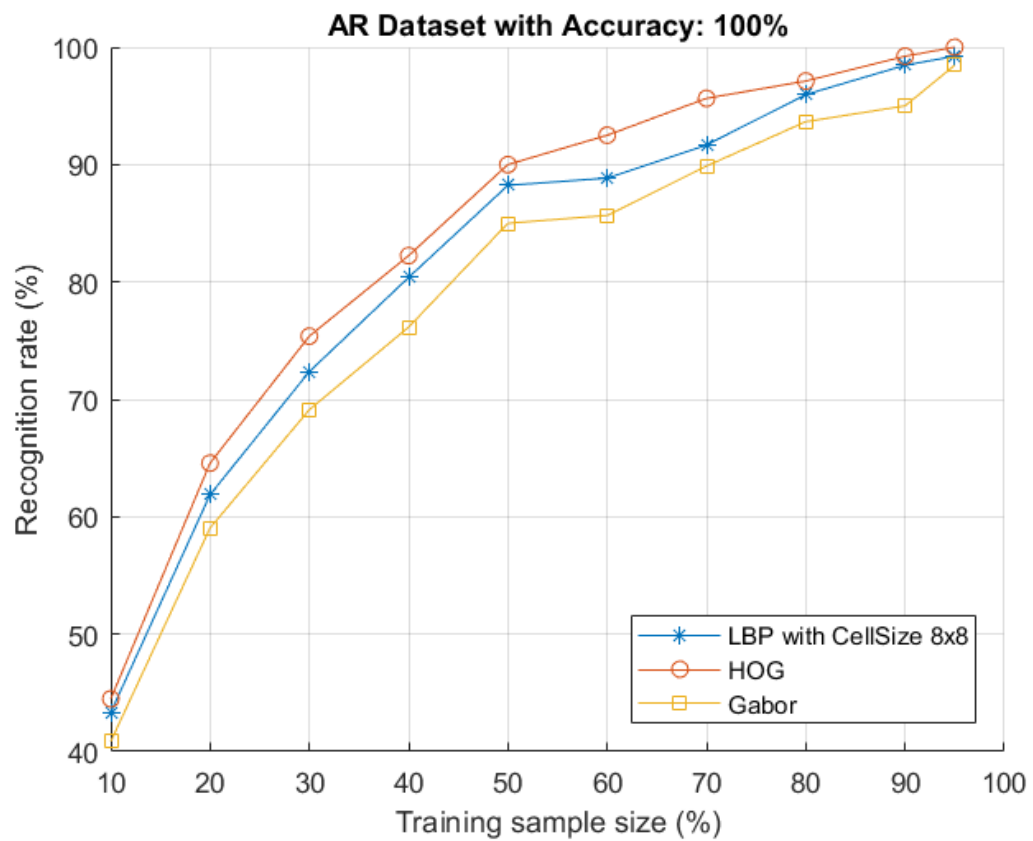


**Figure 4.12** The recognition rate using LBP with cell size of 8x8, HOG, and Gabor with OSTs

#### **4.11.1.11      *Experiment 11: GLPF LBP using OTS***

The results of LBP can be improved using a preprocessing stage which is GLPF, where the recognition rate is increased from about 42% to about 46% for OTS.

#### **4.11.1.12      *Experiment 12: GLPF LBP using OSTs***

The results of LBP can be improved using a preprocessing stage which is GLPF, where the recognition rate is increased from about 45% to about 48%. The experiment is carried out using OSTs.

#### **4.11.1.13      *Experiment 13: Using flipped images***

In this experiment, the flipped face images are used instead of symmetrical images, where the original face images are used along with the flipped one to train the system. The experiment is carried out using Gabor filter and HOG as feature extraction methods. The experimental results show that the use of the original images along with the flipped images performs better than using only the original images for training, but not as much as using the original with symmetrical images for training.

The obtained results for the previous experiments are summarized in **Table 4.3**.

As we can see from the table, as the number of training samples increase, the accuracy increases too. Also, the results using original with symmetrical samples are in general better than using the original samples alone.

The use of GLPF improves the accuracy of the LBP by about (3%), also, selecting a small size for LBP plays a significant role in improving accuracy, for instance, using a cell size of 8x8 increases the accuracy from (45%) to (99%).

In addition, the accuracy of GLCM is very low, although this can be improved using extended GLCM and extended normalized GLCM, still performs worse than other methods, nevertheless, it can be used to support other methods like LBP where the accuracy increases from (45%) using LBP up to (53%) using LBP with extended normalized GLCM.

Finally, the Gabor and HOG are performing well, where the accuracy is (98%) for Gabor, and the best result is obtained using HOG with accuracy (100%) using original with symmetrical images.

**Table 4.3** The recognition rates of the different methods on the AR dataset, using the OTS and the OSTs.

Preprocessing Method	Feature Extraction Method		Training set %									
			10	20	30	40	50	60	70	80	90	95
			Recognition Rate %									
No	LBP	OTS	13	18	20	24	28	29	33	34	38	42
		OSTS	14	20	23	28	31	32	33	36	38	45
GLPF	LBP	OTS	14	20	23	27	30	33	34	35	39	45
		OSTS	14	21	24	29	32	34	36	38	45	48
No	LBP 8x8	OTS	43	62	72	80	87	88	92	96	96	97
		OSTS	43	62	72	80	88	89	92	96	98	99
No	GLCM	OTS	5	5	6	6	7	7	7	8	9	9
		OSTS	6	7	8	8	9	10	11	12	14	15
No	Extended GLCM	OTS	5	6	6	7	8	8	10	11	12	13
		OSTS	5	7	8	9	10	11	12	13	16	17
No	Extended Norm. GLCM	OTS	5	6	6	6	7	8	10	11	14	15
		OSTS	6	8	10	11	11	13	13	15	19	22
No	LBP with Extended norm. GLCM	OTS	12	19	24	26	31	32	37	38	40	46
		OSTS	15	21	26	30	33	34	39	41	46	53
No	HOG	OTS	42	63	73	82	89	91	94	96	97	98
		OSTS	44	65	75	82	90	93	96	97	99	100
		Flip	43	64	73	72	89	92	93	96	96	99
No	Gabor	OTS	37	54	64	72	81	83	87	91	93	94
		OSTS	41	59	69	76	85	86	90	94	95	98
		Flip	38	56	65	73	81	85	87	92	95	95

#### 4.11.2 Experimental Results: Illumination and Occlusion

In this part, the AR dataset is divided into three groups, the first group includes the images that have illumination variation, the second group is for the images with sunglasses occlusion, and the last group is for the images with scarf occlusion.

#### 4.11.2.1 Experiment 14: Illumination

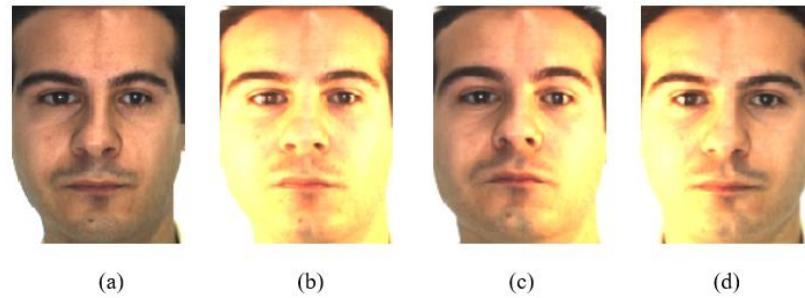


**Figure 4.13** Illumination difference. (a) normal illumination. (b) high illumination. (c) and (d) variations in illumination. (Example images from AR dataset)

In this experiment, the group of illumination variation is selected to test the system, an example is shown in **Figure 4.13**. The experiment is carried out using LBP with cell size 8x8, Gabor and HOG, the results are shown in **Figure 4.14**.

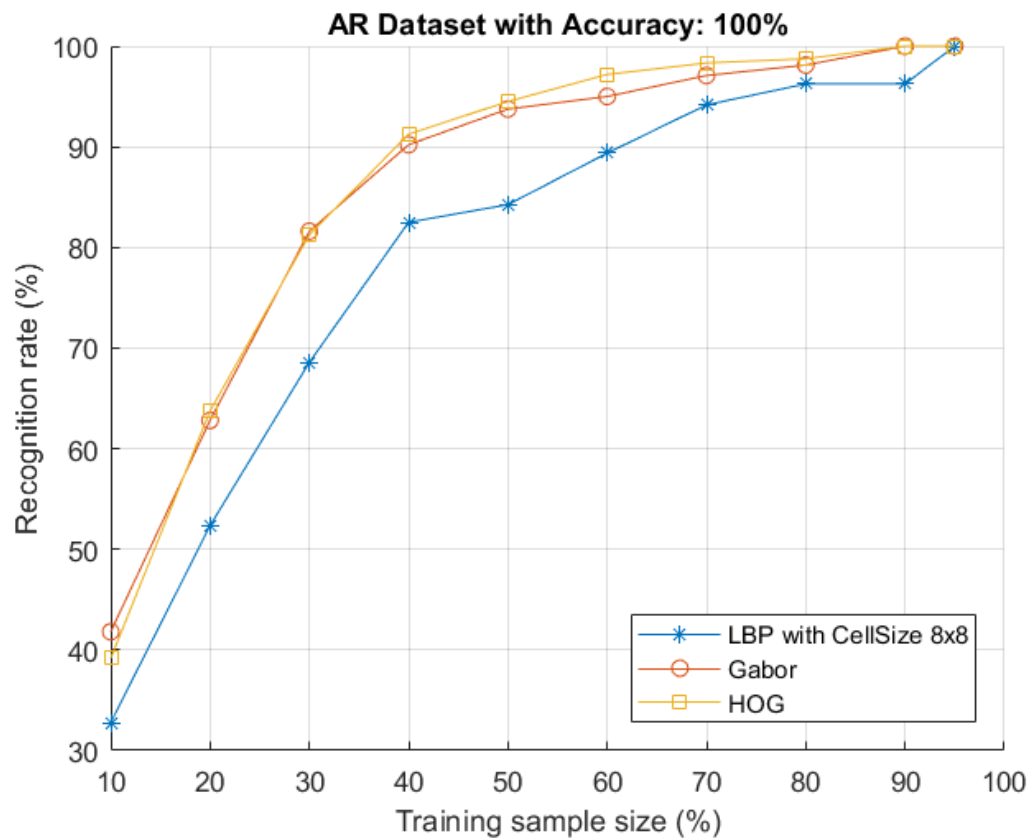


**Figure 4.14** The recognition rate using LBP 8x8, Gabor and HOG using images of illumination from AR dataset

#### 4.11.2.2 Experiment 15: Occlusion (Sunglasses)

In this experiment, the group of sunglasses occlusion is selected to test the system against occlusion, the methods LBP 8x8, Gabor and HOG are used for feature extraction, the results as in **Figure 4.15**.

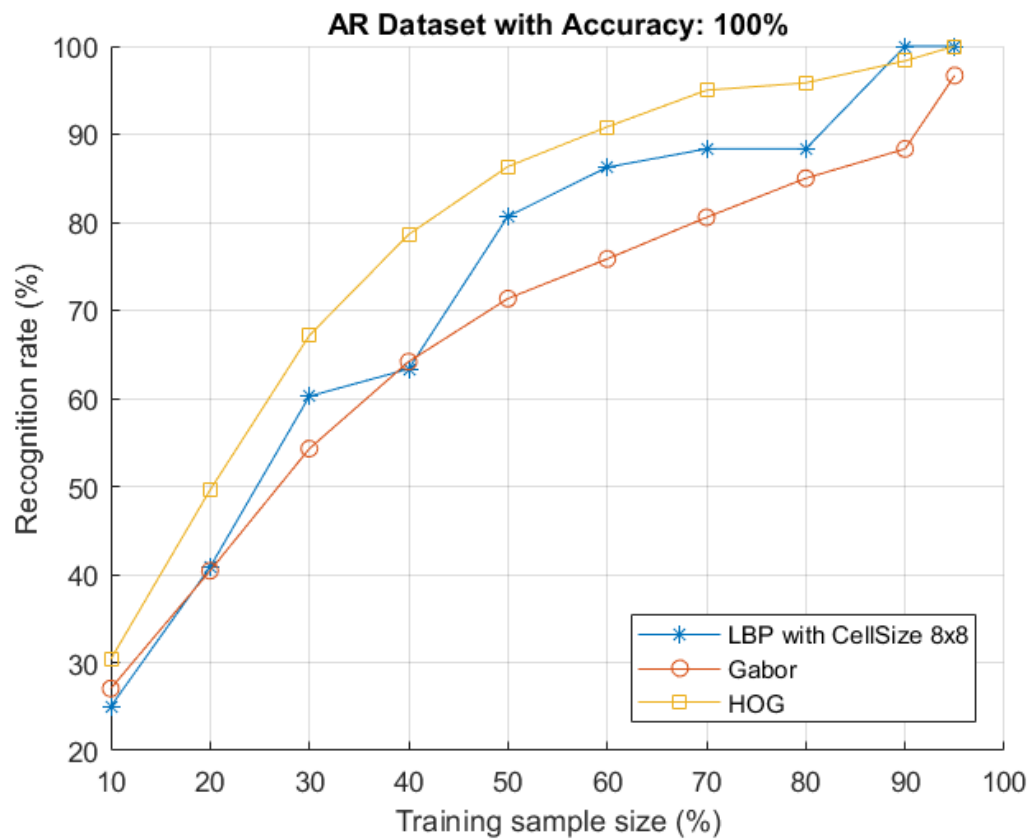


**Figure 4.15** The recognition rate using LBP 8x8, Gabor and HOG using images of occlusion (sunglasses) form AR dataset

#### 4.11.2.3 Experiment 16: Occlusion (Scarf)

In this experiment, the robustness of the recognition system is also tested against the occlusion using different extraction methods with images of scarf, the obtained result as in **Figure 4.16**.

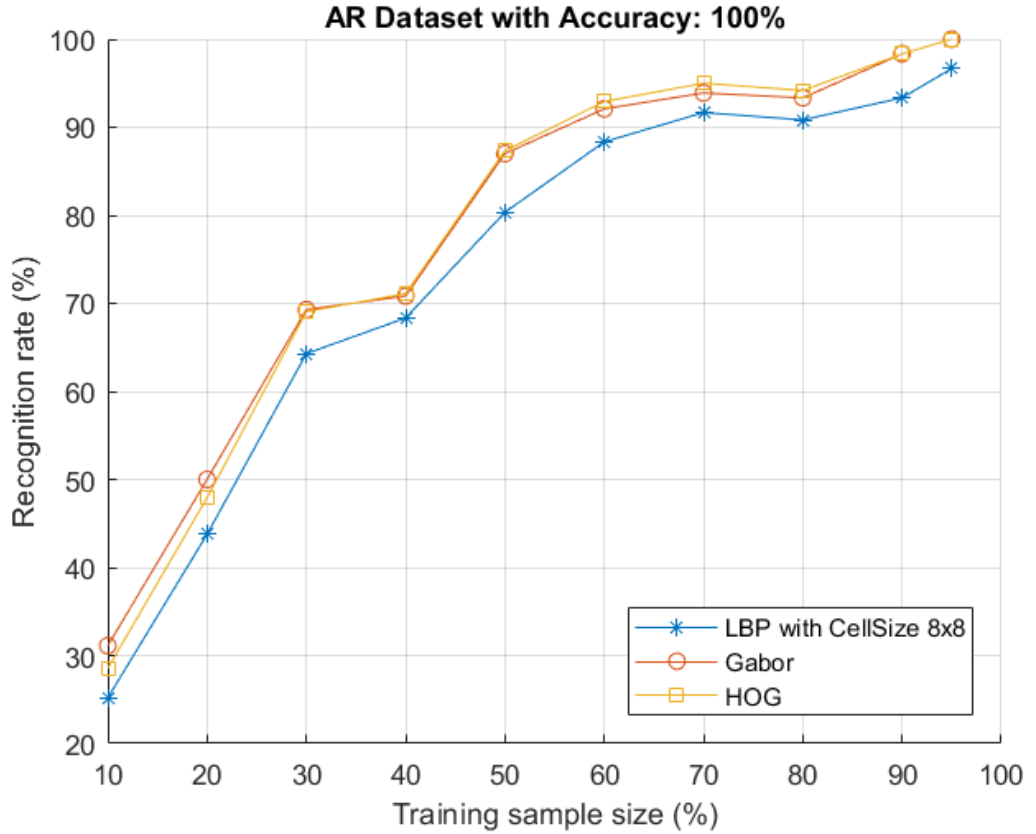


**Figure 4.16** The recognition rate using LBP 8x8, Gabor and HOG using images of occlusion (scarf) form AR dataset

In the previous three experiments, we select the best three methods among the methods that we have studied, these methods are LBP with cell size of 8x8, Gabor and HOG. These methods are implemented for some part of AR dataset with illumination variations and occlusions, and from **Figure 4.14**, **Figure 4.15** and **Figure 4.16** the three methods are performing well and we can conclude the following:

For the images with illumination variations: for 95% of the data as training, the three methods give accuracy of (100%), but for smaller size of training samples, the LBP

with cell size of  $8 \times 8$  performs less than the other two methods (Gabor and HOG). the performance of Gabor and HOG are close to each other.

In addition, the occlusion with sunglasses, the best results are obtained using HOG, while the occlusions with scarf, the performance of Gabor and HOG are close to each other and perform better than the LBP with cell size of  $8 \times 8$  but still HOG performs better. Therefore, for this reason we recommend using HOG.

# CHAPTER 5

## SYMMETRY IN FEATURE DOMAIN

### 5.1 Feature Extraction using Image Stripes (FEIS)

The aim of using the feature extraction methods is to transfer the image from the image space to a feature space. For a specific feature extraction method, the extracted features set for a unique image should be also a unique. The features of the image are another way to represent the image since they can be used easier in the image processing systems than using the images.

In this thesis, a new feature extraction method is introduced. The idea of this method is inspired by the LBP algorithm mechanism, where LBP using a circle to formulate the features, as explained in section 3.2.2, this method uses lines or (image stripes) as shown in **Figure 5.3**, so we call it Feature Extraction using Image Stripes (FEIS).

The FEIS depends, like the most of feature extraction methods, on the relation between the pixel of interest and its neighbors. This method also transforms the image from the images space to the feature space but the extracted features using this method have a very interesting characteristic which is implementing the use of symmetry in the feature domain, as it is explained in section 5.1.2. This is not exist for the features that are extracted using the traditional methods.

If an image  $A$  with pixels with gray level values  $g_{11}, g_{12} \dots g_{mn}$  such as:

$$A_{mn} = \begin{pmatrix} g_{11} & g_{12} & \cdots & g_{1n} \\ g_{21} & g_{22} & \cdots & g_{2n} \\ \vdots & \vdots & \ddots & \vdots \\ g_{m1} & g_{m2} & \cdots & g_{mn} \end{pmatrix}$$

The image  $A$  is converted to a vector  $\vec{A}$  so that:

$$\vec{A} = (g_{11} \ g_{21} \ \cdots \ g_{m1} \ g_{12} \ g_{22} \ \cdots \ g_{m2} \ \cdots \ g_{1n} \ g_{2n} \ \cdots \ g_{mn})$$

The binary result can be obtained by defining a function  $S$  which compares each element  $g_i$  in  $\vec{A}$  with its neighbor  $g_{i-1}$  as:

$$S(\vec{A}) = S(g_i - g_{i-1}) = \begin{cases} 1, & g_i \geq g_{i-1} \\ 0, & g_i < g_{i-1} \end{cases} \quad (5.1)$$

where  $S$  is a sign function, then by assigning a binomial factor  $2^i$  for each  $S(g_i - g_{i-1})$  and introducing a new variable  $\lambda$ , such as  $\lambda$  is the length of the sub-vector from vector  $S(\vec{A})$  that is being converted to a decimal value, the method of Feature Extraction using Image Stripes (FEIS) is achieved as:

$$FEIS = \sum_{i=0}^{\lambda-1} S(g_i - g_{i-1}) 2^i \quad (5.2)$$

If  $A(5 \times 3)$  is an image with pixel values as shown in **Figure 5.1**

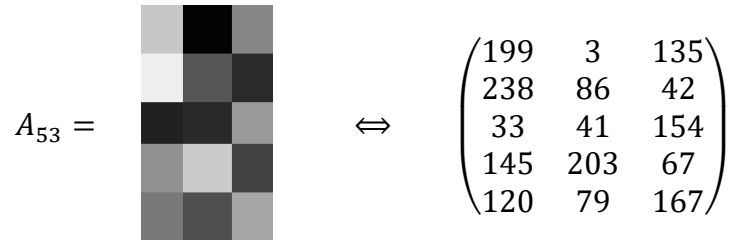


**Figure 5.1** An example of an image

Then the vector  $\vec{A}$  is given as:

$$\begin{aligned} \vec{A} \\ = [199 \ 238 \ 33 \ 145 \ 120 \ 3 \ 86 \ 41 \ 203 \ 79 \ 135 \ 42 \ 154 \ 67 \ 167] \end{aligned}$$

And the binary result  $S(\vec{A})$  can be obtained as:

$$S(\vec{A}) = [1 \ 1 \ 0 \ 1 \ 0 \ 0 \ 1 \ 0 \ 1 \ 0 \ 1 \ 0 \ 1 \ 0 \ 1]$$

For  $\lambda = 5$ :

$$s(\vec{A}) = \left[ \underbrace{1 \ 1 \ 0 \ 1 \ 0}_{26} \quad \underbrace{0 \ 1 \ 0 \ 1 \ 0}_{10} \quad \underbrace{1 \ 0 \ 1 \ 0 \ 1}_{21} \right]$$

$$FEIS(\lambda = 5) = [26 \ 10 \ 21]$$

The extracted features depend on the value of  $\lambda$ , as the value of  $\lambda$  is changed, the number and values of extracted features are changed too.

For  $\lambda = 3$ :

$$s(\vec{A}) = \left[ \underbrace{1 \ 1 \ 0}_6 \quad \underbrace{1 \ 0 \ 0}_4 \quad \underbrace{1 \ 0 \ 1}_5 \quad \underbrace{0 \ 1 \ 0}_2 \quad \underbrace{1 \ 0 \ 1}_5 \right]$$

$$FEIS(\lambda = 3) = [6 \ 4 \ 5 \ 2 \ 5]$$

**Figure 5.2** shows the extracted features for different values of  $\lambda$

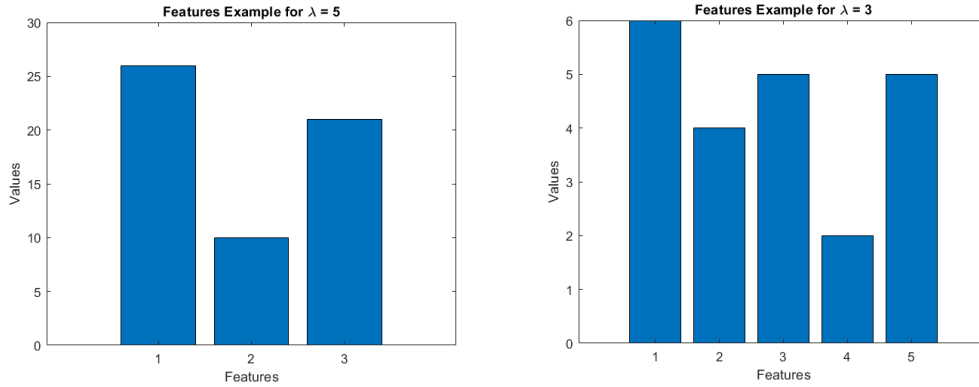


**Figure 5.2** An example of extracted features for different values of  $\lambda$

For a real image from ORL dataset as shown in **Figure 5.3** (a) and its stripes **Figure 5.3** (b), the features can be extracted using the previous steps, the resulting features are shown in **Figure 5.4**.



**Figure 5.3** The original image (a), and its stripes (b), (Example image from ORL dataset)

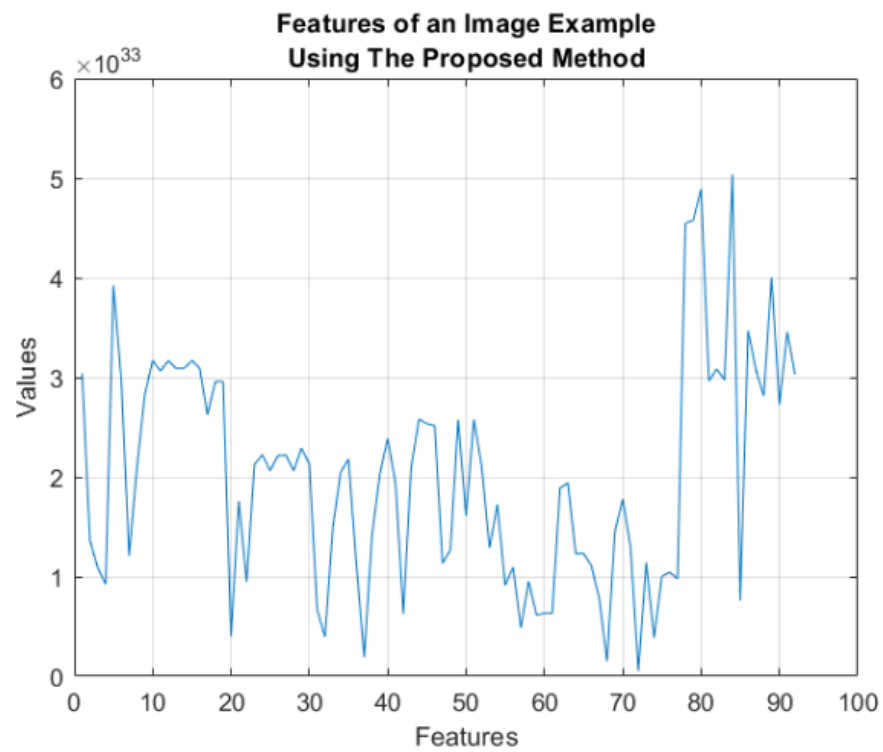


**Figure 5.4** Features example for an image from ORL dataset

The obtained feature vector of the image also depends on the value of  $\lambda$  that is selected as shown in **Figure 5.5**.

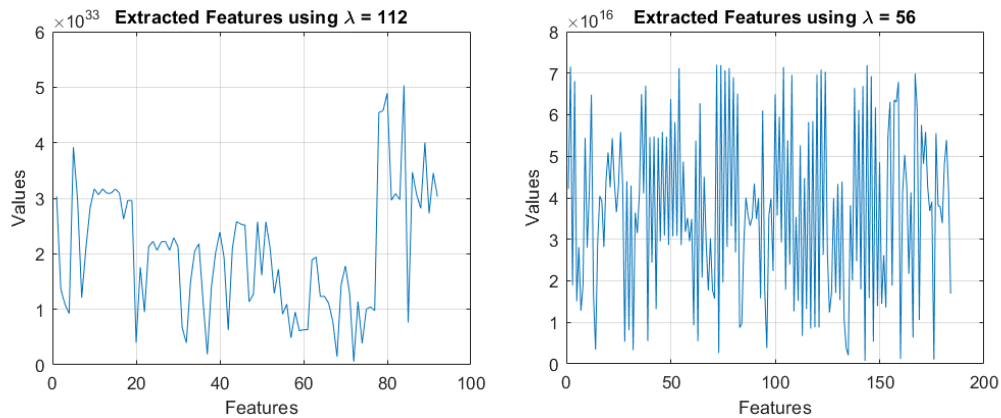


**Figure 5.5** Different sets of features using different values of  $\lambda$

### 5.1.1 The FEIS method and symmetry

The traditional symmetry procedure can be implemented in the image space by integrating the mirrored face halves (left and right) with the corresponding one as shown in **Figure 5.6**.

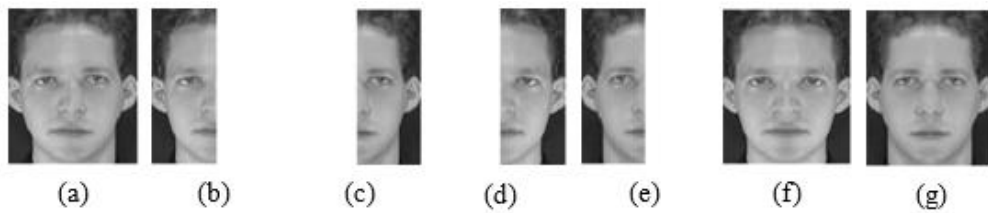


**Figure 5.6** Original image, b) left side, c) right side, d) mirror of left side, e) mirror of right side, f) integrating left side with mirror, g) integrating right side with mirror

The features of the three images (original and two generated ones) can be extracted using the known feature extraction methods such as LBP, GLCM, Gabor and HOG and this gives three sets of features. As stated in the previous chapter. **Figure 5.7** shows the symmetry procedure in the image domain.

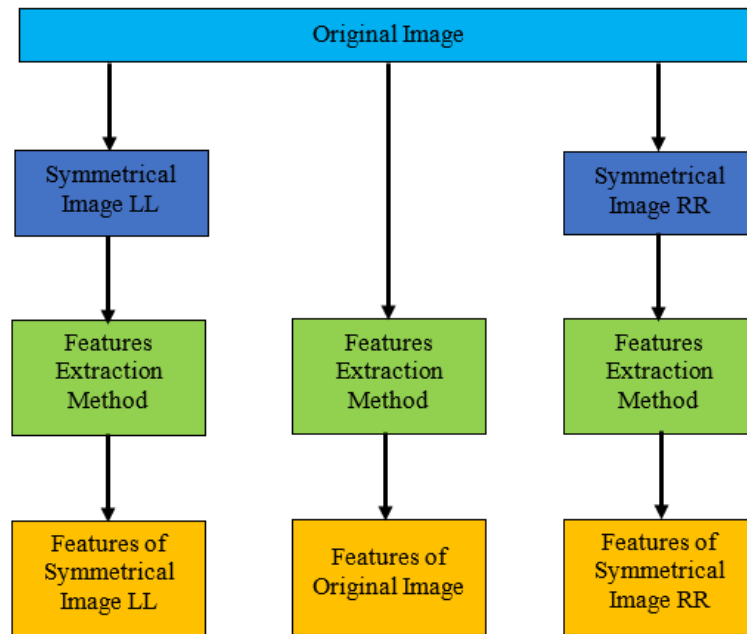


**Figure 5.7** The symmetry procedure in the image space

The only way that exists to do the symmetry procedure is to be implemented in the image space, it means, generating new images using the symmetry property of the face then extracting the features from the original and generated images.

### 5.1.2 The symmetry procedure in the features space

The proposed method is the first method that can be used to implement the symmetry procedure in the feature space as in **Figure 5.8**.

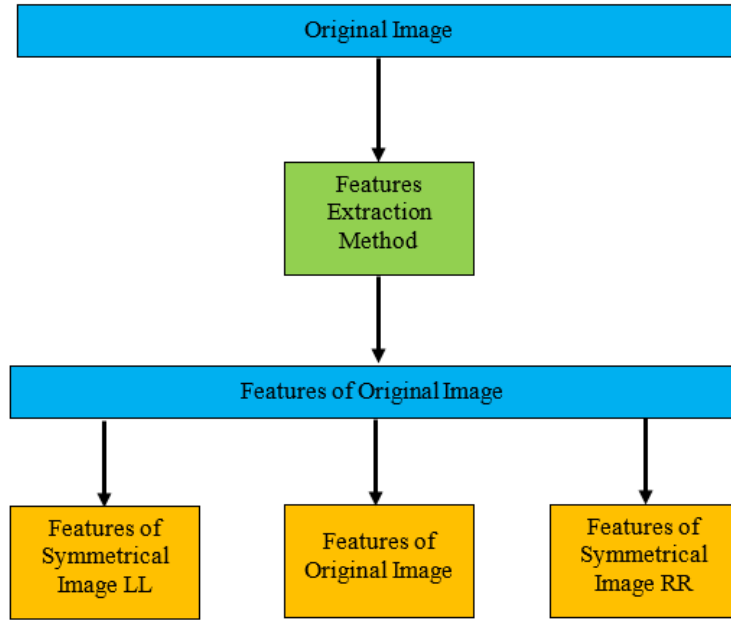


**Figure 5.8** The symmetry procedure in the features space

All the known feature extraction methods have no facility to do the symmetry procedure in the feature space since their transformation from the image space to the feature space is a nonlinear transformation. Such a procedure can also be implemented in the features space in an easy way; this can be achieved only by using the proposed method.

For simplicity, we call the feature vector of the original image as the parent feature vector as in **Figure 5.9**, from this feature vector, we generate two feature vectors and we call them as children vectors as in **Figure 5.10**.

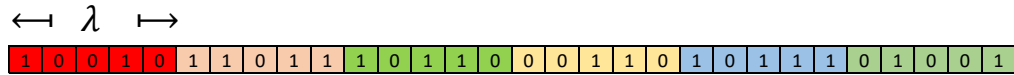


**Figure 5.9** The features of the original image (parent)

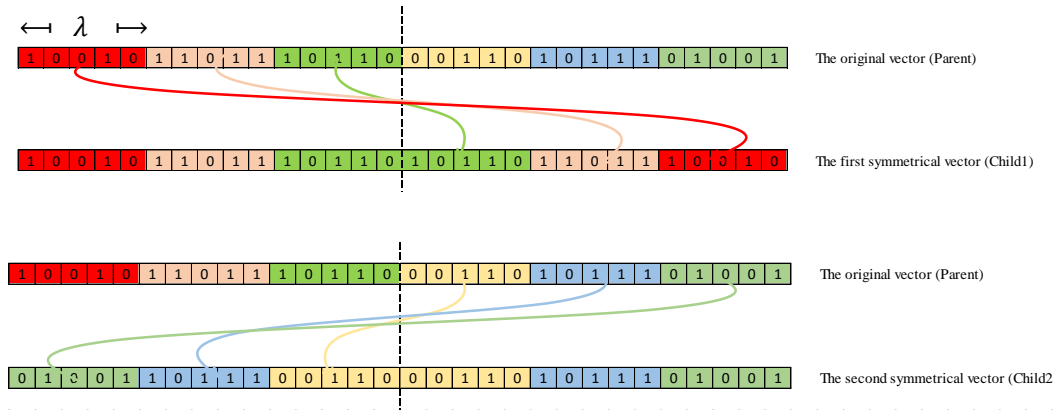


**Figure 5.10** Generating the symmetrical features (children) from the original features (parent)

The vectors of parent and children are used to calculate the features of the original and symmetrical features respectively.

### 5.1.3 The FEIS method for face recognition

The face recognition system is implemented using the proposed method. First, the procedure is carried out using only the features of the original face images. Then the procedure is repeated using the symmetrical features. And finally, the recognition rates are compared with the results obtained from using the methods in the literature. In addition, different values of  $\lambda$  are tested with different training set sizes.

### 5.1.4 The effect of $\lambda$ on recognition rates

Some experiments are implemented to examine the effect of  $\lambda$  on recognition rates. The experiments are carried out using original features and original with symmetrical features using images from AR dataset. The results show that the value of  $\lambda$  has an impact effect on the recognition rates, since a small chosen value of  $\lambda$  leads to a better recognition rates as shown in **Figure 5.11** to **Figure 5.14**. All the results are summarized in **Table 5.1** and **Table 5.2**.

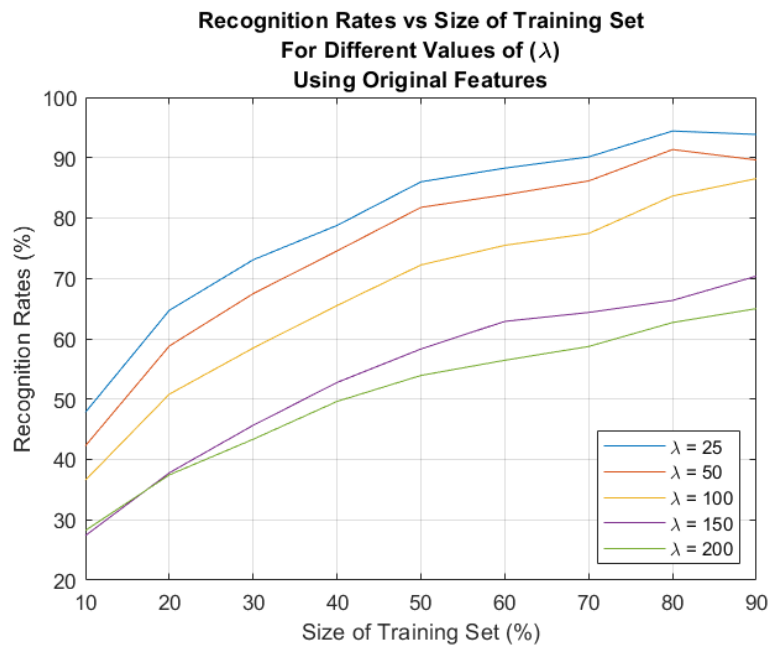


**Figure 5.11** Recognition rates vs size of training set for different values of  $\lambda$  using original features



**Figure 5.12** Recognition rates vs size of training set for different values of  $\lambda$  using original with symmetrical features

For the second part of the experiments, different values of  $\lambda$  is examined using training set sizes 70%, 80% and 90% respectively. The experiments are implemented using original features and original with symmetrical features, as shown in **Figure 5.13** and **Figure 5.14**.

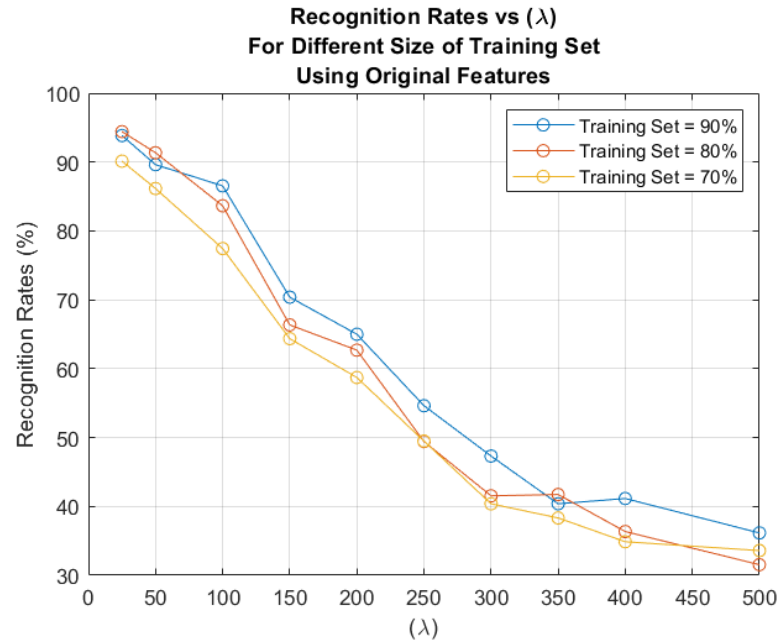


**Figure 5.13** Recognition rates vs  $\lambda$  for different sizes of training set using original features

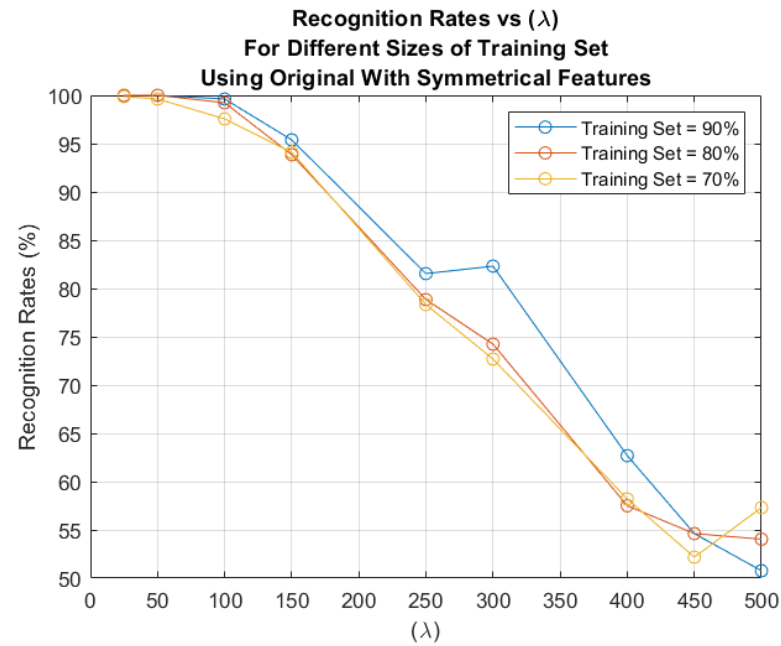


**Figure 5.14** Recognition rates vs  $\lambda$  for different sizes of training set using original with symmetrical features

The obtained results are summarized in **Table 5.1** and **Table 5.2**.

**Table 5.1** The results using original features with different values of  $\lambda$  and different training sample sizes

Training set %	Values of $\lambda$								
	1	3	5	10	25	50	100	150	200
	Accuracy %								
10	51.75	51.75	49.53	49.53	47.82	42.27	36.58	27.39	28.25
20	69.62	69.62	67.69	67.69	64.71	58.80	50.82	37.79	37.45
30	78.02	78.02	76.87	76.59	73.08	67.47	58.46	45.66	43.35
40	82.56	82.56	82.12	82.12	78.78	74.55	65.51	52.76	49.62
50	90.77	90.77	89.46	89.46	86.00	81.77	72.23	58.31	53.92
60	92.31	92.31	90.77	90.77	88.27	83.85	75.48	62.88	56.44
70	93.59	93.59	92.44	92.31	90.13	86.15	77.44	64.36	58.72
80	96.35	96.35	95.38	94.81	94.42	91.35	83.65	66.35	62.69
90	96.35	96.35	96.15	96.15	93.85	89.62	86.54	70.38	65.00

**Table 5.2** The results using original with symmetrical features with different values of  $\lambda$  and different training sample sizes

Training set %	Values of $\lambda$							
	1	3	5	10	25	50	100	150
	Accuracy %							
10	88.46	88.46	86.62	85.85	83.21	79.57	69.87	59.19
20	96.30	96.30	95.72	95.38	94.47	91.30	84.81	73.85
30	98.35	98.35	97.75	97.69	97.14	95.49	90.99	82.20
40	99.23	99.23	99.23	98.85	98.65	97.24	94.17	87.18
50	99.69	99.62	99.54	99.54	99.23	98.69	96.00	90.62
60	99.71	99.62	99.62	99.52	99.23	98.65	96.35	92.31
70	100.00	100.00	100.00	100.00	99.87	99.62	97.56	94.10
80	100.00	100.00	100.00	100.00	100.00	100.00	99.23	93.85
90	100.00	100.00	100.00	100.00	100.00	100.00	99.62	95.38

### 5.1.5 Comparing the FR performance using the original features and the FR performance using the original with symmetrical features

In this experiment, the performance of the FR system using the original features is compared with the performance of the FR system using the original with symmetrical features. The experiments are carried out using images from AR dataset and the comparison is implemented using two values of ( $\lambda$ ) when  $\lambda = 25$  and when  $\lambda = 50$ . The results as shown in **Figure 5.15**.

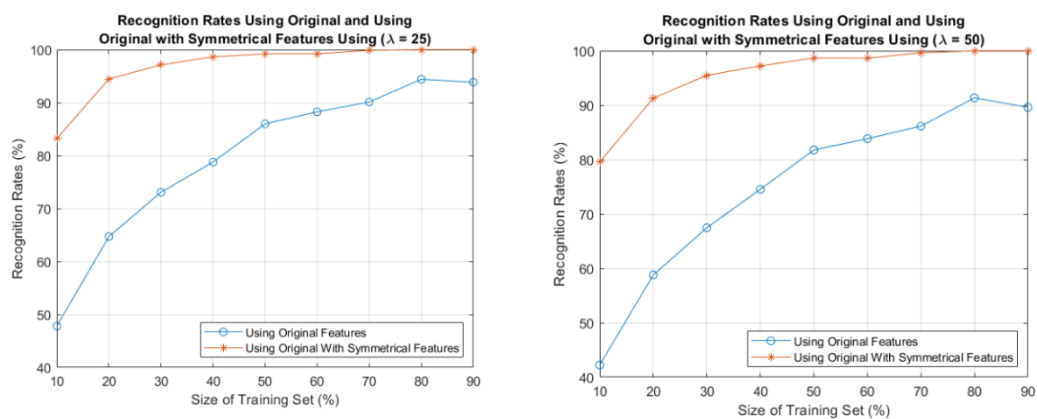


**Figure 5.15** The FR performance using the original features and the FR performance using the original with symmetrical features for different values of  $\lambda$

### 5.1.6 The speed of the proposed method compared with other methods

In this experiment, the speed of extracting the features for one image using the proposed method is measured and compared with other methods, these methods are LBP, GLCM, Gabor and HOG. An image with size 112x92 from ORL dataset is used for this test as shown in **Figure 5.16**. The experiment is carried out using a laptop computer equipped with an Intel Core i7-7700HQ CPU @ 2.80 GHz and 16 GB of memory; GPU acceleration is not used. The test results are shown in **Figure 5.17** and **Table 5.3**.



**Figure 5.16** A 112x92 image from ORL dataset used for speed test

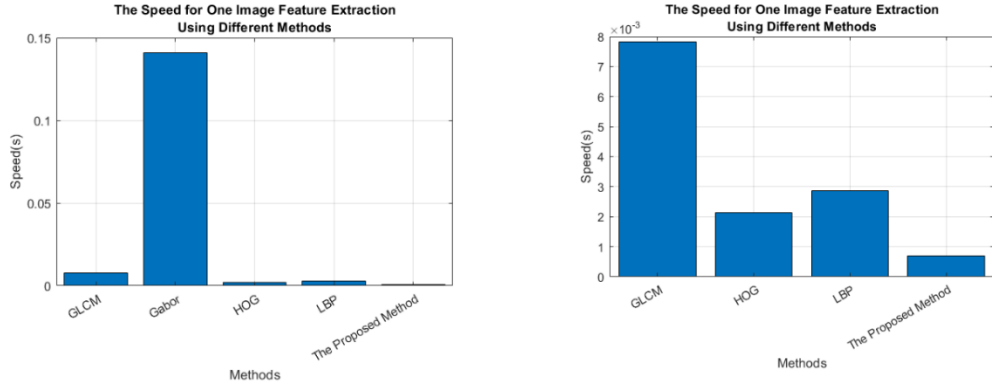


**Figure 5.17** The speed of the proposed method compared with other methods

**Table 5.3** The speed of the proposed method compared with other methods

Method	LBP	GLCM	Gabor	HOG	The propose method
Time(s)	$2.87 \times 10^{-3}$	$7.82 \times 10^{-3}$	$1.41 \times 10^{-1}$	$2.14 \times 10^{-3}$	$7.07 \times 10^{-4}$

### 5.1.7 The performance of the FR system using the proposed method compared with the other methods

The performance of the proposed method when  $\lambda = 25$  is compared with the performances of some FR methods. From the experimental results show that the recognition accuracy of the original proposed method FEIS (without using symmetry) reaches (93.85%) and this accuracy is higher than Support Vector Machine (SVM) [30], with accuracy of (55.8%), Sparse representation based classification (SRC) [44] with (80.8%) and Discriminative Multi Manifold Analysis (DMMA) [128] (92.1%).

Although the original proposed method FEIS method is perform less than collaborative probabilistic labels (CPL) [129] (94.2%) and local structure based multi-phase collaborative representation classifier (LSMPCRC) [130] (98.9%), the upgraded FEIS (using symmetry in feature domain) reaches (100%) which is higher than those methods. Using AR dataset, the best performance of the proposed method is compared with the best performance of other methods as shown in **Table 5.4**.

**Table 5.4** The performance of the proposed method compared with other methods

Method	Accuracy %
Support Vector Machine (SVM) [30]	55.8
Sparse Representation based Classifier (SRC) [44]	80.8
Discriminative Multi-Manifold Analysis (DMMA) [128]	92.1
Collaborative Probabilistic Labels (CPL) [129]	94.2
Local Structure Based Multi-phase Collaborative Representation Classifier (LSMPCRC) [130]	98.9
LBP 8x8 (OSTS)	99
HOG (OSTS)	100
Gabor (OSTS)	98
Proposed Method 1: Original Features	93.85
Proposed Method 2: Original with Symmetrical Features	100

For the sake of completeness, the performance of FEIS method using the symmetry in feature space is examined using all datasets, ORL, Yale and AR with different possibilities of training samples. The results are compared with the best results that we have obtained using symmetry in image domain, LBP 8x8, LBP-GLCM, Gabor and HOG. Also, the proposed method is compared with the results of the methods in the literature CRC [127], SRC [44], and SCRC [5, 6]. Moreover, the results are compared with the state-of-the-art Deep Metric Learning (DML) using residual network ResNet 34 model [89] based features. The experiments for FEIS are carried out using  $\lambda = 1$ .

The obtained results are summarized in **Table 5.5**, **Table 5.6** and **Table 5.7**.

**Table 5.5** The recognition rates of the FEIS method on the ORL dataset compared with the other methods.

Feature Extraction Method	No. of Training Images								
	1	2	3	4	5	6	7	8	9
	Recognition Rate %								
FEIS	87.5	95	97.5	95	100	100	100	97.5	100
DML	98	99	100	100	100	100	100	100	100
LBP-GLCM	72.5	85	90	95	95	97.5	97.5	100	100
Gabor	90	97.5	100	100	100	100	100	100	100
CRC [127]	72	84	86	91	91	94	93	94	93
SRC [44]	76	89	90	94	94	94	95	96	95
SCRC [5, 6]	76	90	92	94	94	95	96	96	95

**Table 5.6** The recognition rates of the FEIS method on the Yale dataset compared with the other methods.

Feature Extraction Method	No. of Training Images									
	1	2	3	4	5	6	7	8	9	10
	Recognition Rate %									
FEIS	94	99	100	100	100	100	100	100	100	100
DML	100	100	100	100	100	100	100	100	100	100
LBP	95	98	100	100	100	100	100	100	100	100
Gabor	97	100	100	100	100	100	100	100	100	100
CRC [127]	87	93	94	99	98	96	98	95	96	100
SRC [44]	87	90	90	98	92	92	98	100	100	100
SCRC [5, 6]	88	95	97	99	100	100	100	100	100	100

**Table 5.7** The recognition rates of the FEIS method on the AR dataset compared with the other methods.

Feature Extraction Method	Training set %								
	10	20	30	40	50	60	70	80	90
	Recognition Rate %								
FEIS	88	96	98	99	100	100	100	100	100
DML	90	94	98	99	100	100	100	100	100
LBP 8x8	43	62	72	80	88	89	92	96	98
HOG	44	65	75	82	90	93	96	97	99
Gabor	41	59	69	76	85	86	90	94	95
CRC [5, 127]	76	77	78	78	78	78	78	78	78
SRC [5, 44]	72	74	74	74	75	74	74	75	75
SCRC [5, 6]	77	80	81	81	80	81	81	80	81

From **Table 5.5**, **Table 5.6** and **Table 5.7** the FEIS performs well as a new feature extraction method. It is fast because it is based on one-pixel comparison, with higher recognition rates than other methods except DML. Although, the FEIS, in some cases, performs less than DML, it is very fast compared with the DML, since, for each pixel it needs to do only one comparison operation to construct the result, not like the DML which is more complex than the FEIS and takes more time to process the features.

# CHAPTER 6

## CONCLUSION AND FUTURE WORK

In this thesis, a complete system for face recognition based on original and symmetrical training data is proposed.

Although there are many face recognition systems proposed, these systems are not robust against the limited number of training sets in addition with the effect of illumination and pose variations. This thesis presents an effective method to overcome the restricted number of the face training images using the symmetry property of the face. Moreover, the use of this property also reduces the effect of illumination and pose variations.

In order to increase the accuracy of the face recognition rates, and also to eliminate the above-mentioned drawbacks, first, we generate a new set of face images using the left and right halves of each face. Second, we use the original and generated face images to training the face recognition system.

The original and generated face images are preprocessed before extracting their features. This procedure is achieved using the 2-D DWT, GLPF, and DoG. Then the features of these samples are extracted using the LBP, the GLCM, the Gabor Filter and the HOG methods. Finally, the Euclidean Distance and Cosine similarity classifiers are used to obtain the results of the recognition. The proposed method is examined and tested using three of benchmarks datasets. The proposed method is tested against a number of well-known methods in the literature and a superior performance is obtained against these methods.

On the other hand, the use of the GLCM alone is not recommended, but it could support the performance of the LBP by using the combined features from both methods. It could be well-observed that combining features from different methods provided a better performance, as opposed to using a single method. The Gabor filter and HOG are indeed very helpful tools in FR. This thesis also showed that the use of

the preprocessing stage in the recognition system improved the accuracy of the face recognition, as compared to not using any of the preprocessing stages.

Although the method is especially effective when the set of training samples is small, it took more time to process the increased number of training samples.

In this thesis, a new method for feature extraction is also proposed, this method uses the stripes of the image to extract the features, so we call it Feature Extraction using Image Stripes (FEIS). The FEIS method has the ability to do the symmetry procedure either in the image space or in the feature space, thence the feature space is another way to achieve the benefit of using the symmetry property of the face to improve the recognition rates. Although, there lots of methods for feature extraction are presented, none of them can utilize the symmetry property in the feature space. The FEIS method is the first proposed method can do that in both feature and image spaces. The FEIS method is examined and tested for face recognition using data from ORL and AR dataset and experimental results shows that it has a performance higher than methods in the literature. In addition, the speed of the FEIS method is measured and compared with other methods (LBP, GLCM, Gabor Filter, and HOG) and found that it is faster than these methods.

## **6.1 Future Directions**

As a future work, we first plan to run our system on more datasets to show the robustness of the proposed methods.

In order to improve our classifier and also the performance of the system, the Convolutional Neural Network (CNN) can be used for huge datasets. Since ORL, Yale and AR are not huge datasets.

In addition, we aim to upgrading the FEIS algorithm to be based on the gradient of the pixies' values as in HOG.

Also, we need to do more study concerned with the effects of the mutation and crossover operations for the parent genes of the image that are obtained using FEIS method.

Moreover, the idea of using the reflected images along with the original and symmetrical images to increase the size of the dataset by generating more images and hence adding more improvement to the system performance.

Lastly, the feature extraction methods like FEIS, LBP and Gabor can be improved by new optimization methods like Crow search, Cow search, whale search algorithm.

## REFERENCES

- [1] Vallabh, H., "Authentication using finger-vein recognition," University of Johannesburg, 2012.
- [2] Yousefi, F., "Analysis of methods for finger vein recognition," *MIDDLE EAST TECHNICAL UNIVERSITY*, 2013.
- [3] Ahonen, T., Hadid, A., & Pietikainen, M., "Face description with local binary patterns: Application to face recognition," *IEEE transactions on pattern analysis and machine intelligence*, vol. 28, pp. 2037-2041, 2006.
- [4] Tan, X., Chen, S., Zhou, Z.-H., & Zhang, F., "Face recognition from a single image per person: A survey," *Pattern Recognition*, vol. 39, pp. 1725-1745, 2006/09/01/ 2006.
- [5] Liu, Z., Pu, J., Wu, Q., & Zhao, X., "Using the original and symmetrical face training samples to perform collaborative representation for face recognition," *Optik-International Journal for Light and Electron Optics*, vol. 127, pp. 1900-1904, 2016.
- [6] Peng, Y., Li, L., Liu, S., Lei, T., & Wu, J., "A New Virtual Samples-Based CRC Method for Face Recognition," *Neural Processing Letters*, vol. 48, pp. 313-327, August 01 2018.
- [7] Liu, L., Fieguth, P., Guo, Y., Wang, X., & Pietikäinen, M., "Local binary features for texture classification: Taxonomy and experimental study," *Pattern Recognition*, vol. 62, pp. 135-160, 2017.
- [8] Julsing, B., "Face recognition with local binary patterns," *Research No. SAS008-07, University of Twente, Department of Electrical Engineering, Mathematics & Computer Science (EEMCS)*, 2007.
- [9] Ahonen, T., Hadid, A., & Pietikäinen, M., "Face recognition with local binary patterns," in *Computer vision-eccv 2004*, 2 ed: Springer, 2004, pp. 469-481.
- [10] Yang, P. & Yang, G., "Feature extraction using dual-tree complex wavelet transform and gray level co-occurrence matrix," *Neurocomputing*, vol. 197, pp. 212-220, 7/12/ 2016.
- [11] Sun, Y. & Yu, J., "Facial Expression Recognition by Fusing Gabor and Local Binary Pattern Features," in *International Conference on Multimedia Modeling*, 2017, pp. 209-220.
- [12] Ojala, T., Pietikäinen, M., & Mäenpää, T., "Multiresolution gray-scale and rotation invariant texture classification with local binary patterns," *Pattern Analysis and Machine Intelligence, IEEE Transactions on*, vol. 24, pp. 971-987, 2002.

- [13] Arabi, P. M., Joshi, G., & Deepa, N. V., "Performance evaluation of GLCM and pixel intensity matrix for skin texture analysis," *Perspectives in Science*, vol. 8, pp. 203-206, 2016.
- [14] Li, W., Mao, K., Zhang, H., & Chai, T., "Designing compact Gabor filter banks for efficient texture feature extraction," in *2010 11th International Conference on Control Automation Robotics & Vision*, 2010, pp. 1193-1197.
- [15] Tan, X. & Triggs, B., "Fusing Gabor and LBP feature sets for kernel-based face recognition," in *International Workshop on Analysis and Modeling of Faces and Gestures*, 2007, pp. 235-249.
- [16] Makandar, A. & Halalli, B., "Image enhancement techniques using highpass and lowpass filters," *International Journal of Computer Applications*, vol. 109, 2015.
- [17] Anila, S. & Devarajan, N., "Preprocessing technique for face recognition applications under varying illumination conditions," *Global Journal of Computer Science and Technology*, 2012.
- [18] Jadhav, D. V. & Holambe, R. S., "Feature extraction using Radon and wavelet transforms with application to face recognition," *Neurocomputing*, vol. 72, pp. 1951-1959, 2009.
- [19] Azeem, A., Sharif, M., Raza, M., & Murtaza, M., "A survey: Face recognition techniques under partial occlusion," *Int. Arab J. Inf. Technol.*, vol. 11, pp. 1-10, 2014.
- [20] Mehta, G. & Vatta, S., "An Introduction to a Face Recognition System using PCA, FLDA and Artificial Neural Networks," *IJARCSSE*, vol. 3, 2013.
- [21] Samaria, F. S. & Harter, A. C., "Parameterisation of a stochastic model for human face identification," in *Applications of Computer Vision, 1994., Proceedings of the Second IEEE Workshop on*, 1994, pp. 138-142.
- [22] Georgiades, A., Belhumeur, P., & Kriegman, D., "Yale face database," *Center for computational Vision and Control at Yale University*, <http://cvc.cs.yale.edu/cvc/projects/yalefaces/yalefaces.html>, vol. 2, p. 6, 1997.
- [23] Martinez, A. & Benavente, R., "The AR face database," CVC Tech. Report1998.
- [24] Liu, X., Lu, L., Shen, Z., & Lu, K., "A novel face recognition algorithm via weighted kernel sparse representation," *Future Generation Computer Systems*, vol. 80, pp. 653-663, 2018.
- [25] Tilki, Ö., "PCA based face recognition: An application," 2014.
- [26] Arar, N. M., "Fusing Local Appearance Models For Face Recognition," Bogaziçi University, 2012.

- [27] Harguess, J. D., "Face recognition from video," 2011.
- [28] Kim, K., "Face recognition using principle component analysis," in *International Conference on Computer Vision and Pattern Recognition*, 1996, pp. 586-591.
- [29] Naeem, M., Qureshi, I., & Azam, F., "FACE RECOGNITION TECHNIQUES AND APPROACHES: A SURVEY," *Science International*, vol. 27, 2015.
- [30] Meshgini, S., Aghagolzadeh, A., & Seyedarabi, H., "Face recognition using Gabor-based direct linear discriminant analysis and support vector machine," *Computers & Electrical Engineering*, vol. 39, pp. 727-745, 2013.
- [31] Turk, M. & Pentland, A., "Eigenfaces for recognition," *Journal of cognitive neuroscience*, vol. 3, pp. 71-86, 1991.
- [32] Belhumeur, P. N., Hespanha, J. P., & Kriegman, D. J., "Eigenfaces vs. fisherfaces: Recognition using class specific linear projection," *Pattern Analysis and Machine Intelligence, IEEE Transactions on*, vol. 19, pp. 711-720, 1997.
- [33] Wiskott, L., Fellous, J.-M., Kruger, N., & von der Malsburg, C., "Face recognition by elastic bunch graph matching," *Intelligent biometric techniques in fingerprint and face recognition*, vol. 11, pp. 355-396, 1999.
- [34] Girisha, H., Sreepathi, B., & Karibasappa, K., "Multi-view face recognition using local binary pattern," *International Journal of Computer Science and Information Technologies*, vol. 5, pp. 2978-2981, 2014.
- [35] Bargavi, B. S. & Santhi, C., "Global and local facial feature extraction using Gabor filters," *International Journal of Science, Engineering and Technology Research (IJSETR)*, vol. 3, pp. 1020-1023, 2014.
- [36] Pentland, A., Moghaddam, B., & Starner, T., "View-based and modular eigenspaces for face recognition," 1994.
- [37] Du, S., "Image-based face recognition under varying pose and illuminations conditions," University of British Columbia, 2008.
- [38] Moujahdi, C., Ghouzali, S., Mikram, M., & Aboutajdine, D., "Multi-View Face Recognition," *Journal of Communications and Computer Engineering*, vol. 2, p. 46, 2012.
- [39] Dai, M. & Zhou, M., "On automatic human face recognition," *Advances Biometrics*, vol. 1, pp. 41-48, 2003.
- [40] Gan, J.-Y. & Zhang, Y.-W., "A new approach for face recognition based on singular value features and neural networks," *Acta Electronica Sinica*, vol. 32, pp. 170-173, 2004.

- [41] Gan, J.-y., Zhang, Y.-w., & Mao, S.-y., "Adaptive Principal Components Extraction Algorithm and Its Application In the Feature Extraction of Human Face," *Acta Electronica Sinica*, vol. 30, pp. 1013-1016, 2002.
- [42] Er, M. J., Chen, W., & Wu, S., "High-speed face recognition based on discrete cosine transform and RBF neural networks," *IEEE Transactions on neural networks*, vol. 16, pp. 679-691, 2005.
- [43] Zhao, W., Chellappa, R., Phillips, P. J., & Rosenfeld, A., "Face recognition: A literature survey," *ACM computing surveys (CSUR)*, vol. 35, pp. 399-458, 2003.
- [44] Wright, J., Yang, A. Y., Ganesh, A., Sastry, S. S., & Ma, Y., "Robust face recognition via sparse representation," *IEEE transactions on pattern analysis and machine intelligence*, vol. 31, pp. 210-227, 2009.
- [45] Yang, M. & Zhang, L., "Gabor feature based sparse representation for face recognition with gabor occlusion dictionary," in *Computer Vision–ECCV 2010*, ed: Springer, 2010, pp. 448-461.
- [46] Mairal, J., Ponce, J., Sapiro, G., Zisserman, A., & Bach, F. R., "Supervised dictionary learning," in *Advances in neural information processing systems*, 2009, pp. 1033-1040.
- [47] He, X., Yan, S., Hu, Y., Niyogi, P., & Zhang, H.-J., "Face recognition using Laplacianfaces," *Pattern Analysis and Machine Intelligence, IEEE Transactions on*, vol. 27, pp. 328-340, 2005.
- [48] Turk, M. A. & Pentland, A. P., "Face recognition using eigenfaces," in *Computer Vision and Pattern Recognition, 1991. Proceedings CVPR'91., IEEE Computer Society Conference on*, 1991, pp. 586-591.
- [49] Tunç, B. & Gökmen, M., "Manifold learning for face recognition under changing illumination," *Telecommunication Systems*, vol. 47, pp. 185-195, 2011.
- [50] Tran, C. K., Tseng, C. D., & Lee, T. F., "Improving the Face Recognition Accuracy under Varying Illumination Conditions for Local Binary Patterns and Local Ternary Patterns Based on Weber-Face and Singular Value Decomposition," in *2016 3rd International Conference on Green Technology and Sustainable Development (GTSD)*, 2016, pp. 5-9.
- [51] Wiskott, L., Fellous, J.-M., Kuiger, N., & Von Der Malsburg, C., "Face recognition by elastic bunch graph matching," *Pattern Analysis and Machine Intelligence, IEEE Transactions on*, vol. 19, pp. 775-779, 1997.
- [52] Georghiades, A. S., Belhumeur, P. N., & Kriegman, D. J., "From few to many: Illumination cone models for face recognition under variable lighting and pose," *Pattern Analysis and Machine Intelligence, IEEE Transactions on*, vol. 23, pp. 643-660, 2001.

- [53] Shashua, A. & Riklin-Raviv, T., "The quotient image: Class-based re-rendering and recognition with varying illuminations," *Pattern Analysis and Machine Intelligence, IEEE Transactions on*, vol. 23, pp. 129-139, 2001.
- [54] Zhou, S. & Chellappa, R., "Rank constrained recognition under unknown illuminations," in *Analysis and Modeling of Faces and Gestures, 2003. AMFG 2003. IEEE International Workshop on*, 2003, pp. 11-18.
- [55] Zhang, L. & Samaras, D., "Face recognition from a single training image under arbitrary unknown lighting using spherical harmonics," *Pattern Analysis and Machine Intelligence, IEEE Transactions on*, vol. 28, pp. 351-363, 2006.
- [56] Lu, Z. & Zhang, L., "Face recognition algorithm based on discriminative dictionary learning and sparse representation," *Neurocomputing*, vol. 174, pp. 749-755, 2016.
- [57] Kim, T.-K. & Kittler, J., "Locally linear discriminant analysis for multimodally distributed classes for face recognition with a single model image," *Pattern Analysis and Machine Intelligence, IEEE Transactions on*, vol. 27, pp. 318-327, 2005.
- [58] Jaiswal, S., "Comparison between face recognition algorithm-eigenfaces, fisherfaces and elastic bunch graph matching," *International Journal of Global Research in Computer Science (UGC Approved Journal)*, vol. 2, pp. 187-193, 2011.
- [59] Pentland, A., Moghaddam, B., & Starner, T., "View-based and modular eigenspaces for face recognition," in *Computer Vision and Pattern Recognition, 1994. Proceedings CVPR'94., 1994 IEEE Computer Society Conference on*, 1994, pp. 84-91.
- [60] Gross, R., Matthews, I., & Baker, S., "Eigen light-fields and face recognition across pose," in *Automatic Face and Gesture Recognition, 2002. Proceedings. Fifth IEEE International Conference on*, 2002, pp. 1-7.
- [61] Zhou, S. K. & Chellappa, R., "Illuminating light field: Image-based face recognition across illuminations and poses," in *Automatic Face and Gesture Recognition, 2004. Proceedings. Sixth IEEE International Conference on*, 2004, pp. 229-234.
- [62] Blanz, V. & Vetter, T., "Face recognition based on fitting a 3D morphable model," *Pattern Analysis and Machine Intelligence, IEEE Transactions on*, vol. 25, pp. 1063-1074, 2003.
- [63] Basri, R. & Jacobs, D. W., "Lambertian reflectance and linear subspaces," *Pattern Analysis and Machine Intelligence, IEEE Transactions on*, vol. 25, pp. 218-233, 2003.

- [64] Ramamoorthi, R., "Analytic PCA construction for theoretical analysis of lighting variability in images of a Lambertian object," *Pattern Analysis and Machine Intelligence, IEEE Transactions on*, vol. 24, pp. 1322-1333, 2002.
- [65] Vasilescu, M. A. O. & Terzopoulos, D., "Multilinear subspace analysis of image ensembles," in *Computer Vision and Pattern Recognition, 2003. Proceedings. 2003 IEEE Computer Society Conference on*, 2003, pp. II-93-9 vol. 2.
- [66] Wang, R., Shan, S., Chen, X., & Gao, W., "Manifold-manifold distance with application to face recognition based on image set," in *Computer Vision and Pattern Recognition, 2008. CVPR 2008. IEEE Conference on*, 2008, pp. 1-8.
- [67] Shin, D., Lee, H.-S., & Kim, D., "Illumination-robust face recognition using ridge regressive bilinear models," *Pattern Recognition Letters*, vol. 29, pp. 49-58, 2008.
- [68] Prince, S. J., Warrell, J., Elder, J. H., & Felisberti, F. M., "Tied factor analysis for face recognition across large pose differences," *Pattern Analysis and Machine Intelligence, IEEE Transactions on*, vol. 30, pp. 970-984, 2008.
- [69] Kusuma, G. P. & Chua, C.-S., "PCA-based image recombination for multimodal 2D+ 3D face recognition," *Image and Vision Computing*, vol. 29, pp. 306-316, 2011.
- [70] Al-Shiha, A. A. M., Woo, W. L., & Dlay, S. S., "Multi-linear neighborhood preserving projection for face recognition," *Pattern Recognition*, vol. 47, pp. 544-555, 2014.
- [71] Banerjee, P. K. & Datta, A. K., "Class specific subspace dependent nonlinear correlation filtering for illumination tolerant face recognition," *Pattern Recognition Letters*, vol. 36, pp. 177-185, 2014.
- [72] Givens, G. H., Beveridge, J. R., Phillips, P. J., Draper, B., Lui, Y. M., & Bolme, D., "Introduction to face recognition and evaluation of algorithm performance," *Computational Statistics & Data Analysis*, vol. 67, pp. 236-247, 2013.
- [73] Li, S., Gong, D., & Yuan, Y., "Face recognition using Weber local descriptors," *Neurocomputing*, vol. 122, pp. 272-283, 2013.
- [74] Luan, X., Fang, B., Liu, L., & Zhou, L., "Face recognition with contiguous occlusion using linear regression and level set method," *Neurocomputing*, vol. 122, pp. 386-397, 2013/12/25/ 2013.
- [75] Zhou, C., Wang, L., Zhang, Q., & Wei, X., "Face recognition based on PCA image reconstruction and LDA," *Optik-International Journal for Light and Electron Optics*, vol. 124, pp. 5599-5603, 2013.

- [76] Wang, H., Leng, Y., Wang, Z., & Wu, X., "Application of image correction and bit-plane fusion in generalized PCA based face recognition," *Pattern Recognition Letters*, vol. 28, pp. 2352-2358, 2007.
- [77] Hsieh, P.-C. & Tung, P.-C., "A novel hybrid approach based on sub-pattern technique and whitened PCA for face recognition," *Pattern Recognition*, vol. 42, pp. 978-984, 2009.
- [78] Luh, G.-C. & Lin, C.-Y., "PCA based immune networks for human face recognition," *Applied soft computing*, vol. 11, pp. 1743-1752, 2011.
- [79] Oh, S.-K., Yoo, S.-H., & Pedrycz, W., "Design of face recognition algorithm using PCA-LDA combined for hybrid data pre-processing and polynomial-based RBF neural networks: Design and its application," *Expert Systems with Applications*, vol. 40, pp. 1451-1466, 2013.
- [80] Zhang, D. & Zhou, Z.-H., "(2D) 2PCA: Two-directional two-dimensional PCA for efficient face representation and recognition," *Neurocomputing*, vol. 69, pp. 224-231, 2005.
- [81] Tan, K. & Chen, S., "Adaptively weighted sub-pattern PCA for face recognition," *Neurocomputing*, vol. 64, pp. 505-511, 2005.
- [82] Sun, Y., Liang, D., Wang, X., & Tang, X., "Deepid3: Face recognition with very deep neural networks," *arXiv preprint arXiv:1502.00873*, 2015.
- [83] Wan, L., Liu, N., Huo, H., & Fang, T., "Face Recognition with Convolutional Neural Networks and subspace learning," in *Image, Vision and Computing (ICIVC), 2017 2nd International Conference on*, 2017, pp. 228-233.
- [84] Parkhi, O. M., Vedaldi, A., & Zisserman, A., "Deep face recognition," in *bmvc*, 2015, p. 6.
- [85] Goswami, G., Ratha, N., Agarwal, A., Singh, R., & Vatsa, M., "Unravelling robustness of deep learning based face recognition against adversarial attacks," in *Thirty-Second AAAI Conference on Artificial Intelligence*, 2018.
- [86] Li, S. & Deng, W., "Deep facial expression recognition: A survey," *arXiv preprint arXiv:1804.08348*, 2018.
- [87] Pramerdorfer, C. & Kampel, M., "Facial expression recognition using convolutional neural networks: state of the art," *arXiv preprint arXiv:1612.02903*, 2016.
- [88] Zhou, L.-F., Du, Y.-W., Li, W.-S., Mi, J.-X., & Luan, X., "Pose-robust face recognition with Huffman-LBP enhanced by Divide-and-Rule strategy," *Pattern Recognition*, 2018.

- [89] He, K., Zhang, X., Ren, S., & Sun, J., "Deep residual learning for image recognition," in *Proceedings of the IEEE conference on computer vision and pattern recognition*, 2016, pp. 770-778.
- [90] Tan, X. & Triggs, B., "Enhanced local texture feature sets for face recognition under difficult lighting conditions," in *International Workshop on Analysis and Modeling of Faces and Gestures*, 2007, pp. 168-182.
- [91] Kasar, M. M., Bhattacharyya, D., & Kim, T.-h., "Face recognition using neural network: a review," *International Journal of Security and Its Applications*, vol. 10, pp. 81-100, 2016.
- [92] Goh, Y., Teoh, A. B., & Goh, M. K., "Wavelet based illumination invariant preprocessing in face recognition," in *Image and Signal Processing, 2008. CISP'08. Congress on*, 2008, pp. 421-425.
- [93] Liu, D.-H., Lam, K.-M., & Shen, L.-S., "Illumination invariant face recognition," *Pattern Recognition*, vol. 38, pp. 1705-1716, 2005.
- [94] Sompura, M. & Gupta, V., "A Review on Feature Extraction Methods and Classifiers," *International Journal*, vol. 3, 2015.
- [95] Dixon, S. J. & Brereton, R. G., "Comparison of performance of five common classifiers represented as boundary methods: Euclidean distance to centroids, linear discriminant analysis, quadratic discriminant analysis, learning vector quantization and support vector machines, as dependent on data structure," *Chemometrics and Intelligent Laboratory Systems*, vol. 95, pp. 1-17, 2009.
- [96] Nikisins, O. & Greitans, M., "Local binary patterns and neural network based technique for robust face detection and localization," in *2012 BIOSIG - Proceedings of the International Conference of Biometrics Special Interest Group (BIOSIG)*, 2012, pp. 1-6.
- [97] Ravat, C. & Solanki, S. A., "Survey on Different Methods to Improve Accuracy of The Facial Expression Recognition Using Artificial Neural Networks," 2018.
- [98] Davis, T. A. & Ramanujacharyulu, C., "Statistical analysis of bilateral symmetry in plant organs," *Sankhyā: The Indian Journal of Statistics, Series B*, pp. 259-290, 1971.
- [99] Endress, P. K., "Symmetry in flowers: diversity and evolution," *International Journal of Plant Sciences*, vol. 160, pp. S3-S23, 1999.
- [100] Arrigo, D. J., *Symmetry analysis of differential equations: an introduction*: John Wiley & Sons, 2015.
- [101] Maldacena, J., "The symmetry and simplicity of the laws of physics and the Higgs boson," *European Journal of Physics*, vol. 37, p. 015802, 2015.

- [102] Chen, X., Flynn, P. J., & Bowyer, K. W., "Fully automated facial symmetry axis detection in frontal color images," in *Automatic Identification Advanced Technologies, 2005. Fourth IEEE Workshop on*, 2005, pp. 106-111.
- [103] Zhao, W. Y. & Chellappa, R., "Illumination-insensitive face recognition using symmetric shape-from-shading," in *Computer Vision and Pattern Recognition, 2000. Proceedings. IEEE Conference on*, 2000, pp. 286-293.
- [104] Pan, G. & Wu, Z., "3D face recognition from range data," *International Journal of Image and Graphics*, vol. 5, pp. 573-593, 2005.
- [105] Farin, G., Femiani, J., Bae, M., & Lockwood, C., "3D face authentication and recognition based on bilateral symmetry analysis," 2005.
- [106] Saha, S. & Bandyopadhyay, S., "A symmetry based face detection technique," in *Proceedings of the IEEE WIE National Symposium on Emerging Technologies*, 2007, pp. 1-4.
- [107] Xu, Li, Y., Zhang, Z., Yang, B., & You, J., "Sample diversity, representation effectiveness and robust dictionary learning for face recognition," *INS Information Sciences*, vol. 375, pp. 171-182, 2017.
- [108] Swarnalatha, S., Satyanarayana, P., & Babu, B. S., "Wavelet Transforms, Contourlet Transforms and Block Matching Transforms for Denoising of Corrupted Images via Bi-shrink Filter," *Indian Journal of Science and Technology*, vol. 9, 2016.
- [109] Dalali, S. & Suresh, L., "Daubechives Wavelet Based Face Recognition Using Modified LBP," *Procedia Computer Science*, vol. 93, pp. 344-350, 2016.
- [110] Mistry, D., *DISCRETE WAVELET TRANSFORM USING MATLAB* vol. 4, 2013.
- [111] Gonzalez & Woods, *Digital image processing*, 2 ed.: Prentice Hall, 2002.
- [112] Winnemöller, H., Kyprianidis, J. E., & Olsen, S. C., "XDoG: an extended difference-of-Gaussians compendium including advanced image stylization," *Computers & Graphics*, vol. 36, pp. 740-753, 2012.
- [113] Davidson, M. W. & Abramowitz, M., "Molecular expressions microscopy primer: Digital image processing-difference of gaussians edge enhancement algorithm," *Olympus America Inc., and Florida State University*, 2006.
- [114] Haralick, R. M., Shanmugam, K., & Dinstein, I. H., "Textural Features for Image Classification," *IEEE Trans. Syst., Man, Cybern. IEEE Transactions on Systems, Man, and Cybernetics*, vol. 3, pp. 610-621, 1973.
- [115] The MathWorks, L., "Image Processing Toolbox User's Guide, Using a Gray-Level Co-Occurrence Matrix (GLCM),"

<http://matlab.izmiran.ru/help/toolbox/images/enhanc15.html>, Accessed on 14 July 2019.

- [116] Haralick, R. M., Shanmugam, K., & Dinstein, I. H., "Textural features for image classification," *Systems, Man and Cybernetics, IEEE Transactions on*, pp. 610-621, 1973.
- [117] Vatamanu, O. A., Frandes, M., Ionescu, M., & Apostol, S., "Content-based image retrieval using local binary pattern, intensity histogram and color coherence vector," in *E-Health and Bioengineering Conference (EHB), 2013*, 2013, pp. 1-6.
- [118] Thomas, L. L., Gopakumar, C., & Thomas, A. A., "Face Recognition based on Gabor Wavelet and Backpropagation Neural Network," *J. Sci. and Eng. Research*, vol. 4, pp. 2114-2119, 2013.
- [119] Dobrisek, S., Struc, V., Krizaj, J., & Mihelic, F., "Face recognition in the wild with the probabilistic Gabor-Fisher classifier," *FG 2015*, 2015.
- [120] Haghighat, M., Zonouz, S., & Abdel-Mottaleb, M., "Identification using encrypted biometrics," in *International Conference on Computer Analysis of Images and Patterns*, 2013, pp. 440-448.
- [121] Nisperos, S., *Gabor Filter Experiment*, 2014.
- [122] Kamarainen, J.-K., Kyrki, V., & Kalviainen, H., "Invariance properties of Gabor filter-based features-overview and applications," *IEEE Transactions on image processing*, vol. 15, pp. 1088-1099, 2006.
- [123] Rahma, A. S., Bisono, E. F., Arifin, A. Z., Navastara, D. A., & Indraswari, R., "Generating automatic marker based on combined directional images from frequency domain for Dental Panoramic Radiograph Segmentation," in *Informatics and Computing (ICIC), 2017 Second International Conference on*, 2017, pp. 1-6.
- [124] Dalal, N. & Triggs, B., "Histograms of oriented gradients for human detection," in *Computer Vision and Pattern Recognition, 2005. CVPR 2005. IEEE Computer Society Conference on*, 2005, pp. 886-893.
- [125] Nicolini, C. A. & Vakula, S., *From neural networks and biomolecular engineering to bioelectronics*. New York: Plenum Press, 2013.
- [126] Xiang, Z., Tan, H., & Ye, W., "The excellent properties of a dense grid-based HOG feature on face recognition compared to Gabor and LBP," *IEEE Access*, 2018.
- [127] Zhang, L., Yang, M., & Feng, X., "Sparse representation or collaborative representation: Which helps face recognition?," in *Computer vision (ICCV), 2011 IEEE international conference on*, 2011, pp. 471-478.

- [128] Lu, J., Tan, Y.-P., & Wang, G., "Discriminative multimanifold analysis for face recognition from a single training sample per person," *IEEE transactions on pattern analysis and machine intelligence*, vol. 35, pp. 39-51, 2013.
- [129] Ji, H.-K., Sun, Q.-S., Ji, Z.-X., Yuan, Y.-H., & Zhang, G.-Q., "Collaborative probabilistic labels for face recognition from single sample per person," *Pattern Recognition*, vol. 62, pp. 125-134, 2017.
- [130] Liu, F., Tang, J., Song, Y., Bi, Y., & Yang, S., "Local structure based multi-phase collaborative representation for face recognition with single sample per person," *Information Sciences*, vol. 346, pp. 198-215, 2016.

## CURRICULUM VITAE

### Personal Information

---

**Name Surname** : Saad Omran Elhashmi ALLAGWAIL

**Date of Birth** : 1977

**Phone** : +905522186566

**Email** : [saad.elhashmi@gmail.com](mailto:saad.elhashmi@gmail.com)

### Education

---

Sep. 2004 – Sep. 2005      Coventry University      United Kingdom

M.S. Degree in Control Engineering

Sep. 1993 – Sep. 1997      Faculty of Electronic Engineering      Libya

B. S. Degree in Control Engineering

### Professional Skills

---

#### Languages

Arabic, English and Beginner in Turkish

#### Programming Languages

Matlab, VBasic and Beginner in Python

### **Awards**

---

The Control Theory and Applications Centre (CTAC) Prize of Coventry university in 2005.

### **Work Experience**

---

2000 - 2007	Waha Oil Company	Libya
-------------	------------------	-------

Operations Department, Automation Section

### **Training Programs**

---

2004	Waha Oil Company	Libya
------	------------------	-------

Programmable Logic Controller (PLC), Training Course

## **PUBLICATIONS**

- [1] S. Allagwail, O. S. Gedik, and J. Rahebi, “Face Recognition with Symmetrical Face Training Samples Based on Local Binary Patterns and the Gabor Filter,” *Symmetry*, vol. 11, p. 157, 2019.
- [2] S. Allagwail and O. S. Gedik, “Face Recognition Based on Symmetry in Feature Domain" *Symmetry*”, (In progress to publication).
- [3] S. Allagwail and O. S. Gedik, “Face Recognition with Symmetrical Face Training Samples Based on Local Binary Patterns and Gaussian Low-Pass Filter”, *International Multidisciplinary, Engineering, Science, Education and Technology Conference*, September 20-21, 2019 in Kuala Lumpur, United Malaysia. (accepted).